Part III.

Hurricane Surge Hazard Analysis

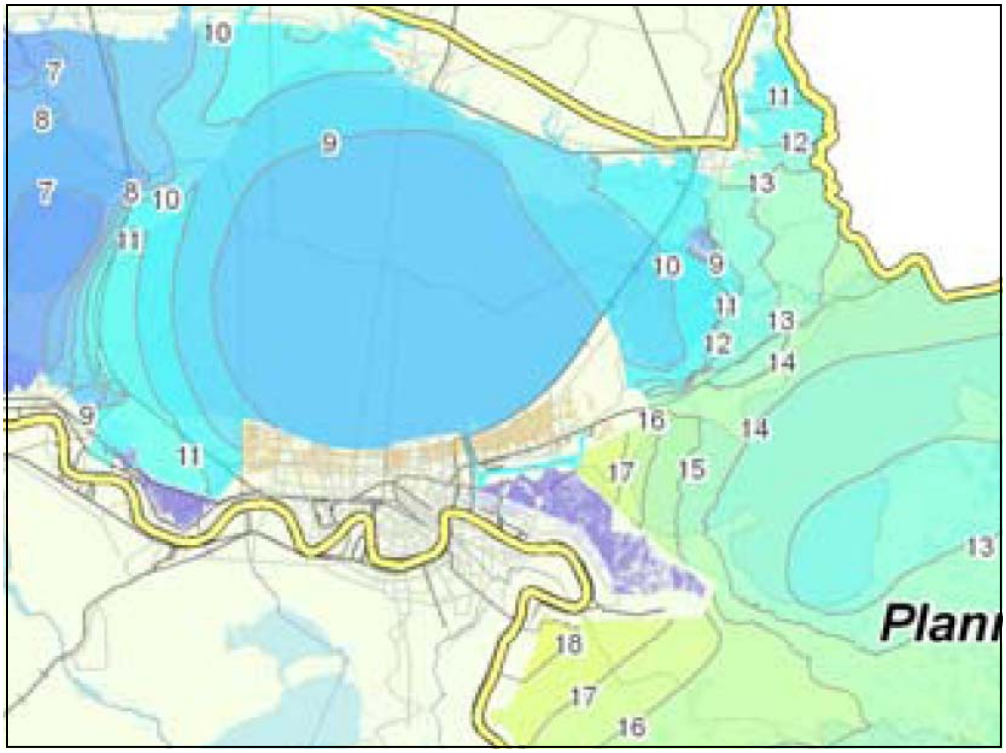

USACE 2009

As discussed in the Introduction, the full range of hurricane surge risk management programs—perimeter structures, evacuation, property flood damage insurance, building codes, coastal restoration, etc.—requires good surge hazard information. Hydrologists describe surge and other flood hazards using a return frequency analysis (see GTN-1) to quantify the recurrence probability of surge by magnitude. The estimated surge hazard varies across a region in accordance with hurricane joint probability characteristics (see Part I) and the physics of surge interaction with local coastal landscape features (see Part II).

Return frequency analysis relies on sophisticated mathematical techniques to provide seemingly exact hazard estimates—such as surge SWL elevations and wave height to the nearest 0.1 ft for the 100- and 500-year return period. However, the apparent accuracy of these probability estimates is belied by major uncertainties in critical inputs regarding hurricane climatology and the modeling of surge physics (see Parts 1 and II). A significant limitation is the short duration of records on which inputs are based. Despite these uncertainties, the advantages of probabilistic surge elevation estimates include:

- The estimates can be used to further support detailed quantitative risk assessment and cost-benefit analysis for risk management alternatives (e.g., optimal perimeter structure height).
- Estimates for different locations that are developed with the same methodology can be compared and the relative differences can be used to establish regional risk management priorities.
- A variety of useful probabilities can be calculated—such as the probability of a 100-year surge occurring at a particular location over the term of a typical mortgage; or the probability of a 500-year surge occurring across a wide region over an agency's planning horizon.

This Part III reviews the state of the practice in hurricane surge SWL and wave return frequency analysis, including the following subjects:

Section 12., the direct approach involving analysis of data records from tide gauge stations and other observations to estimate local surge SWL and wave hazards. If sufficiently long and reliable records are available, a direct analysis provides the best estimate of local surge hazard;

Section 13., the JPA approach to combining the results of hurricane JPA and deterministic surge modeling. As tide gauge records are not widely available, this technique is usually employed—in a way similar to that used in characterizing riverine flood hazards; and

Section 14., recent applications of the JPA approach, including the surge hazard analysis performed by the USACE for the southeast Louisiana.

Sections 12 and 13 examine the established literature and ongoing research, including methods, assumptions, and limitations. Section 14 addresses the published information on surge analyses performed as part of FISs. Afterwards, findings and conclusions are presented, together with recommendations for improving future hurricane surge hazard analyses.

The ensuing Part IV discusses hazard analyses for interior polder inundation associated with surge overtopping and breaching of perimeter protection. The USACE has employed analysis of perimeter overtopping and breaching in designing post-Katrina upgrades to the New Orleans regional hurricane protection systems. Part V examines additional technical approaches to evaluating hurricane surge hazard for future conditions and surge estimates for selected storm-scenarios.

Section 12. Analysis of Surge Records

12.1 Analysis of Tide and HWM Data

As with riverine flood hazard analysis, surge SWL return frequencies can be evaluated using long term gauge station records (FEMA February 2007). Gauge stations which provide daily maximum water levels are maintained by NOAA, USGS, and USACE in coastal sounds, bays, lakes, and rivers and near important coastal works. NOAA has four CN-GoM tide stations with records dating back many decades at Pensacola FL (80+ years), Dauphin Island AL (40+ years), Grand Isle LA (60+ years), and Sabine Pass TX (50+ years). The USGS gauge record for Biloxi MS covers over 100 years.

Important limitations in the direct analysis of tide gauge data include the following:

- The record may not be sufficiently long to reasonably estimate a particular return period event. As discussed in GTN-1, the probability of a 100-yr (or greater) surge occurring during a given 100-yr tide record is 63%. The probabilities do not exceed 95% and 99% for at least one occurrence until the record approaches 300 and 500 years. Note that this limitation is not unique to tide records. The records used to establish joint probability characteristics for regional hurricane climatology are also subject to length limitations.
- The uncertainties associated with extrapolating extreme events—with return periods many times longer than the record length—can be very large.
- Tide stations often fail during major surge events. Peak SWL values for recent events can sometimes be estimated using nearby SWL HWM data. However, for many events HWM data may not be available in close proximity to the station or, if available, may not be reliable.
- Tide data must be converted to the proper geoid reference (NAVD88 and epoch, see GTN-2). Conversion of older data must account for regional and local sources of coastal subsidence (see Section 18). Long-term tide data are also affected by SLR.
- The analysis only applies to a small geographical area in close proximity to the gauge station—e.g., up to a few miles at most. Coastal landscape features can significantly alter surge magnitude (see Section 7).
- Changes in the coastal landscape over time impact gauge data representativeness and usability. Examples include changing coastal pass bathymetry; construction of levees, roads, and other embankments; subsidence and erosion; loss of coastal barriers and dunes; etc. Coastal hydrologists often study the effect of landscape changes on the tidal exchange and water quality for important estuaries (Jacobsen and Dill 2007, McCorquodale et al 2007).

GTN-1 describes the estimation of return periods from a data series using observed rankings. The observed return frequency (F_R, equal to the inverse of the return period) is typically defined as:

$$F_R = n/\tau \text{ ; or sometimes as } F_R = (n - a) \,/\, (\tau + 1 - 2a)$$

where

n is the observed rank,
τ is the record length, and
a provides a minor adjustment to the observed return period.

To extrapolate recurrence estimates from the observed return frequency (or return period) hydrologists use probability distribution functions. These functions account for normal or log-normal distributions

around a mean, skewness, kurtosis, and other factors typical of recurrence data distribution. Example distributions include

- Log-Normal distribution, takes the logarithm of the return period (log (100) = 2) and uses a normal distribution of the magnitude versus log transformed return period (or return frequency); defined by two parameters, mean and the variance.
- Log Pearson Type III distribution, adds the coefficient of skewness to the Log-Normal Distribution and reduces to the Log-Normal Distribution when coefficient of skewness equals zero.
- Generalized Extreme Value, (GEV) distribution includes three parameters (the mean, variance, and a shape parameter allowing for a higher probability of extreme values, i.e., a "fat tail") which are grouped according to three types: Type I, (Gumbel) distribution; Type II, (Frechet) distribution; and Type III (Weibull) distribution.
- Generalized Pareto distribution, a three parameter power law function.

The selection of a particular function is somewhat arbitrary but can be aided by visual inspection or more rigorous fitting techniques. Figure 12.1 illustrates the use of the GEV distribution function, and a modified function, with data from the NOAA Pensacola tide station, by Xu and Wang (2008). Note that the GEV derived level is nearly three feet less than the observed value for the 82-yr return period.

In addition to extrapolating extreme return period values, the functions can be used to estimate uncertainty bands. Most probability distribution functions for estimating return frequency are skewed distributions and thus the uncertainty bands will also be skewed. Note the authors of Figure 12.1 did not include an uncertainty band but the difference between the two curves is over 5 ft at 500 years.

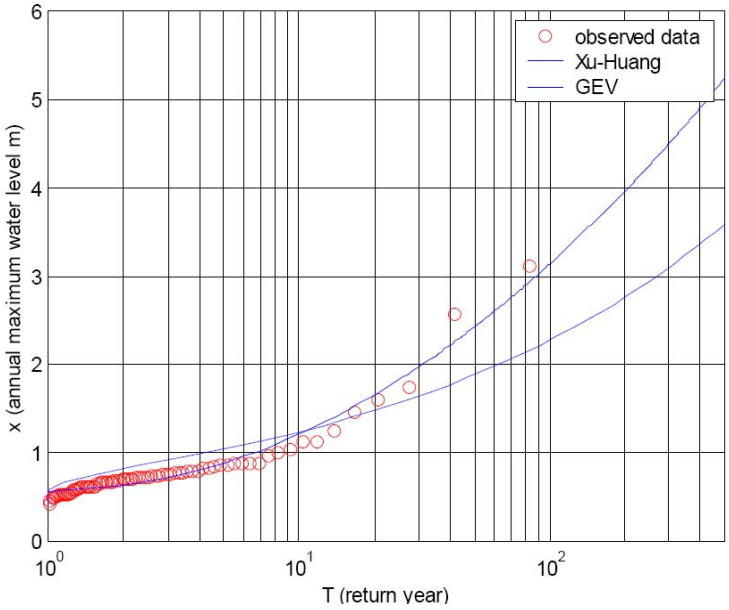

Figure 12.1. Observed Annual Maximums at Pensacola Tide Station with GEV and Modified Distribution Functions

(The GEV curve has the lower water level at the 100-yr return)

Xu and Wang 2008

12.2 Recent Evaluations of Tide Gauge Data

The following is a discussion of two recent return frequency studies encompassing multiple CN-GoM tide stations.

A return frequency analysis of unreferenced tide data was published in 2005 (prior to Hurricane Katrina) by Chris Zervas of NOAA. The objective of this report was to support sea level rise assessment and not to provide a detailed return frequency analysis. Annual high SWLs relative to the gauge Mean Higher High Water (MHHW) in meters were analyzed using the GEV distribution for 117 US tide stations, including five along the CN-GoM. Zervas noted that GoM stations required a positive shape parameter (Type II, Frechet) due to higher probabilities of extreme SWLs associated with hurricane surge, but provided no detailed information about the GEV equation. The report does not present complete return frequency graphs or tabulated results for the various stations. The 1% return frequency magnitudes (in ft above gauge MHHW) are approximately:

- Pensacola, FL 6.5 ft
- Dauphin Island, AL 5.4 ft
- Grand Isle, LA 4.9 ft
- Eugene Island, LA 6.4 ft
- Sabine River, TX 4.5 ft

Grand Isle MHHW is about 0.5 ft above LMSL or 0.7 ft NAVD88-2006.81 (NOAA). Thus, this estimate of the 1% return frequency SWL corresponds to approximately 5.6 ft NAVD88-2006.81.

While Zervas did not focus on assessing local hurricane surge return frequency he noted that

> The GEV exceedance probability curves . . . are best constrained at the more frequent return periods and less well constrained near the 1% annual exceedance probability level . . . . In addition, if the GEV distribution has a positive shape factor (Frechet), the 95% confidence intervals widen considerably for the longer return periods, since they are dependent on the presence or absence of a few rare events in the data series. (Zervas 2005)

Zervas goes on to state that the 1% return frequency SWL for Grand Isle "may have been underestimated." (Zervas 2005)

Shortly after Hurricane Katrina a FEMA contractor was tasked to conduct a return frequency analysis for several regional tide stations in order to provide local governments with advisories on potential changes to NFIP 100- and 500-yr flood elevations. (FEMA issues these advisories in order to expedite rebuilding as the development of detailed FIRMs takes several years.)[1] URS Corporation analyzed data for four NOAA tide stations (Pensacola FL, ,Dauphin Island, AL, Waveland MS, and Grand Isle LA) and two USGS gauges (Pascagoula MS and Biloxi MS). The NOAA tide data were adjusted to gauge MSL and the USGS gauge data were assumed to be equivalent to MSL. No adjustments were made for long-term SLR or station subsidence.

The annual maximum data were plotted using the following formula:

[1] An early draft copy of this report entitled *Preliminary Flood Frequency Analysis for Hurricane Katrina* (URS Corporation 2005) has been obtained. The report appears to have been subsequently revised and is referenced as the *Hurricane Katrina Flood Frequency Analysis* in a later, broader report: *Hurricane Katrina in the Gulf Coast, Mitigation Assessment Team Report*, p. 1-19 (URS Corporation 2006). The later version could not be obtained.

$$F_R = \frac{n - 0.4}{\tau + 0.2}$$

Figure 12.2 illustrates the log-log plot of the annual maximum data for the USGS Biloxi MS gauge. The SWL for Hurricane Katrina is the highest rank value, which for 100 records yielded a plotted return frequency of `0.6%, or a return period of 167 years. The 100-yr return period on the plot corresponds to a SWL of 17.8 ft.

The data for all six stations were analyzed using several probability distribution functions, including the GEV and Log Pearson Type III. The results for the 100-yr return period SWL for these two PDFs—in feet above LMSL—are shown in Table 12.1, along with the results of Zervas' analysis for three of the stations. With the addition of the Hurricane Katrina data, the URS GEV 100-yr SWL estimate for Dauphin Island AL was higher than Zervas' GEV estimate by more than 1 ft. The URS GEV estimate rose slightly for Grand Isle LA (by 0.2 ft) and remained the same for Pensacola FL. The Log Pearson Type III estimates were slightly higher than the GEV estimates for all six locations. URS did not provide an uncertainty analysis for these estimates.

In a separate 2006 report URS provided the following estimates of return period SWL:

- Biloxi MS, 15.7 ft (100-yr) and 28.7 ft (500-yr); Hurricane Katrina HWM of 24 ft (250-yr);
- Pascagoula MS, 11.9 (100-yr); Hurricane Katrina HWM of 13 ft (125-yr);
- Waveland MS, 17.6 ft (100-yr) and 22.8 ft (200-yr); Hurricane Katrina HWM of 23 ft (200-yr);
- Dauphin Island AL, 6 ft (50-yr) and 7.5 ft (100-yr); Hurricane Katrina HWM of 5.8 ft (50-yr); and
- Pensacola FL, 5.8 ft (50-yr) and 7.3 ft (100-yr); Hurricane Katrina HWM of 6.1 ft (50-yr).

Note that the Xu-Wang curve in Figure 12.1 indicates a 100-yr SWL for Pensacola FL of closer to 10.5 ft.

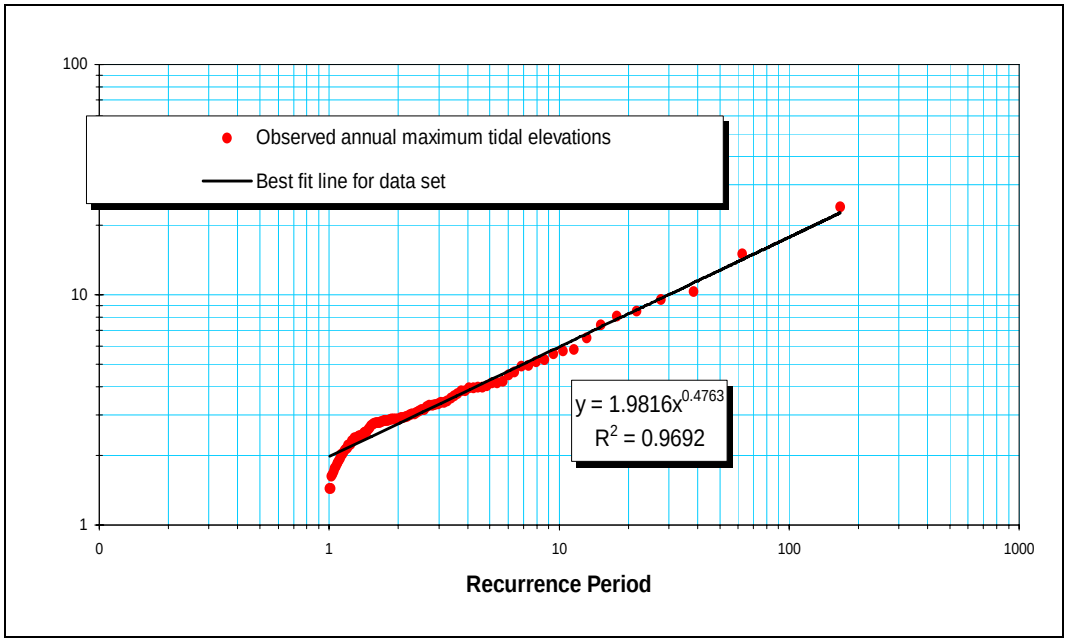

Figure 12.2. Annual Maximum Series for Biloxi MS Tide Gauge
URS Corporation 2005

Table 12.1. Estimates of 100-yr Surge SWL

URS Corporation 2005

Tide Station	URS Post Katrina		Zervas Pre-Katrina
	GEV	Log-Pearson Type III	GEV
Grand Isle, LA	5.6	5.7	5.6
Waveland, MS	23.5	25.8	-
Biloxi, MS	14.8	15.2	-
Pascagoula, MS	11.4	11.6	-
Dauphin Island, AL	7.3	7.5	6.1
Pensacola, FL	7.2	7.3	7.2

NOAA (Tides and Currents, Extreme Water Levels) recently began publishing updated return frequency analyses—employing the GEV distribution— for selected tide gauges on their website. CN-GoM gauges include Pensacola FL, Dauphin Island AL, Grand Isle and Eugene Island LA, and Sabine Pass TX. Figure 12.3 presents the NOAA return period graph for Grand Isle LA, with the water elevation converted to NAVD88-2006.81. The mean, 95%UCL, and LCL levels for the 100-yr return period are 7.1, 11.5,and 5.1 ft. The current mean estimate of 7.1 ft is 1.5 ft higher than the URS value shown in Table 12.1 for the GEV, reflecting NOAAs refinements to the gauge's 60+ years of data—including 2008 observations for Hurricanes Gustav and Ike. This increase indicates the sensitivity of 100-yr return period estimates to record length and quality. Figure 12.3 shows the notable asymmetry of the confidence limits and that the GEV distribution based mean 100-yr level is less than the highest observed value (about 7.5 ft).

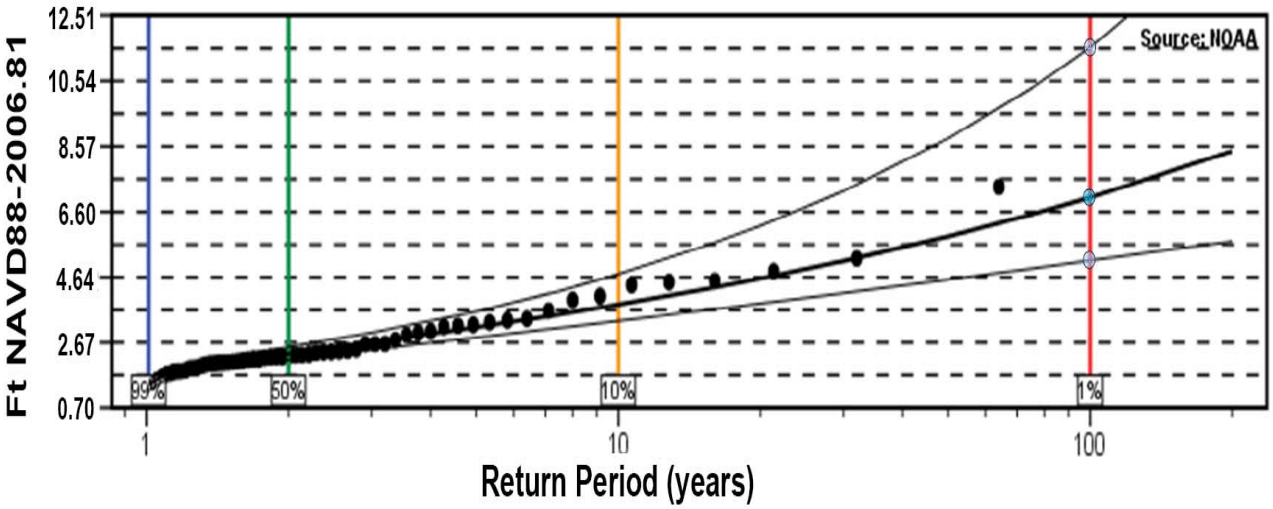

Figure 12.3. Grand Isle LA Tide Station Return Frequency

NOAA (http://tidesandcurrents.noaa.gov/est/est_station.shtml?stnid=8761724)

12.3 Recent Evaluations of HWM Data

In 2010 Needham developed a surge database for the US GoM shoreline covering the 130-yr period of 1880 to 2009. The database

> identifies the maximum surge height and peak surge location for storm surge events. Although this information does not depict the regional extent of specific surges, or a list of all historic surge levels at a particular location, these data are useful for understanding surge height potentials for the entire basin and regions within the basin, identifying locations that observe enhanced or reduced numbers of peak surges, and potentially for understanding the relationship between specific tropical cyclone characteristics and resultant surge heights. (Needham 2010)

Needham's search of tropical cyclone data sets identified a total of 421 storms, with 463 landfalls (42 storms involved double landfalls) which he classified as having at the potential to generate a peak SWL of 4 ft or higher (above LMSL). This equates to a frequency of more than 3.5 US GoM tropical cyclone landfalls per year. By investigating tide gauge records, scientific and technical literature, HWM studies, newspaper reports, and other data sources Needham confirmed 193 peak SWL events of 4 ft or higher. For the CN-GoM, he identified 76 events of 4 ft or higher and 32 of 8 ft or higher (frequencies of 58% and 25%, respectively). Table 12.2 lists the 76 events.

Needham analyzed frequency and magnitude time-series for the 193 surge events for evidence of long-term trends associated with the SO, AMO, and NAO (see Section 2). He noted a period of relatively suppressed surge frequency and magnitude from the 1970s through the 1990s attributable to the cooler AMO phase. He also described statistical correlations of US Gulf-wide surge events with the AMO, SO, and NAO. Needham did not attempt to define an overall cycle for GoM surge events.

Needham also analyzed 181 peak SWL records for the period from 1900 to 2009 to evaluate US Gulf-wide return frequency surge magnitude. Needham analyzed the series using several probability distribution functions, including the Gumbel, Huff-Angel, and Southern Regional Climate Center (SRCC) distributions. (The latter two equations were previously developed for evaluating rainfall frequency.) Table 12.3 presents the results of his analysis, with the estimate of the US Gulf-wide 100-yr surge ranging from 23.8 to 32.8 ft.

Two important limitations with Needham's US Gulf-wide return period analysis include the following.

1. Lumping surge HWM data for different coastal regions ignores the dramatic effects on surge magnitude associated with a) particular hurricane track Loop Current interactions; b) regional continental shelf conditions; and c) local landscape features.
2. The surge HWM data are subject to many error sources, including lack of a true local peak measurement and the quality of LMSL vertical referencing;

Needham did not provide an uncertainty analysis for his Gulf-wide return period estimates. Uncertainty bands are crucial as the probability of a 100-yr event occurring at least once within a particular 100-yr span is only 66.9%.

Table 12.2. List of CN-GoM Surge HWMs

Needham 2010

Storm Name	Year	Peak Surge Location	Peak SWL (ft LMSL)
Katrina	2005	Pass Christian MS	27.8
Camille	1969	Pass Christian MS	24.6
Eloise	1975	Dune Allen Beach	18.2
New Orleans	1917	Southeastern LA, S of New Orleans LA	17.0
Cheniere Caminada	1893	Cheniere Caminada (W of Grand Isle) LA	16.0
Frederic	1979	Gulf State Park	15.3
Betsy	1965	Pointe a la Hache	15.2
Rita	2005	Cameron LA	15.0
Grand Isle	1909	Terrebonne Bay/ Bayou Portage (N of Pass Chris) LA/ MS	15.0
Ivan	2004	Destin, FL to Mobile, AL FL/Al	15.0
Unnamed	1947	Chandeleur Light LA	14.0
Opal	1995	Florida Panhandle FL	14.0
Unnamed	1906	Galt, Santa Rosa County FL	14.0
Audrey	1957	west of Cameron	13.9
Gustav	2008	Southeast LA, near Bay Gardene LA	13.0
Flossy	1956	Ostrica Lock LA	13.0
Terrebonne Parish	1926	Terrebonne Parish 1926 Terrebonne Parish LA	12.5
Lili	2002	Crewboat Channel (Calumet) LA	12.3
Unnamed	1886	Johnson's Bayou LA	12.0
Georges	1998	Fort Morgan AL	11.9
Unnamed	1916	Mobile AL	11.6
Unnamed	1888	Southeastern LA LA	10.9
Unnamed	1896	Fort Walton Beach	10.0
Isidore	2002	Rigolets, LA and Gulfport Harbor, MS MS/LA	8.3
Andrew	1992	Cocodrie LA	8.0
Juan	1985	Cocodrie LA	8.0
Danny	1985	South Central LA Coast LA	8.0
Edith	1971	Vermillion & Cote Blanche Bays LA	8.0
Unnamed	1923	Biloxi MS	8.0
Unnamed	1901	Port Eads and Mobile LA/AL	8.0
Earl	1998	Northwest FL- Big Bend area E of Apalach FL	8.0
Unnamed	1901	Port Eads and Mobile LA/AL	8.0
Hilda	1964	Cocodrie LA	7.8
Ethel	1960	Quarantine Bay LA	7.0
Unnamed	1918	Creole LA	7.0
Erin	1995	just west of Navarre Beach FL	7.0
Ida	2009	Bay Gardene LA	6.5
Danny	1997	HWY 182W, b/t Gulf Shores & Fort Morgan AL	6.5
Unnamed	1931	Frenier LA	6.5
Unnamed	1932	Mobile AL	6.5
Unnamed	1940	Frenier LA	6.4
Bob	1979	Gulfport and Harrison County CD MS	6.3

Table 12.2. List of CN-GoM Surge HWMs, Continued

Needham 2010

Storm Name	Year	Peak Surge Location	Peak SWL (ft LMSL)
Cindy	2005	SE LA, MS, Lakes Borgne & Pont MS/LA	6.0
Florence	1988	Bayou Bienvenue LA	6.0
Chris	1982	Cameron Parish LA	6.0
Carmen	1974	South Central LA Coast LA	6.0
Debbie	1965	Industrial Canal in New Orleans LA	6.0
TS Brenda	1955	Shell Beach LA	6.0
Unnamed	1948	MS Coast MS	6.0
Unnamed	1943	Chef Menteur LA	6.0
Unnamed	1920	Lake Borgne and Mississippi Sound MS/LA	6.0
Unnamed	1897	Sabine Pass TX/ LA	6.0
Unnamed	1936	Fort Walton Beach, Panama City, Valparaiso FL	6.0
Unnamed	1929	Panama City to Apalachicola FL	6.0
Unnamed	1897	Sabine Pass TX/ LA	6.0
Matthew	2004	Frenier LA	5.8
Debra	1978	Atchafalaya Bay to Vermillion Bay LA	5.7
Bill	2003	Bayou Bienvenue MS	5.5
Beryl	1988	Bayou Bienvenue LA	5.5
Baker	1950	Pensacola FL	5.5
Bonnie	1986	Sabine Pass TX	5.2
Hanna	2002	Gulfport Harbor MS	5.1
Claudette	1979	Sabine Coast Guard Station TX	5.0
Babe	1977	Southeastern LA LA	5.0
Esther	1957	MS Coast MS	5.0
Arlene	2005	Walton County FL	5.0
Alberto	1994	Okaloosa Island to Destin FL	5.0
Claudette	1979	Sabine Coast Guard Station TX	5.0
Babe	1977	Southeastern LA LA	5.0
Bertha	1957	west end of Vermillion Bay LA	4.7
TS No.1	1956	Biloxi MS	4.7
Unnamed	1912	Mobile AL	4.4
Ella	1958	Texas and Louisiana Coasts TX/LA	4.0
Unnamed	1938	Cameron and Vermillion Parishes LA	4.0
Ella	1958	Texas and Louisiana Coasts TX/LA	4.0
Unnamed	1916	Mobile AL	4.0

Table 12.3. US Gulf-Wide Surge SWL Return Period Estimates

Needham 2010

Return Period (yr)	Probability Distribution Function		
	Gumbel	Huff-Angel	SRCC
2	9.5	9.1	9.0
5	13.3	12.5	13.2
10	15.9	15.6	16.3
20	18.3	19.6	19.4
25	19.1	21.2	20.5
50	21.5	26.2	23.5
100	23.8	32.8	26.6

12.4 Analysis of Wave Data

Extreme wind waves in the GoM originate with hurricanes. Marine engineers and scientists involved in the design of ocean going vessels and offshore oil and gas exploration and production platforms (such at those at OceanWeather, Inc.) have studied extreme GoM waves. Data on waves off the CN-GoM shore have been collected at regional NOAA buoys since the 1970s. Over the recent decades the network of buoys has expanded to over 100 stations (see NOAA National Data Buoy Center website).

Panchang and Dongcheng (2006) analyzed data from three deep GoM buoys which each had records extending over 25 years. Using a Gumbel distribution, the 100-yr H_s values were found to be between 34.2 and 37.1 ft. The authors noted that the 95% confidence band associated with this 100-yr estimate is on the order of ±3 feet. The $H_{1\%}$ in a wave field is usually estimated at $1.52H_s$; thus, an estimate of the 100-yr $H_{1\%}$ in the deep GoM would exceed 60 ft, allowing for a margin of uncertainty. A major limitation of this analysis, acknowledged by the authors, is the short record duration. Temporary buoys deployed near the transition to the Continental Shelf during Hurricane Ivan recorded H_s up to 58.7 ft. This H_s value is higher than the 100-yr range noted above, but may reflect shallower depth.

Since 1999 the Louisiana State University Coastal Studies Institute has installed seven wave monitoring stations for analyzing the nearshore seasonal wave characteristics and extreme hurricane waves. However, it will likely be many years before a sufficient record is available for direct analysis of extreme nearshore wave conditions.

In the absence of sufficiently long wave records, wave scientists have primarily relied on the stochastic approaches to evaluating extreme GoM waves employing hindcasts of GoM hurricanes dating back over 50 years (e.g., see Jonathan and Ewans February 2011 and May 2011).

Section 13. Surge JPA

13.1 Overview of Surge JPA

The JPA for evaluating hurricane climatology (described in Section 4) can be readily coupled with deterministic high resolution surge hydrodynamic modeling (encompassing wind, SWL, and wave setup components, see Section 9) to estimate the surge hazard at any coastal location of interest (LOI). As described in GTN-1 Sections K and L, JPA of flood return frequency is a common tool in hydrology.

The JPA of surge return frequency can be summarized in a mathematical formulation (from Resio et al 2007 and Toro 2008):

$$\boldsymbol{F}(SWL_i) = \int\int\int\int\int \boldsymbol{p}(CPD, R_{max}, V_f, \theta, X)\, \boldsymbol{H}[\boldsymbol{\Psi}(CPD, R_{max}, V_f, \theta, X) - SWL_i]\, d(CPD)\, d(R_{max})\, d(V_f)\, d(\theta)\, d(X)$$

where

- CPD, R_{max}, V_f, θ, and X are five major hurricane characteristics influencing local surge response, with X being the landfall distance with respect to the LOI (or X and Y for a full areal range). Additional characteristics could be included—such as V_{max} (instead of, or in addition to, CPD), IKE, Holland B, asymmetry, double eye walls, track passage over the Loop Current, intensification and decay dynamics, etc.
- $\boldsymbol{\Psi}$(CPD, R_{max}, V_f, θ, X) is the deterministic *surge response function.* $\boldsymbol{\Psi}$ defines the SWL at the LOI for the range of hurricane characteristics using a high spatial resolution wind/surge/wave-setup model (e.g., PBL plus ADCIRC-STWAVE), incorporating the influence of the regional coastal landscape on surge routing. Mathematically, $\boldsymbol{\Psi}$ is a six dimensional (6D) surface.
- $\boldsymbol{p}$(CPD, R_{max}, V_f, θ, X) is the joint PDF of the five characteristics. Example PDFs for CPD, R_{max}, V_f, and θ were previously shown in Figure 4.2 and 4.3. The joint probability is also a 6D function—of the five attribute probabilities: $\boldsymbol{p}$(CPD), $\boldsymbol{p}$(R_{max}), $\boldsymbol{p}$(V_f), $\boldsymbol{p}$(θ), and $\boldsymbol{p}$(X).
- H[] evaluates if the local SWL determined by $\boldsymbol{\Psi}$ for a particular hurricane is greater than some SWL_i ; if it is, H[]= 1; if not, H[] = 0. The combined term—$\boldsymbol{p}$(CPD, R_{max}, V_f, θ, X) $\boldsymbol{H}$[Ψ(CPD, R_{max}, V_f, θ, X) – SWL_i]—is thus the discrete (mass) probability for the interval [Ψ(CPD, R_{max}, V_f, θ, X) – SWL_i].
- $\boldsymbol{F}(SWL_i)$ is the cumulative probability at SWL_i , integrating $\boldsymbol{p}$(SWL) over the full range of CPD, R_{max}, V_f, θ, and X. Thus, $\boldsymbol{F}(SWL_i)$ provides the surge cumulative distribution function (CDF). The local surge CDF is typically presented as a 2D graph of SWL versus return frequency or period. The return frequency, F_r equal to 1 – $\boldsymbol{F}(SWL_i)$. is the *surge hazard response function*.

Hurricane surge JPA requires a stochastic approach, coupling a good representation of both the probabilistic hurricane climatology for the LOI—$\boldsymbol{p}$(CPD, R_{max}, V_f, θ, X)—with the deterministic model of hurricane driven surge interactions with the local coastal landscape—$\boldsymbol{\Psi}$(CPD, R_{max}, V_f, θ, X). In this approach a synthetic set of hurricanes is typically used to represent the hurricane climatology. As discussed in Section 4, a *full JPM* set approximates the entire range of the 5D (CPD, R_{max}, V_f, θ, X) storms by employing a sufficient combinations of attributes. However, with more values per attribute the number of storm combinations increases drastically. For five values per five attributes 3125 storms would be required to provide the CDF for one location.

An alternative to the full JPM is the *Monte Carlo JPM* which only employs the number of randomly selected storms—drawn from the 5D range—to construct a synthetic record of sufficient length to

confidently contain return frequencies of interest. Thus, for a synthetic 1000-yr record for a LOI that experiences an average landfall of 16 GHMs/century the set would only need to include 160 storms.

With either the Full or Monte Carlo JPM each hurricane in the synthetic set is simulated with the wind/surge/wave-setup model. Each simulation result represents one increment—d(CPD) d(R_{max}) d(V_f) d(θ) d(X)—of the above 5D integrand. Modeling each storm in the set provides all the increments in the integrand, and numerical integration—or quadrature—is then used to compute the surge CDF.

In a regional surge hazard study this entire stochastic analysis must be replicated at a reasonable LOI spacing. The location spacing can be addressed by establishing offsets for each storm such that intermediate points experience nearly the same peak SWL as the nearest landfall point. In theory, conditions along the coast can be represented by replicating each storm in the JPM every $2X_{max}$, where X_{max} is the maximum radial distance at which the peak SWL for that storm is relatively undiminished.[1] X_{max} is not the same for every storm. If the regional study employs a uniform landfall spacing for all storms the landfall spacing should be equal to or less than the shortest $2X_{max}$.

High resolution surge models require the dedication of large HPPC system for hours per storm simulation. Given the time and expense associated with such models further reduction of the synthetic hurricane set size is desirable—provided any increased error is acceptable. Researchers have devised two primary techniques for defining an optimized subset or sample, (OS): the *JPM-OS* and the *Surge Response OS* (Toro et al 2008 and Resio et al 2007).

In addition to SWL, surge return frequency analysis must also consider wave hazards. The return frequency of shoreline and overland (inundated region) surge waves, at a LOI, are typically evaluated by estimating wave field conditions (which encompasses a Rayleigh distribution, see Section 5) associated with the SWL at those return frequencies. The shoreline and overland wave field conditions at any SWL are typically a function of localized, depth-depended wave regeneration, propagation, and transformation processes (see Section 6).

The following sections provide a further explanation of surge JPA using JPM-OS and Surge-Response-OS, the selection of landfall spacing, the treatment of bias and uncertainty in surge JPA, key steps involved in implementing surge JPA, and wave hazard analysis. Approaches to future conditions surge JPA—for examining the influence of potential changes in RSLR, SST, etc. on hazards—are discussed in Part IV.

13.2 JPM-OS

In the JPM-OS approach (Toro 2008) the OS is optimized to represent the hurricane climatology as depicted in the joint probability ***p***(CPD, R_{max}, V_f, θ, X) 6D surface. The targeted error for the JPM-OS relative to ***p*** is reduced by adjusting the number (*n)*, characteristics, and weighting of the JPM-OS hurricanes. The error in the JPM-OS representation of the ***p***() benchmark is mathematically evaluated by comparing their 6D surfaces using numerical integration—also referred to as quadrature (Toro employed the Bayesian quadrature method.) The JPM-OS can be selected to minimize the overall variance or variance within a particular probability range—e.g., around the 100-yr return period. Importantly, the JPM-OS may allow for different relative errors at different return periods.

[1] An assumption is that storms which make landfall farther away can also be represented by the $2X_{max}$ spacing developed from representing the peak SWL. This assumption is generally valid as the SWL slope becomes more gradual with distance from landfall.

Assessing the suitability of a particular JPM-OS to represent ***p*** is analogous to assessing a set of *n* blocks (3D prisms) with varying heights to represent a mathematical 3D surface, as illustrated in Figure 13.1. Increments for each of the 5D independent variables can be refined or coarsened, and thus *n* can be raised or lowered—as shown in Figures 13.1.a and 14.1.b. In addition, varying sized increments can also be employed—as depicted in Figure 13.1.c.—in which case the bases of the 6D prisms are described in terms of their relative—weighted—sizing.

When the JPM-OS is being coupled with a wind model a *wind hazard benchmark* can be used to further optimize the selection. Similarly, when the set is being coupled with a surge model a *surge hazard benchmark* can be employed in refining the optimization. For a surge JPA the surge hazard benchmark has the additional advantage of incorporating interaction between hurricane characteristics and coastal features.

A surge hazard benchmark for a LOI is created by employing a large set of (*N*) storms—e.g., 3,125 storms if five increments were employed for each of the five attributes. This large storm set is coupled with a very *simplified*, much less computationally demanding, surge model. The model is simpler both in terms of the physics and coastal features represented—such as a SLOSH or a low resolution ADCIRC model without wave setup. In some cases, the simplified surge model may use an idealized coastal region, or the analysis may employ the hurricane climatology and a surge model for a similar coastal region. Thus, the surge hazard benchmark serves as a reference only in that it reflects a high resolution of possible storm characteristics. It does <u>not</u> reflect a high resolution of the coastal hydrodynamics. (Depending on the degree of surge model simplification the surge hazard benchmark may not offer much improvement over a wind hazard or basic joint probabilities benchmark).

The surge hazard benchmark at each LOI can be thought of as a "finely discretized" representation of the local 6D CDF described by the *n* storms. For a JPM-OS with a lower *n,* the increments for CPD, R_{max}, V_f, θ, and *X* (i.e., X_{max}) are more coarsely discretized, producing a rougher approximation of the 6D surge CDF. The suitability of any trial JPM-OS, (n_1, n_2, n_3, etc.) can then be evaluated by comparing the associated trial surface to the benchmark surface.

The development of a JPM-OS employing a surge hazard benchmark is illustrated in Figure 13.2.

Potential increments in CPD, R_{max}, V_f, and θ for the JPM-OS can be developed initially based on representing the shape of the surge response—as discussed in the following section. However, the advantage of the JPM-OS is that it is optimized to represent the shape of surge *hazard* response, which may contain critical inflections. Thus increments are adjusted and added in order to best capture the response of SWL at varying hurricane characteristic probabilities—especially combinations that may correspond to hazard levels of interest (e.g., 100- , 500-, 1000-yr etc. levels). As with surge response (see below), an overly simplified surge model's representation of coastal conditions can influence the depiction of surge hazard response. These limitations should be assessed to determine that the benchmark surge model adequately depicts regional hazard response.

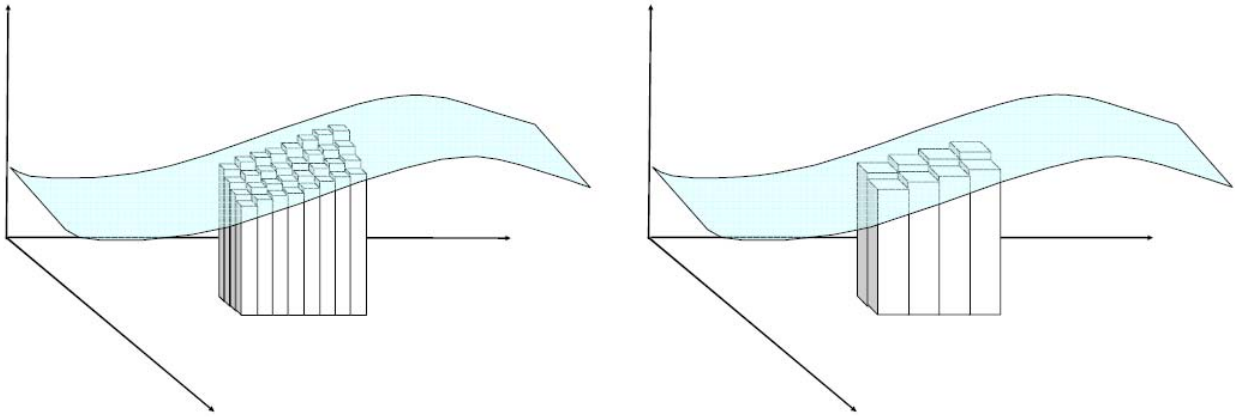

a. Finer Increments (n = 32)

b. Coarser Increments (n = 8)

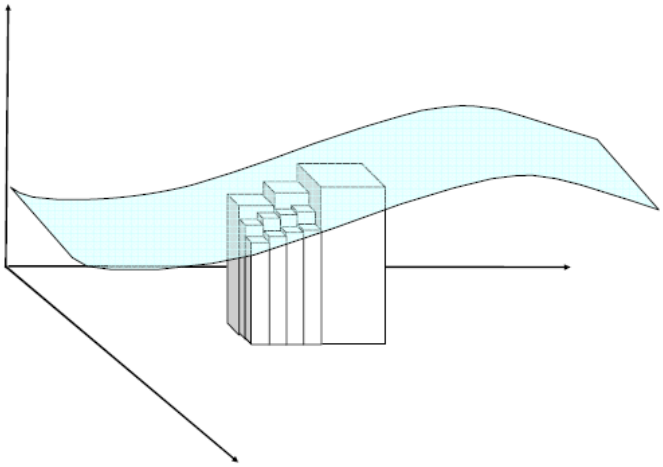

c. Varying Increments (n = 11)

Figure 13.1. Discretization of Volume Under a 3D Surface

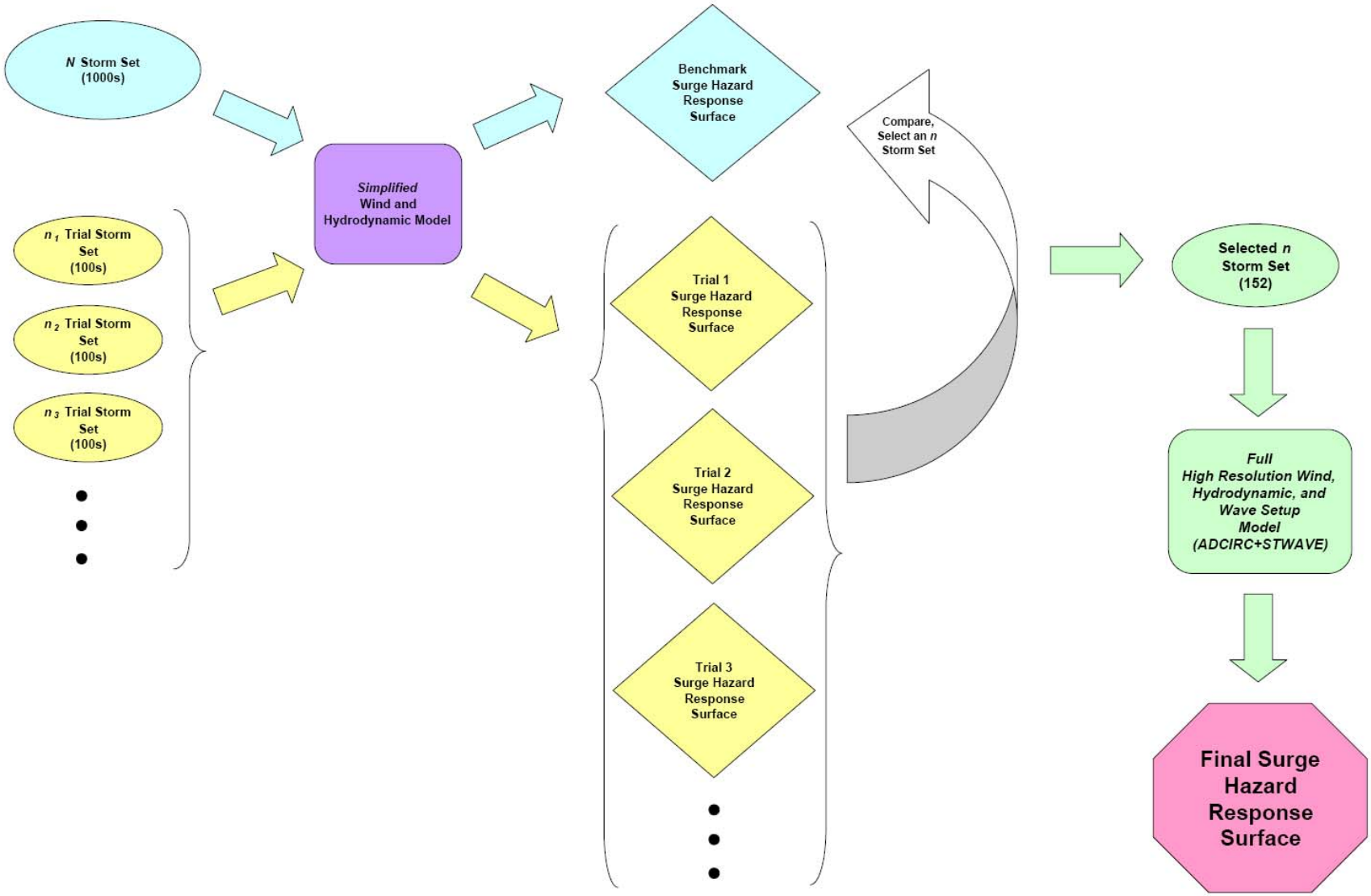

Figure 13.2. Development of JPM-OS Using a Surge Hazard Benchmark

13.3 Surge Response-OS

Another JPM for JPA of hurricane surge is to use an OS of synthetic storms to define the range of the regional surge response $\boldsymbol{\Psi}$ (Resio et al 2007) alone. The approach assumes that a wide range of surge conditions associated with the 5D characteristics can be readily interpolated/extrapolated from limited OS results. In this approach SWL values associated with any combination of storm attributes and their joint probability, as defined by $\boldsymbol{p}$, are obtained from the high spatial resolution Ψ defined with the OS. This OS is more properly considered a part of the deterministic surge hydrodynamic analysis than the joint probability and is referred to in this Report as a *Surge Response-OS*.

This Surge Response OS approach can reduce the size of the storm set when $\boldsymbol{\Psi}$ is considered to have a fairly simple, smooth, response to all five variables—i.e. no abrupt changes in SWL in response with small changes in hurricane characteristics due to regional hurricane-landscape interactions. However, use of a reduced Surge Response-OS also assumes that the interactions of $\boldsymbol{p}$ and $\boldsymbol{\Psi}$ will be fairly smooth. If both of these assumptions are valid, utilizing the Surge Response OS can be an efficient approach.

As noted in Section 1, peak SWLs to the right of landfall increase with increasing CPD, (or V_{max}), R_{max}, V_f, and positive θ (easterly heading with approach to an east-west shoreline). If $\boldsymbol{\Psi}$ is considered to be nearly linear and smooth for all five factors within the region of interest, then an OS can be defined using $\boldsymbol{\Psi}$ alone (i.e., apart from the surge *hazard* response).

Several coastal scientists have recently evaluated the nature and sensitivity of $\boldsymbol{\Psi}$ for the CN-GoM (see Fitzpatrick et al 2010 and Xu 2010), including research supporting JPA OS applications to coastal FISs (Resio et al 2007, Irish et al 2008, URS Corporation 2008, Resio et al 2009, and Irish et al 2009). Major recent findings include:

- CPD—On an idealized coastline, other characteristics being equal, surge SWL increases linearly with increasing CPD (with the V_{max}^2). URS (2008) conducted extensive sensitivity tests using a SLOSH model of the Mississippi coast to evaluate the relationship of CPD and SWL. Using a baseline model with CPD, R_{max}, V_f, and θ values of 70 mb, 30 mi, 12 mph, and 0°, respectively, URS varied CPD between 30 and 110 mb at increments of 10 mb. The SWL results were evaluated at three groups of coastal locations—outer shoreline, inshore river, inland floodplain. Figures 13.3.a, b, and c present results for the three groups of coastal locations. As expected, SWL response to CPD was linear, with steeper slopes further inshore, reflecting the impact of the momentum balance. CPD generally exerts the greatest influence on peak SWL, followed in decreasing order by R_{max}, θ, and finally V_f.
- R_{max}—Irish et al (2008) conducted numerical experiments using a range of idealized shelf slopes to evaluate the affect of R_{max}x on SWL. The simulations employed three R_{max} values (11.5, 23, and 34.5 miles) and six CP values (ranging from 40 to 130 mb). The results, shown in Figure 13.4, also indicate a linear relationship between R_{max} and SWL.
- V_f—URS (2008) used their baseline SLOSH model tested V_f values of 6, 8, 10, 12, 14, 16, and 18 mph. Figure 13.5 illustrates linear response at outer shoreline locations.
- θ—URS (2008) also tested the baseline SLOSH model with headings of -45, -30, -15, 0, +15, +30, and +45 degrees. Figure 13.6 shows that generally SWL increased smoothly, though non-linearly, with more positive θ.
- Holland B—Resio et al (200&) referred to numerical experiments (unpublished) suggesting that modest Holland B variations (e.g., ±20%) are linearly correlated with surge.

a. Outer Shoreline Locations

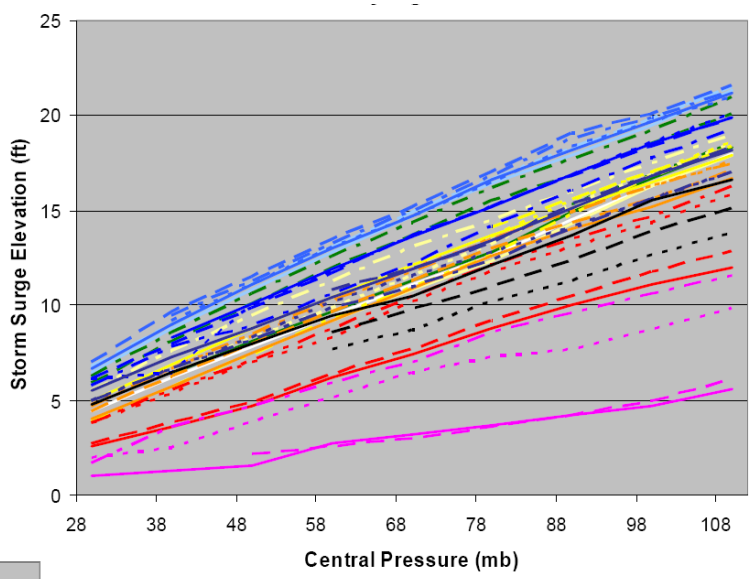

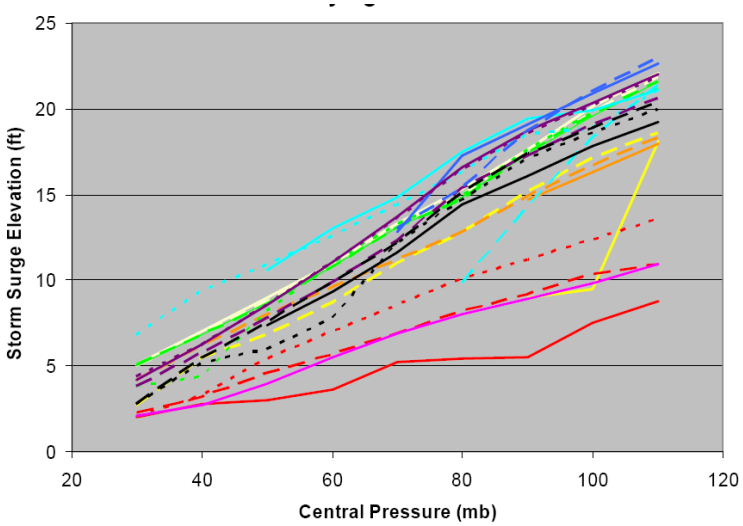

b. Inshore River Locations

c. Inland Floodplain Locations

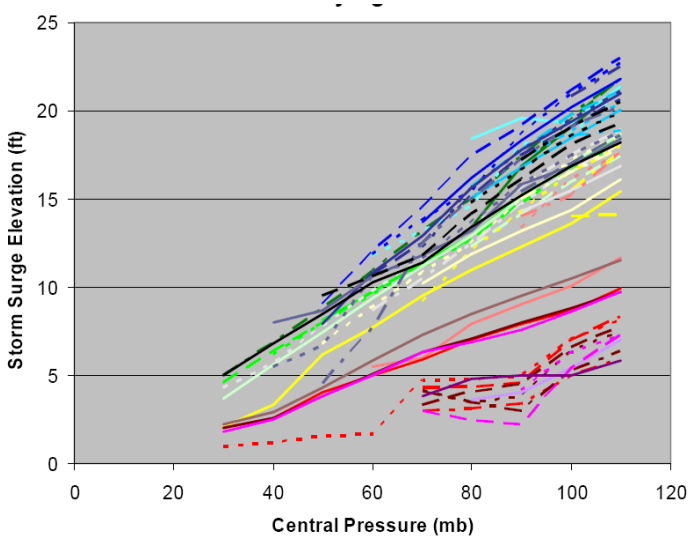

Figure 13.3. Peak SWL versus CPD

(color spectrum blue-red for east-west of landfall)

URS Corporation 2008

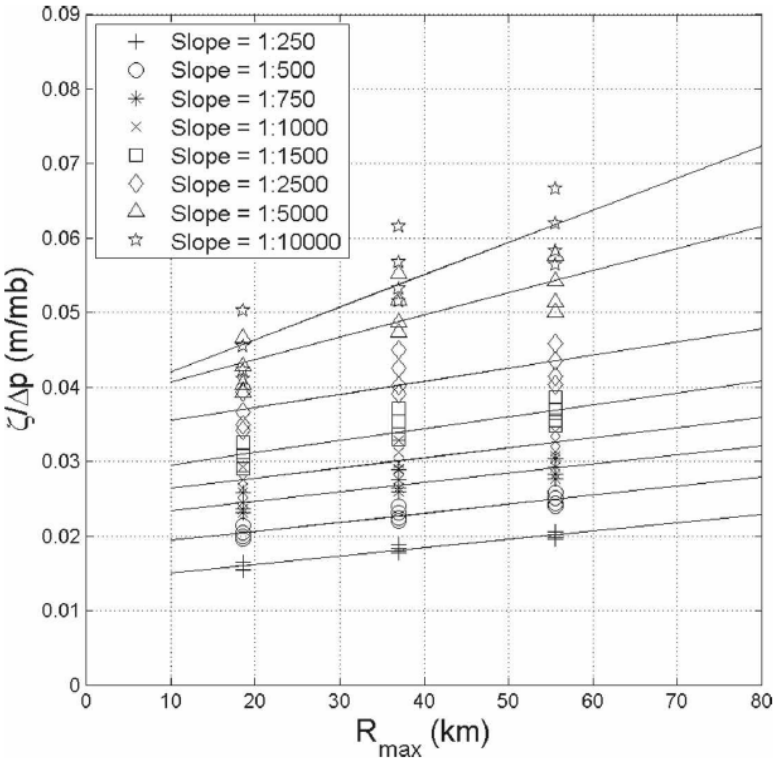

Figure 13.4. Peak SWL versus R_{max} (normalized for CPD)
Irish et al 2008

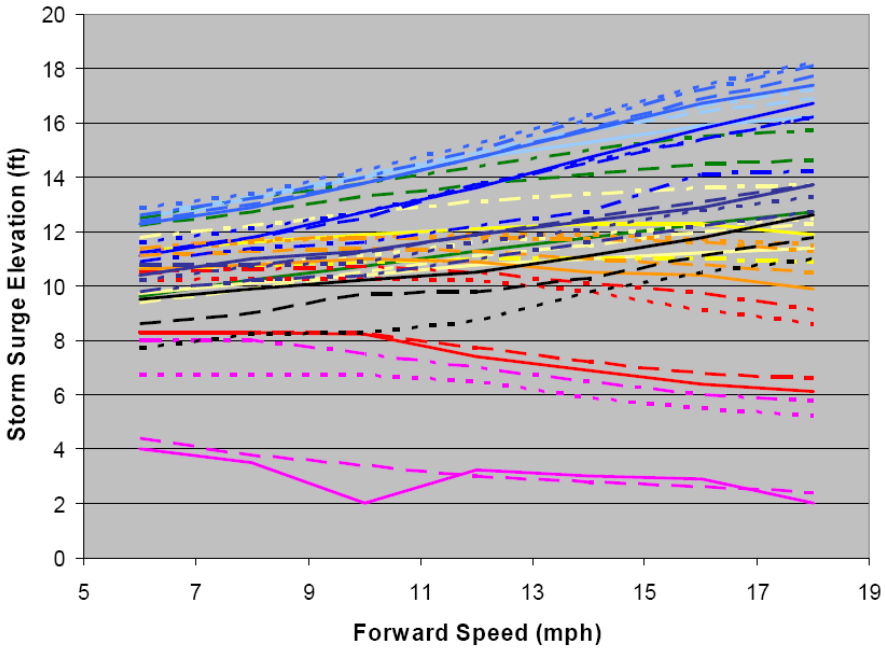

Figure 13.5. Peak SWL versus V_f
URS Corporation 2008

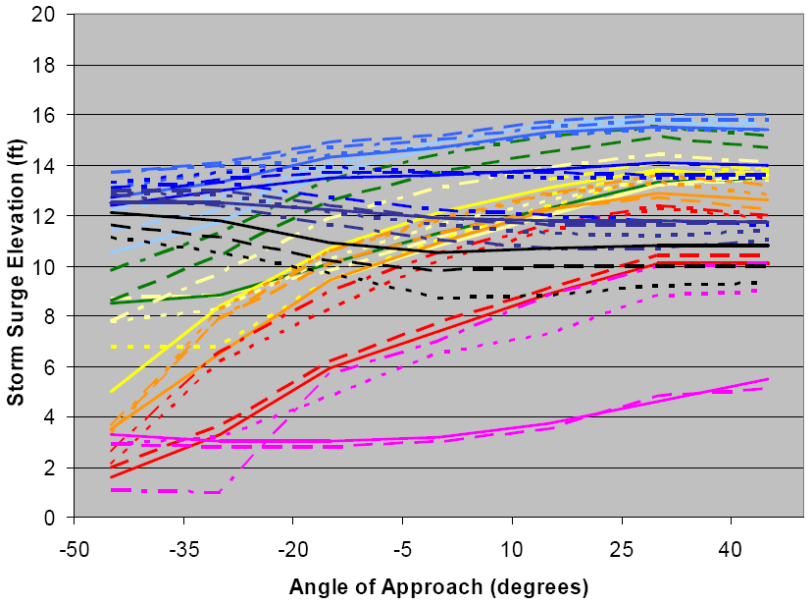

Figure 13.6. Peak SWL versus θ

URS Corporation 2008

However, these indications of smooth response have been based on *very simplified* surge models (e.g., SLOSH). Use of simplified surge models can affect representation of surge response in ways similar to model hindcast performance (see Sections 8, 10, and 11). Seven important simplifications include:

1. Vortex modeling. Simplified vortex models may not reasonably depict wind peaks and durations. The synthetic vortex model simulates the approaching hurricane wind field based on inputs of CPD, R_{max}, V_f, θ, and landfall location, and incorporating correlations on decay, but may not fully account for the observed variability in V_{max} associated with CPD. A major example is Hurricane Katrina, which had a landfall CPD of 100 mb (borderline Category 4/5) but V_{max} winds of 126.5 mph (strong Category 3). In addition, not all vortex models account for storm asymmetry. Finally, vortex models do not describe wind field variability, such as experienced with banding and eye wall replacement.

2. Mesh resolution. Surge hydrodynamic results are sensitive to the terrain fidelity of the model, particularly in the representation of critical coastal landscape features. The simplified models used in OS development may not adequately account for local surge variations that result from the interaction of storm conditions and landscape features. An important example is the local wind setup in sheltered water bodies—such as coastal bays, lakes, and rivers—that is highly sensitive to small variations in storm conditions.

3. Friction. Bottom friction sensitivity to inundation is not addressed in the current SWL models. Thus, it is also not incorporated into simplified models. Furthermore, simplified models may apply uniform friction values across widely differing terrains. The simplification of friction may lead to reducing the number of storms for depicting critical non-linear interactions between surge driving forces and coastal landscape features. The importance of this interaction has been indicated by limited tests on the sensitivity of surge to the presence of coastal marsh (Wamsley et al 2009). Extensive testing of the sensitivity of surge hazard response to friction parameterization, and its interaction with hurricane characteristics, has not be undertaken.

4. Other surge model settings and parameters. Hindcast evaluations of FIS surge models have shown sensitivity to additional settings and parameters, including: numerical method, acceleration terms, time step, eddy viscosity, wind sheltering coefficients, and air-sea drag coefficient. These factors may also influence OS selection.
5. Wave setup. The simplified surge models employed in the development of the OS do not usually include wave radiation stress gradients, and thus do not capture wave setup contribution to SWL, (up to 30%). Furthermore, recent hindcasts of Hurricane Katrina and Rita HWMs indicate that the current wave coupling approach used with the high resolution surge models may not sufficiently depict setup in coastal bays and lakes.
6. Baroclinic forcing. In limited areas, such as near major coastal passes, temperature and salinity gradients can create forces which require 3D analysis. If future studies indicate a significant localized impact, baroclinic forcing may need to be incorporated into the OS selection.
7. LMMSL rise, pre-storm setup, and astronomical tides. The simplified models typically neglect these factors. In the CN-GoM they can combine to contribute over 2 ft to SWL rise, leading to some non-linear interactions with surge.

The URS tests revealed that $\boldsymbol{\Psi}$ becomes more complex as varying coastal features and more complicated momentum exchanges come into play, e.g., Figures 13.3 b) and c). In investigating $\boldsymbol{\Psi}$ for the southwest Texas coast, Irish et al (2009) found that a simplified, nearly linear $\boldsymbol{\Psi}$ is primarily applicable for open coastlines. Sensitivity analyses using high resolution coastal models of very intricate coastlines—such as those with large sheltered water bodies—would likely reveal more irregular interactions. For complex coastlines, a proper Surge Response-OS requires many more storms and may not offer an advantage over the standard JPM-OS approach. Importantly, a Surge Response-OS does not support further JPA of polder inundation hazards (see Section 16).

13.4 Landfall Spacing

In addition to discretizing CPD, R_{max}, V_f, and θ, selecting the number of JPM-OS or Surge Response-OS storms depends on defining increments for landfall spacing. As noted above, each storm is considered to have an appropriate X_{max}—and hence landfall spacing—defined by the SWL gradient near the landfall at peak. URS (2008) summarized sensitivity tests using the simplified SLOSH model of the Mississippi coast; a storm with CPD, R_{max}, V_f, and θ values of 80 mb, 25 mi, 10 mph, and 0°, respectively; and various landfall spacing in fractions of R_{max}. The study found that landfall spacing equivalent to R_{max}—or X_{max} equivalent to $\frac{1}{2}R_{max}$—could be used with minimal effect on estimates of surge hazard across a region. Employing uniform landfall spacing greater than the R_{max} of the smallest storm will thus introduce some error in the OS which must be evaluated as part of the optimization.

Resio et al (2007) reported on a sensitivity analysis conducted with an idealized linear E-W shoreline model of varying shelf slopes and employing three values for R_{max}, 11.5, 23, and 34.5 mi. The results for a modest shelf slope are shown in Figure 13.7. For the 34.5-mi R_{max} storm, as X approaches $\pm\frac{1}{2}R_{max}$ the local peak SWL reduces by about 10% compared to the peak SWL at landfall. The peak fall-off with normalized distance is less for smaller size storms.

Resio et al reported that modification of the idealized E-W shoreline, with part of the shoreline offset southward, induced surge increases, (Figure 13.8). They suggested these increases (due to conveyance effects) would dominate over spacing influences. However, reduced sensitivity to track spacing with this or greater shoreline complexity, or major landscape features, was not specifically analyzed.

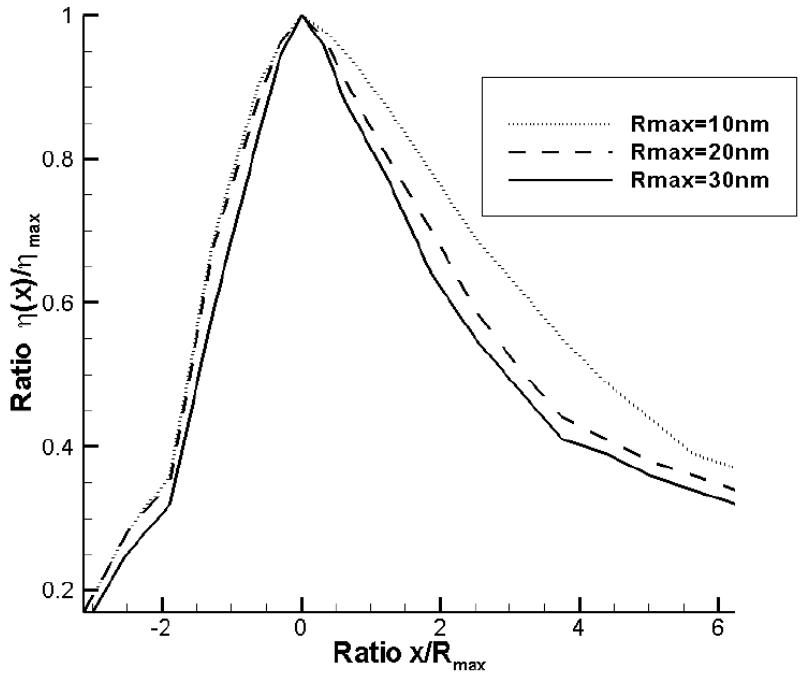

Figure 13.7. Peak SWL versus X

(local peak SWL normalized to landfall peak SWL; X normalized to R_{max})

Resio et al 2007

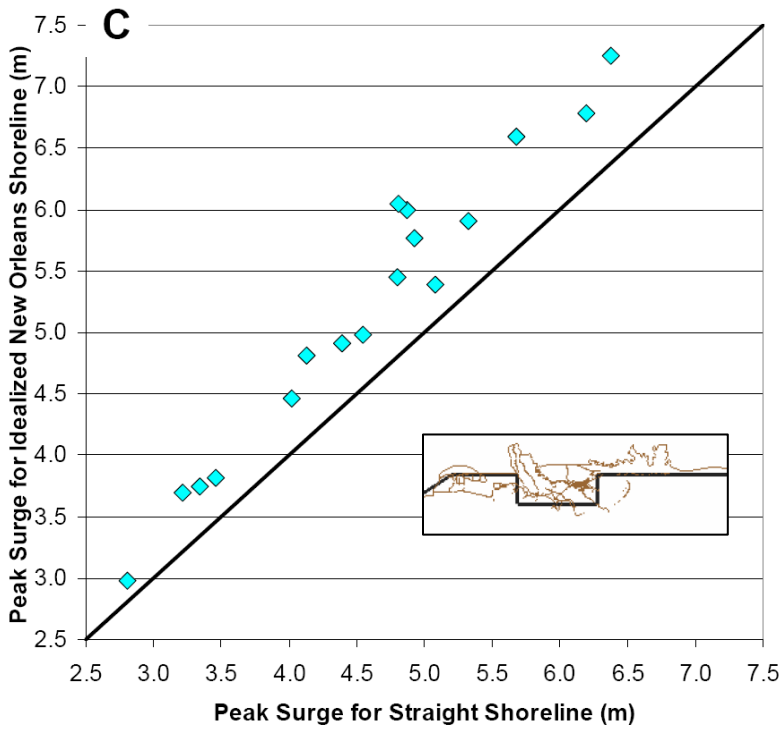

Figure 13.8. Peak SWLs for Modified versus Straight Shoreline

Resio et al 2007

13.5 Bias and Uncertainty in Surge JPA

In employing any methodology scientists typically take steps to identify and correct consistent errors and to define uncertainties. In developing an OS for a surge JPA these steps can include:

- Validation of the benchmark (wind hazard response, surge hazard response, or surge response) with available empirical analysis, such as using a surge return frequency analysis based on the tide records to validate a surge hazard benchmark; development and application of correction factors and uncertainty bands.
- For surge hazard response and surge response benchmarks, validation of the simplified surge model using a hindcast event, and development of associated correction factors and uncertainty bands. Including sufficient number of trials to assess influence of simplified surge model uncertainty on the selection of the OS.
- Assessing the influence of additional storm characteristics on the surge hazard response. Research discussed in Part I suggests it may also be important to account for other variables in hurricane climatology. Fitzpatrick et al (2010) showed that surge is highly correlated with the combined intensity, size, and wind field distribution—i.e., $IKE^{1/2} \cdot V_{max}$. Wind field profile (Holland B), asymmetry, and banding may also be influential.[2] In addition, the role of probabilities associated with certain intensification and decay factors may be important. The FISs to date have tended to regard these parameters as minor and suitable for inclusion in an uncertainty term. In the future, discretization of hurricane characteristics may need to address such parameters directly.
- Expanding trials to assess the influence of discretization of CPD, R_{max}, V_f, θ, and X on the residual error in the selected set's representation of the wind or surge hazard benchmark. Given potential uncertainties, the quality of the JPA results may benefit from enlarging the set to include additional storms that reflect hazards of interest.

An advantage of the JPM-OS is that it can be evaluated versus multiple benchmarks: ***p***, wind hazard, and surge hazard. As the wind model is less computationally demanding, the wind hazard benchmark can be based on a very large storm set.

The biases and uncertainties associated with the selection of an OS will necessarily contribute to biases and uncertainties in the final surge return frequency analysis, together with those associated with the high resolution surge model. Table 13.1 summarizes five major categories of stationary uncertainty, ε, associated with JPA and the use of an OS and how they can be assessed (see Resio et al 2007 and URS Corporation 2008). Importantly, some measured uncertainties encompass more than one ε term.

Research into the nature of uncertainties often distinguishes between uncertainties that are aleatory (inherent in nature and irreducible) versus epistemic (due to reducible limitations on observations and measurements). Distinctions are also often drawn between uncertainties having parametric (system) versus modeling origins (USACE 2009). Methods of quantifying uncertainties, such as model validation, may encompass more than one category.

[2] Irish conducted surge simulations for Texas hurricane landfalls and found that varying Holland B from 0.9 to 1.9 influenced surge SWL by only 15%; but this result may not be applicable to other regions.

Table 13.1. Quantification of Stationary Uncertainties in Surge JPA with OS

Uncertainty In	Distribution	Quantified By	Based On
1. $\varepsilon_{\boldsymbol{p}}$—the hurricane climatology as represented by a function of selected attributes—$\boldsymbol{p}$(CPD ,R_{max}, V_f, θ, X).	Non-Normal (e.g., Gumbel)	CPD return frequency distribution parameters (a_0 and a_1)	Historical data; (note potential discounting of the probability of extremely intense hurricanes, see Figure 3.10)
	Normal	σ_{Rmax}, σ_{Vf}, σ_{ϑ}, σ_X	Historical data.
2. $\varepsilon_{\boldsymbol{W}}$—the hurricane climatology due to attributes not selected—such as CPD-V_{max} variability, asymmetries, spiral banding, eye wall replacement, Holland B ($\varepsilon_{\boldsymbol{B}}$), IKE, etc.	Normal	$\sigma_{\boldsymbol{W}}$ (e.g., $\sigma_{\boldsymbol{B}}$ and $\sigma_{\boldsymbol{PBL}}$)	Validation against a detailed wind hazard benchmark that incorporates more degrees of freedom; or sensitivity tests.
3. ε_{OS}—the coarser discretization of the hurricane climatology relative to the benchmark, i.e. the selected increments in the JPM-OS (not applicable for Surge Response OS); the simplified benchmark; simplified surge response; an example is simplified set of storm tracks	Normal	σ_{OS}	Residual error between two hazard response surfaces; validation against regional tide gauge data or coastal sensitivity tests.
4. ε_{ψ}—the full, coupled high resolution wind/surge/wave-setup model due to imprecision in model physics, setup, geometry, mesh attributes, etc.	Normal	σ_{ψ}	Model validation.
5. ε_T—concurrent contribution of low amplitude tides. (Note this could also include uncertainties in pre-storm meteorological conditions affecting SWL.)	Normal	σ_T	Tide data.

Stationary uncertainty can be normally distributed—mathematically equivalent to a diffusion/spreading term. Such ε terms have an associated RMSE or standard deviation (σ). Multiple, independent ε terms described as normally distributed can be added to provide an overall error term, ε_Σ. When individual σ are in units of SWL the overall σ_Σ can be estimated by summing each individual σ^2 and taking the square root of the sum. Values for σ are not necessarily constant, but can vary with other parameters.

Stationary uncertainty terms can also be non-normally distributed—asymmetric and/or with distorted curves (e.g., fat or pinched tails). In addition to σ these distributions are described with coefficients for skewness, kurtosis, and other shape factors. A major example is uncertainty in the probability distribution for CPD—as CPD is considered the most significant contributor to surge among the hurricane characteristics.. The Louisiana and Mississippi FISs employed Gumbel and Weibull non-normal distributions for CPD. Standard statistical techniques are also available for estimating uncertainties in non-normal distributions (see GTN-1).

Both normal and non-normally distributed uncertainty can be used to construct confidence bands around the estimated the CDF. Furthermore, statistical approaches can be used to also evaluate the influence of combined non-normal and normal distributed uncertainty on the actual CDF (see Resio et al 2012). In addition to evaluating uncertainty, implementation of the JPM-OS approach requires that corrections be applied for any identified bias in the hurricane climatology and/or the high resolution wind/surge/wave-setup model. Non-stationary uncertainty—such as the influence of climate change on hurricane characteristics or RSLR on surge hydrodynamics—must be investigated with separate JPAs by modifying the climatology and wind/surge model (see Part V).

13.6 Preparation of Return Frequency Curves

The simulation of each of the *n* OS storms with the full, high resolution wind/hydrodynamic/wave-setup model produces time-series and peak SWL values at the regional LOIs—mesh nodes as well as intermediate locations with interpolated peak SWL values. Production runs are subject to a series of quality checks to ensure that runs complete successfully—with the specified model setup, parameters, and other input files; that the results over the course of the entire simulation are physically reasonable; and that results do not contain excessive spurious values (non-fatal instabilities that appreciably change the surge SWL peaks). A percentage of runs are usually reviewed in detail, such as by using zoomed animations of surge dynamics near critical coastal areas. Additional quality control procedures are described in FIS documentation (e.g., FEMA February 2007).

Following completion of production runs, the generation of LOI-specific CDF curves involve four steps:

1. CDF integration and smoothing;
2. CDF validation;
3. Adjustments to spatial variations in specific surge hazard levels; and
4. Construction of confidence limits.

STEP 1: CDF Integration and Smoothing

Figure 13.9 illustrates the relative frequencies of surge SWL peaks from a series of JPM-OS storms at a location (URS Corporation 2008). The results have been grouped into 2 cm SWL bins, which are plotted vertically against the joint probability for the storms in the bin. The relative frequency bars depict a very "jagged" distribution and include gaps at many SWL increments. The jaggedness is caused by storms with similar joint probability making landfall at varying X (i.e., at the various landfall spacing). Some minimal smoothing of the PDF can be done to avoid excessive irregularities in integrating the CDF. *However, the smoothing should not significantly distort the CDF and modify the median estimate of surge return frequencies*.

One smoothing approach is to replace each vertical bin bar distribution with a normal distribution—somewhat wider than the vertical bar but having the same area. This spreads out the discrete bin probability over a wider range of SWLs. The value for σ_{Smooth} can be based on some portion of the normally distributed uncertainty described in Section 13.5 above. This spreading of each bin bar in effect incorporates the corresponding portion of ε as an additional dimension of the integrand in the CDF formula (as indicated by Resio et al 2007 and URS Corporation 2008). Figure 13.9 illustrates a smoothed PDF resulting from the use of ε and Figure 13.10 shows the derived CDF.

However, as σ_{Smooth} increases, the PDF and CDF are increasingly modified. Resio et al 2007 (and Resio et al 2012) suggested that this CDF modification could be employed as one way to asses the impact of uncertainty on the 100-yr SWLs—as 100- to 500-yr SWLs were shown to increase notably when σ_{Smooth} was based on both epistemic and aleatory uncertainty. This approach to assessing uncertainty is problematic compared with a traditional approach of computing an undistorted, median, CDF with confidence intervals. In the case of a JPM in which a set of storms is carefully selected, significantly modifying the bin distributions would not seem to support developing a median estimate of the CDF.

Another smoothing approach is to refine the PDF increments. If the Surge Response-OS approach is used the $\boldsymbol{\Psi}$ increments can be refined in the respective dimensions (CPD, R_{max}, V_f, θ, and X) to aid smoothing prior to integration. This is akin to refining the representation in Figure 13.1.c) into the representation in Figure 13.1.a). The intermediate values in surge response are determined through piece-wise interpolations appropriate to each dimension (CPD, R_{max}, V_f, θ, and X). The interpolations in each dimension can use linear or nonlinear fitting techniques—e.g., if a Gumbel distribution is used to characterize the probability of CPD then this function can be used to aid in refining this dimension. Figure 13.11 illustrates the refinement of surge hazard response.

The spreading and refining smoothing techniques can also be used together.

Another technique for developing a smooth CDF would be to employ the results to define values for μ, σ, and coefficients of skewness, kurtosis, etc. These, in turn, would be used to define a surge return frequency curve according to a standard function commonly used in return frequency analysis, such as the Log-Pearson Type III, GEV (e.g., Gumbel, Weibull), etc (see GTN-1).

Comparing the results of different approaches to smoothing and numerical integration can provide a measure of the imprecision associated with this step, which may be crucial for particular surge hazard levels of interest, e.g., 100- and 500-yr SWLs. Importantly, the CDF integration technique itself can be considered to introduce an additional sixth uncertainty, ε_I , beyond the five noted in Table 13.1.

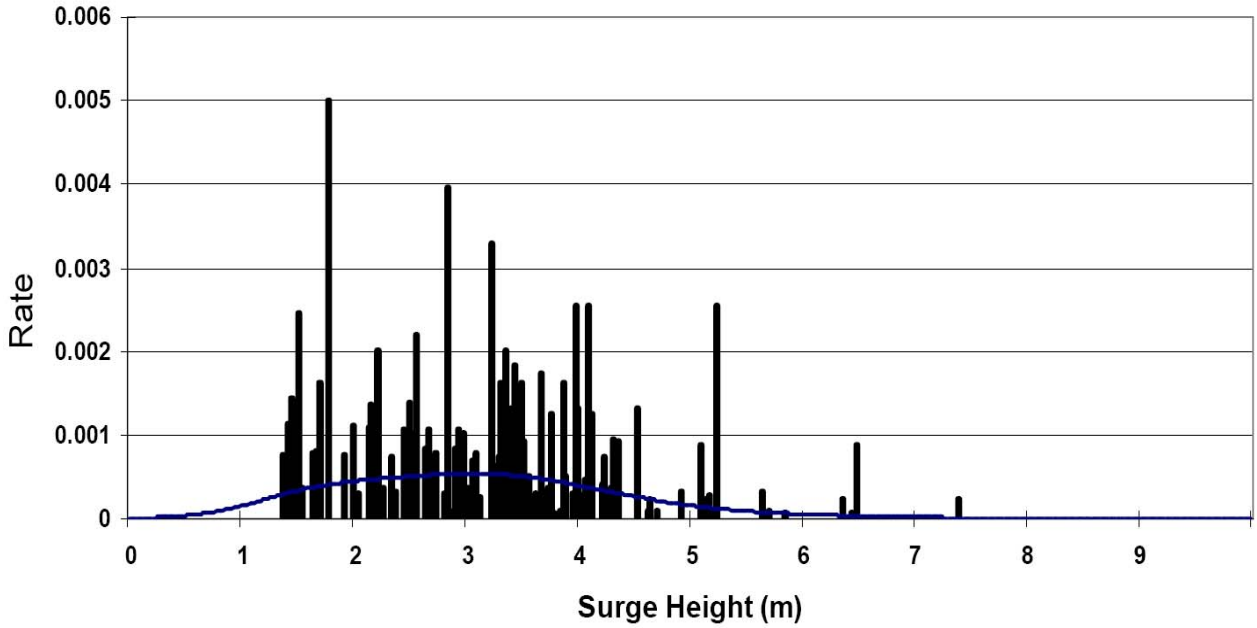

Figure 13.9. Histogram of Relative Frequencies for Peak Surge and Smoothed PDF

black histogram bars = raw SWL values, blue curve = smoothed PDF with uncertainty dampening
URS Corporation 2008

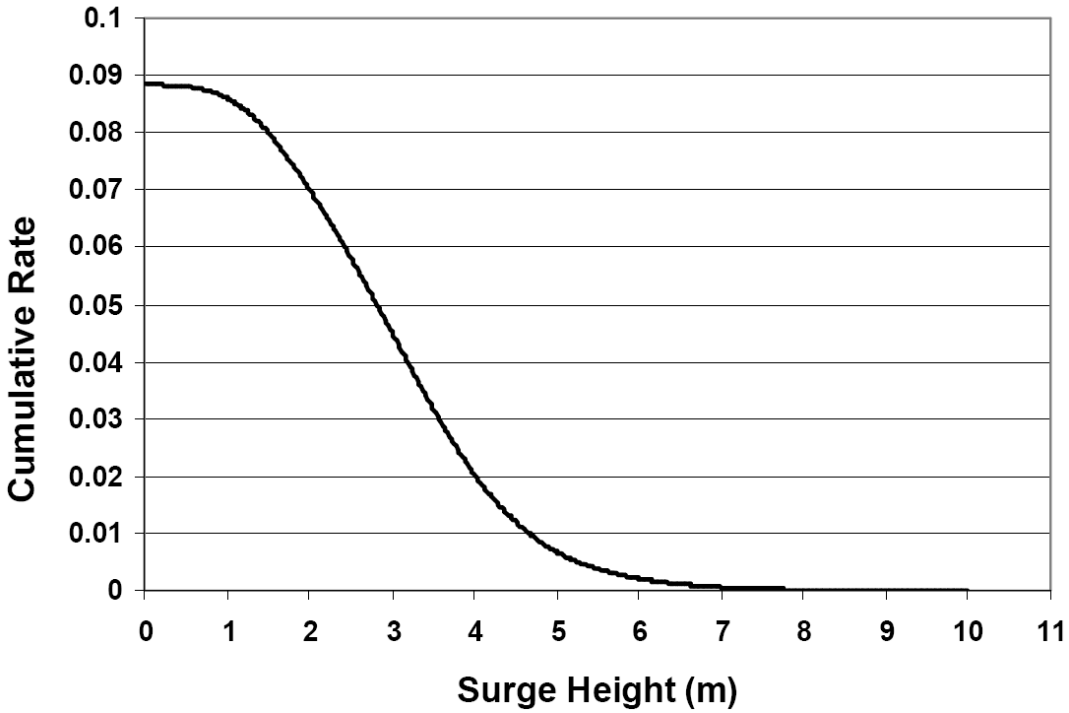

Figure 13.10. Smoothed Surge (Peak SWL) CDF

URS Corporation 2008

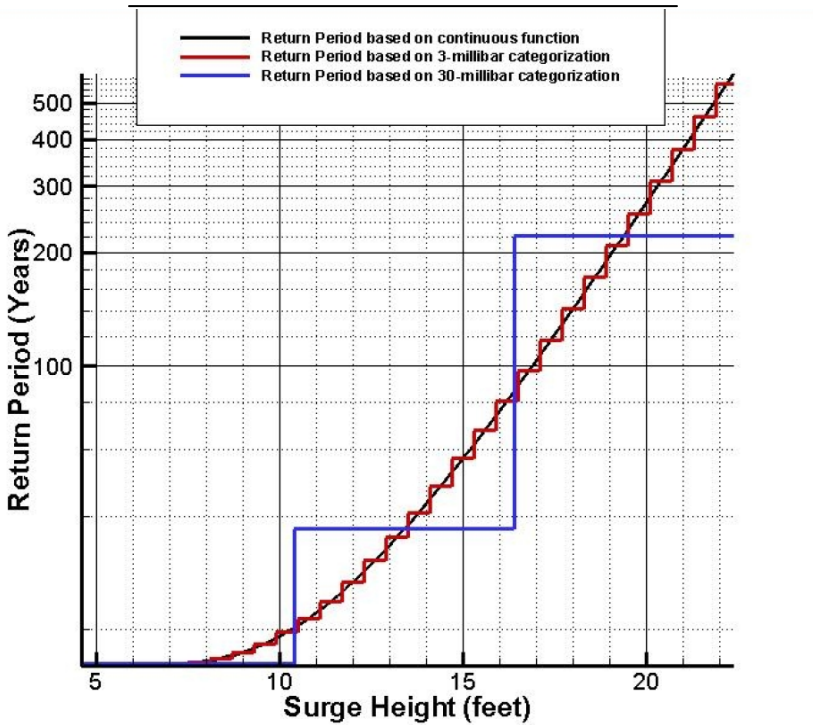

Figure 13.11. Refinement and Interpolation of Surge Hazard Response

Resio et al 2007

STEP 2: CDF Validation

As with any flood return frequency stochastic analysis (see GTN-1), an important post-processing step is comparing the surge hazard CDFs produced in the stochastic analysis against available CDFs derived from gauge return frequency analyses. Comparisons at key locations are used to evaluate residual bias and normally and non-normally distributed uncertainties.

Scientists undertake rigorous investigations of potential bias using

- comparisons of the surge JPA CDF to tide gauge analysis CDF;
- the validation results for the wind/surge/wave-setup model;
- the results of any validations of the OS set; and
- lessons on bias from other studies,

If residual bias is suspected the simulation results for each of the *n* storms must be carefully re-examined, together with the setup and parameterization of models and the selection of the JPM-OS set. If appreciable bias is identified, the source of bias must either be eliminated or appropriate correction factor devised and applied to the surge hazard CDF.

With bias removed or corrected, the magnitude and trends of overall uncertainty can be assessed—e.g., by determining RMSE or σ between the JPA and tide gauge CDFs. The uncertainty may be SWL dependent. If appropriate the smoothing and numerical integration can be revised by incorporating the additional uncertainty. A revision of CDFs to account for bias and uncertainty amounts to a calibration of the JPA CDFs. If JPA CDFs are revised then the estimate of residual uncertainty versus tide gauge CDFs are also updated.

STEP 3. Adjustments to Spatial Variations in Specific Surge Hazard Levels

Following CDF validation the geographic distribution of surge SWL at any return period of interest (e.g., the 100-yr surge SWL) can be depicted as in Figure 13.12. The surge SWL can be overlaid on a variety of regional maps (e.g., topography, land cover, etc.) and aerial imagery and evaluated. The geographic SWL surface is typically examined for irregularities, such as:

a. Lateral misalignments due to resolution limitations in the surge SWL model (e.g., SWL surface incorrectly shown crossing a major topographic crest higher than the SWL); and

b. Sharp gradients not consistent with local topography or land cover.

Identified surge hazard irregularities can be corrected and sharp lateral gradients can be smoothed. These spatial adjustments would, in turn, modify the local CDFs. In theory, rigorous quality control reviews of the individual OS simulations should uncover major problems with surge spatial results prior to this step.

STEP 4: Construction of Confidence Limits

Final residual uncertainty in the JPA CDFs can be evaluated in several ways:

- Assessing the effect of the quantified sources of uncertainty (from Step 2) on the resulting CDF. The linear uncertainty, ε_Σ, can simply be added to (subtracted from) the CDF.
- Comparing CDFs derived with different smoothing/integration techniques.
- Computing a standard curve (e.g., Gumbel distribution) and associated uncertainty bands directly from the stochastic analysis results.
- Comparing JPA and tide gauge CDFs.

These techniques can be employed to construct UCL/LCL bands around a CDF. Bands can be calculated to encompass a range of uncertainty—such as 68.2%, 90%, 95%, 95.4%, 99.6% etc. (equivalent to ± 1σ, 45%, 47.5%, 2σ, 3σ).

As discussed in the Introduction and GTN-1 Section N, FISs are typically based on the median estimated CDF and do not typically employ a CDF with some adjustment for uncertainty or at some confidence limit. The 100-yr flood elevations shown on FEMA maps are not required to reflect allowances for uncertainty. However, the use of confidence limits is more common in other planning and design studies for flood risk management—e.g., the design of flood protection structures. An example of a JPA CDF with confidence limits is shown in Figure 13.13.

Asymmetric uncertainties (associated with skewness, kurtosis, etc.) in the hurricane landfall intensity return frequency (see Figure 3.10) are an important source of asymmetric uncertainty for SWL at higher return periods (e.g., 500-yr). Figure 12.3 illustrates the greater widening of the UCL band relative to the LCL band for Grand Isle LA return frequency at longer return periods. For the 500-yr return period SWL of 11.2 ft, Figure 13.13 shows 95% LCL/UCLs of 8.7 and 14.1 ft. (bands of 2.5 and 2.9 ft, respectively)

In addition to evaluating confidence limits, the quality of a JPA can also be gauged by comparing results in an area common to two adjacent, overlapping, studies, provided they employ reasonably similar rigorous methodologies.

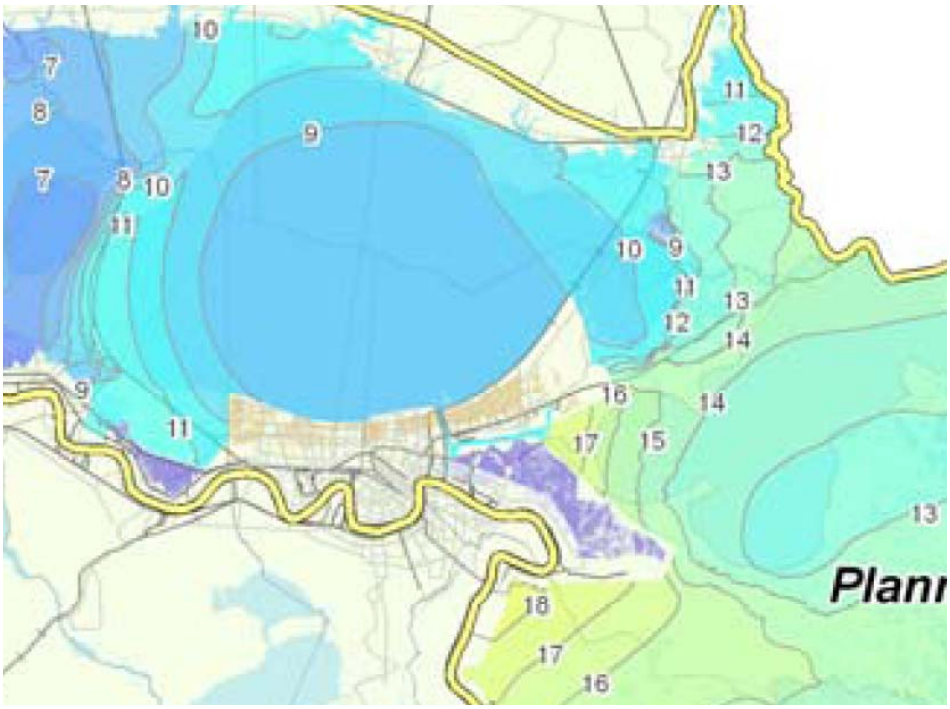

Figure 13.12. Example of Overlay of 100-yr Surge (LACPR Study)
USACE 2009

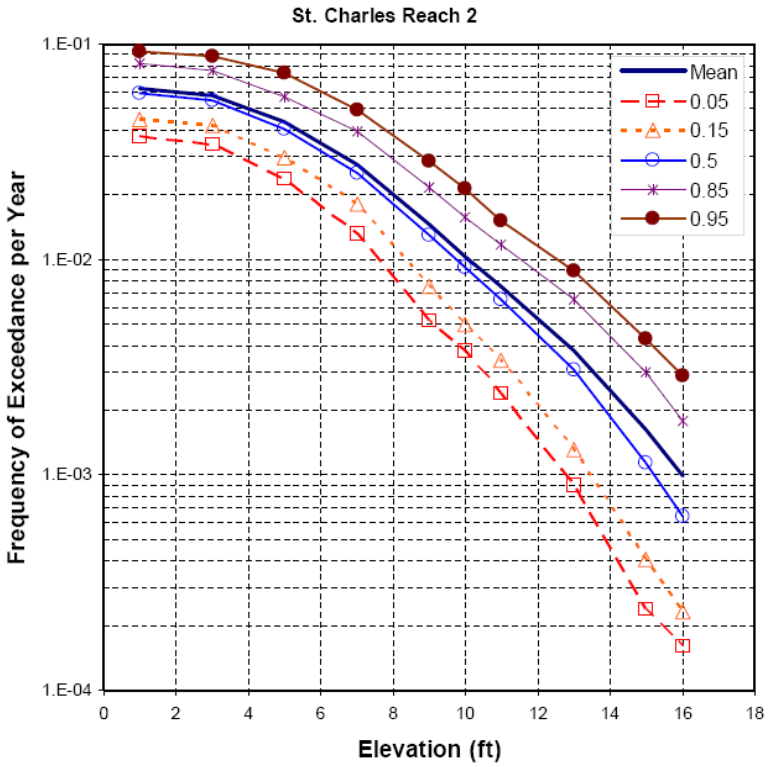

Figure 13.13. Example of Surge CDF with Confidence Limits
(Epistemic Uncertainty Only)
IPET 2009

13.7 Wave Hazard

In overland flood risk applications the wave hazard is considered in terms of the wave height added to the SWL at a particular SWL hazard level, e.g., the 100-year SWL plus associated waves.[3] Currently, wave hazards for most coastal floodplain LOIs are computed under the NFIP, which addresses 1% wave heights using the simple 1D WHAFIS model (see Section 9). This model employs a $H_{1\%}$ depth limitation of 0.78*Depth, and basic assumptions regarding wind speed and direction, boundary conditions, and wave transformation and dampening from friction. If the 100-year SWL can be associated with multiple storm tracks, multiple WHAFIS simulations can be performed to capture wave hazard variations due to differences in wind direction and speed. In this case it would be common practice to employ the "worst-case" wave characteristics—$H_{1\%}$ and T_p— from the multiple simulations.

2D wave models (e.g., STWAVE and SWAN) can also be used to assess H_s, $H_{1\%}$, and other criteria associated with a specific SWL. However, similar assumptions must still be applied. These models can improve the estimation of wave characteristics compared to the 1D WHAFIS model where 2D wave transformations (e.g., refraction and diffraction) are important.

For locales with complicated shorelines or terrain the characteristics of waves during inundation at a particular SWL may be a function of more complex, non-linear, wave physics. In this case Boussinesq models may be employed to assess appropriate values for H_s and T_p (see Section 9).

Important interior water bodies which are enclosed or semi-enclosed—such as long reaches of rivers and canals—but contain significant fetch, may require special analysis to assess the locally generated waves at the SWL of interest. Methods for analyzing these wave conditions include input of assumed wind direction and velocity, fetch, water depth, and duration. By ignoring duration, an estimate can be made of "fully developed" wave fields. Standard methods of analysis, such as developed by Brettschneider, are described in the USACE Coastal Engineering Manual, Part II-2-2 (USACE 2005).

At a specified SWL, depth limitations can cap wave heights where other conditions (boundary, wind speed, fetch, etc.) might otherwise indicate the potential for higher waves. As noted in Section 6 the relationship of H_s to depth is highly variable, with ratios of 0.4 to 0.7 commonly employed.

As discussed in Section 5, coastal scientists and engineers employ the Rayleigh distribution to describe height variability in a wave field. Several relationships dictated by this distribution are:

$H_{avg} = 0.625H_s \approx 5/8\ H_s$;

$H_P = .705H_s\ (-\ln P)^{1/2}$, where P is the Percentile;

$H_{50\%} = 0.59H_s$;

$H_{1\%} = 1.52H_s$; and

$H_{0.1\%} = 1.9H_s$

However, the peak SWL during an extreme surge event typically has a limited duration (e.g., 4 hours or less). Thus, the number of waves occurring during the peak SWL is also limited. For example, during Hurricane Katrina approximately 2,000 waves (with T_p of 7 s , Smith 2007) would have been associated with peak SWL off the south shore of Lake Pontchartrain. For this brief event the Rayleigh distribution may not be representative for ratios of H_s to the top 20 and two wave heights. With a short duration the ratios are likely to be lower.

[3] In offshore applications for vessels and marine structures wave hazards are analyzed apart from SWL variations.

Section 14. Recent Applications of Surge JPA

JPAs of hurricane surge were first undertaken in the 1970s (see Ho and Myers 1975). By the late 1980s researchers on Atlantic Basin and GoM hurricane climatology had provided probabilistic estimates for CP, R_{max}, V_f, and θ, (NOAA-NWS 1987), facilitating wider application of JPM to hurricane surge in combination with the FEMA Surge Model. In 1989 Suhayda completed a surge JPA for Cameron Parish LA using NOAA's latest regional hurricane climatology information, a 685-storm JPM, and the FEMA Surge Model. Interestingly, no surge JPAs were applied to the New Orleans LA region prior to Hurricane Katrina.

In the aftermath of the 2005 hurricane season, JPA with OS has been applied for FISs in Louisiana (in two regions, southeast and southwest) and Mississippi, and is being used in seven ongoing FISs for Texas, North Carolina, South Carolina, Florida—Big Bend, Northeast Florida/Georgia, Northwest Florida/Alabama, and Central Florida—Atlantic. This section describes the application of JPA with OS employed in these and other studies based on available documentation, including OS development, the treatment of bias and uncertainties, and the four post-processing steps.

14.1. Southeast Louisiana FIS

The southeast Louisiana FIS JPA and OS development and post-processing steps are primarily documented in Resio et al 2007.[1] Some supplementary documentation is provided in reports for the four coordinated projects undertaken by the USACE in 2006-09: the FIS (USACE 2008), the HSDRRS design (USACE 2010), the IPET Risk and Reliability Analysis (IPET 2009), and the LaCPR Study of future coastal protection and restoration alternatives (USACE 2009). This section reviews the USACE approach used in the FIS exterior surge SWL and wave hazard analysis—i.e., surge hazards outside the HSDRRS. The subsequent section describes a modified approach used in the IPET Study. The USACE and IPET analyses of wave hazards as modified by the foreshore of HSDRRS structures, HSDRRS overtopping and breaching hazards, and polder inundation hazards, are discussed in Part IV.

OS Development

In their surge JPA for the 151-mile (2½°) segment south of New Orleans Resio et al utilized a Surge Response-OS, as opposed to JPM-OS, (see Section 13). The team conducted numerical experiments of hurricane landfall conditions along an idealized coast line to determine benchmark smooth, SWL response functions for CP, R_{max}, V_f, and θ. The team deferred consideration of the Holland B attribute to the uncertainty term (see below). Full documentation of the simplified surge model and the numerical experiments was not included in the various reports. The authors illustrated an example of a SWL response to CP-R_{max} (see Figure 14.1).

The Resio team discretized the surge response function into 15 CP-R_{max} combinations: three GoM CPs—960, 930, and 900 mb—with six, three, and six R_{max}, variations for each of these three respective CPs. Twelve of the 15 CPD-R_{max} combinations employed one V_f. Two V_f variations were provided for the 20.4 mi storms at 960 and 900 mb, while three were provided at 930 mb. Table 14.1 summarizes the 19 CP-R_{max}-V_f combinations, as well as the 30 CP-R_{max}-V_f-θ combinations, used in the southeast Louisiana study. Resio et al employed a GoM Holland B parameter value of 1.27 for all storms, based on the mean GoM value.

[1] Additional detail is provided in the two part publication: Resio et al 2009 and Irish et al 2009.

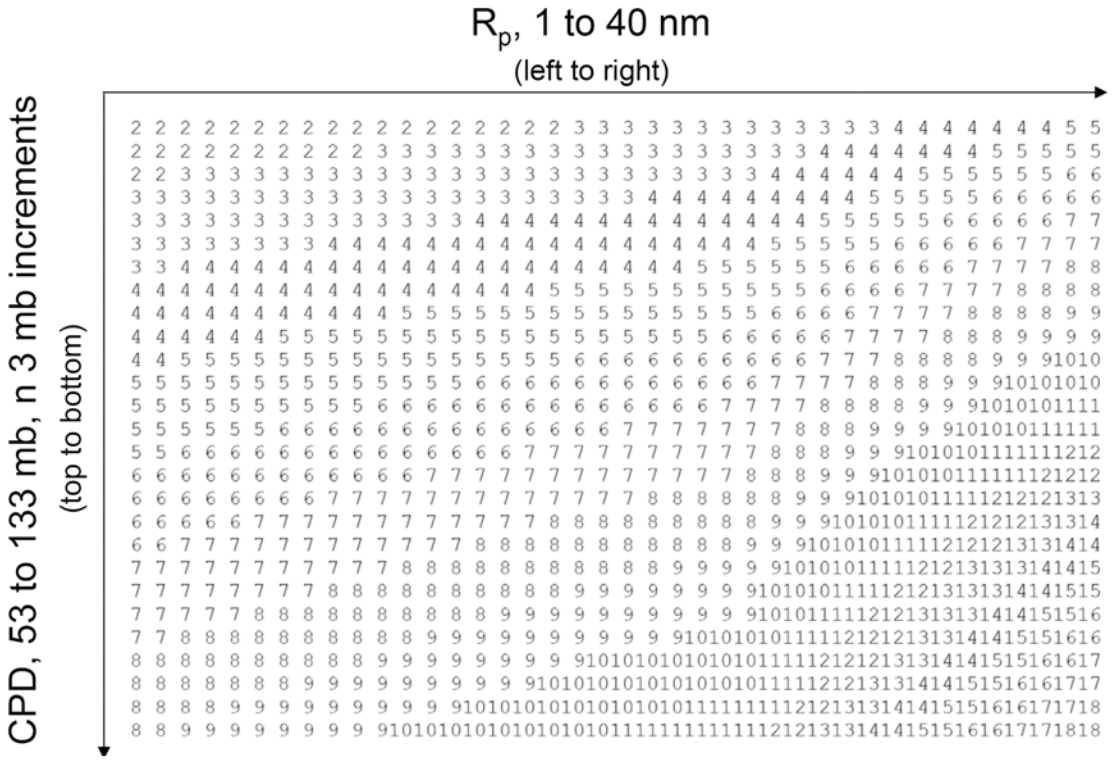

Figure 14.1. Example SWL Response to CPD-R_{max}
Resio et al 2007

To discretize the surge response surface over the study area Resio et al selected five primary landfall locations for the central tracks and four each for the southeast and southwest tracks—with landfall spacing at about 1° longitude, or 30 mi. Intermediate (secondary) landfalls spaced at 15 mi were also used. This arrangement assigned half the storm landfalls within a 1° segment south of New Orleans.

Of the 30 CPD-R_{max}-V_f-θ variations, 24 were employed with primary tracks—12 central, 6 southeast, and 6 southwest, for a total of 108 storms. Thirteen variations were employed with secondary tracks—5 central, 4 southeast, and 4 southwest, for at total of 44 storms. The total combination of attribute variations and tracks provided for 152 storms. The combinations of θ and primary landfall locations are illustrated in Figure 14.2.

Table 14.1 shows that all 152 storms in the Surge Response OS were GMHs, with 50 at Category 3 (960 mb CP, 60 mb CPD), 52 at Category 4 (930 mb CP, 90 mb CPD), and 50 at Category 5 (900 mb CP, 120 mb CPD). Hurricane Katrina's maximum GoM CPD was 118 mb. Of the 50 Category 5 storms, 32 are quite large, with R_{max} above 20 miles. Nine of these large, intense hurricanes are slow moving, with V_f of 6.9 mph. These nine 900 mb CP storms at V_f of 6.9 mph actually have vortex model V_{max} at Category 4.

Resio et al coupled the OS with a vortex model to generate a hurricane wind field. Model winds are provided as 30-minute average winds (in m/s), which can be readily converted to 1-minute winds (in mph). Attachment 1 lists the 152 hurricanes and their GoM and landfall attributes, including the peak GoM and landfall V_{max}, and peak GoM and landfall SSS category (which are assigned on the basis of the 1-minute V_{max}) (USACE 2011). Figure 14.3 illustrates the track of Hurricane No. 26. Figures 14.4 and 14.5 illustrate the GoM winds and at landfall wind field for Hurricane No. 26.

Table 14.1. Southeast Louisiana OS

GoM CP mb	GoM R_{max} miles	Landfall V_f mph	θ direction from	Track Set (Number)
960	40.9	12.7	Central	P (5)
	28.3	12.7	SE	P (4)
			SW	P (4)
	24.2	12.7	Central	P (5)
	20.9	12.7	SE	P (4)
			SW	P (4)
	20.4	12.7	Central	S (4)
			SE	S (3)
			SW	S (3)
		6.9	Central	P (5)
				S (4)
	12.7	12.7	Central	P (5)
930	29.7	12.7	Central	P (5)
	20.4	19.6	Central	P (5)
				S (4)
			SE	P (4)
				S (3)
			SW	P (4)
				S (3)
		12.7	Central	P (5)
		6.9	SE	P (4)
				S (3)
			SW	P (4)
				S (3)
	9.2	12.7	Central	P (5)
900	25.1	12.7	Central	P (5)
	21.2	12.7	SE	P (4)
			SW	P (4)
	20.4	12.7	Central	S (4)
			SE	S (3)
			SW	S (3)
		6.9	Central	P (5)
				S (4)
	17.1	12.7	Central	P (5)
	14.4	12.7	SE	P (4)
			SW	P (4)
	6.9	12.7	Central	P (5)
3 CP	**15 CP-R_{max}**	**19 CP-R_{max}-V_f**	**30 CPD-R_{max}-V_f-θ**	**152 Storms**

Resio et al 2007

P-Primary Track Set; S-Secondary Track Set (Landfall located between Primary Tracks)

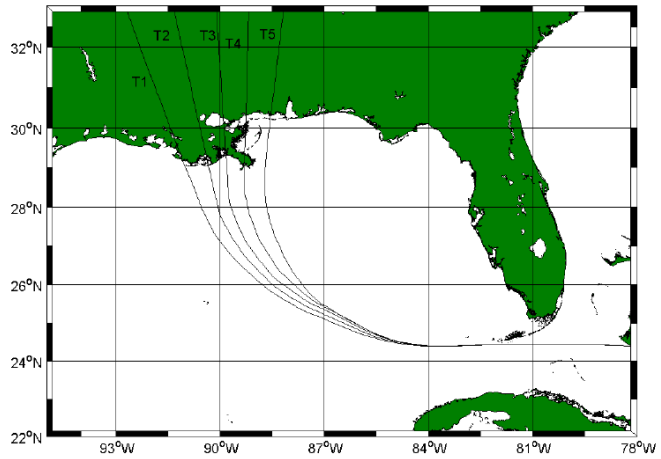

Five Primary Central Tracks (Four Secondary Tracks not shown)

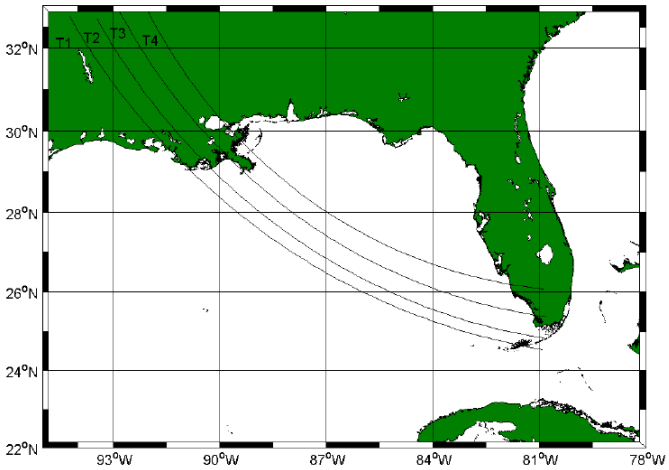

Four Primary Southeast Tracks (Three Secondary Tracks not shown; some origins shifted)

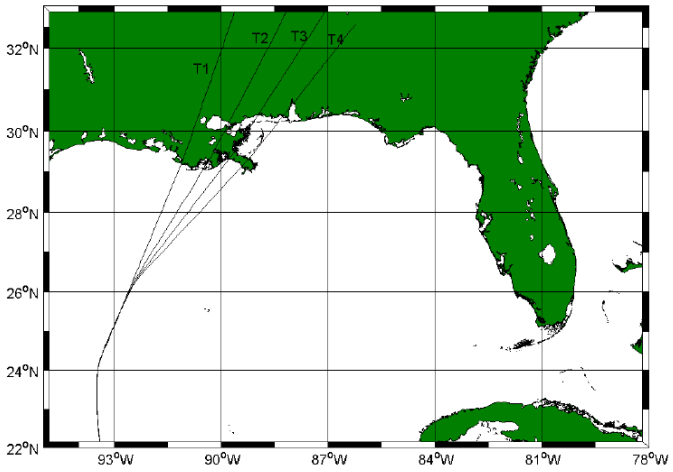

Four Primary Southwest Tracks (Three Secondary Tracks not shown)

Figure 14.2. Hurricane Tracks for Southeast Louisiana JPM-OS

Resio et al 2007

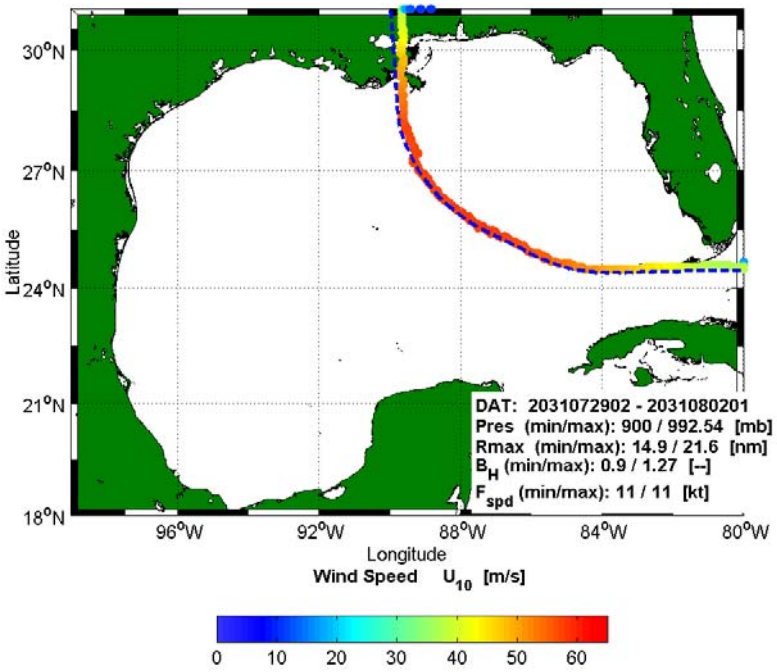

Figure 14.3. Synthetic Hurricane No. 26 Track and V_{max} (30-min winds in m/s)

USACE 2011

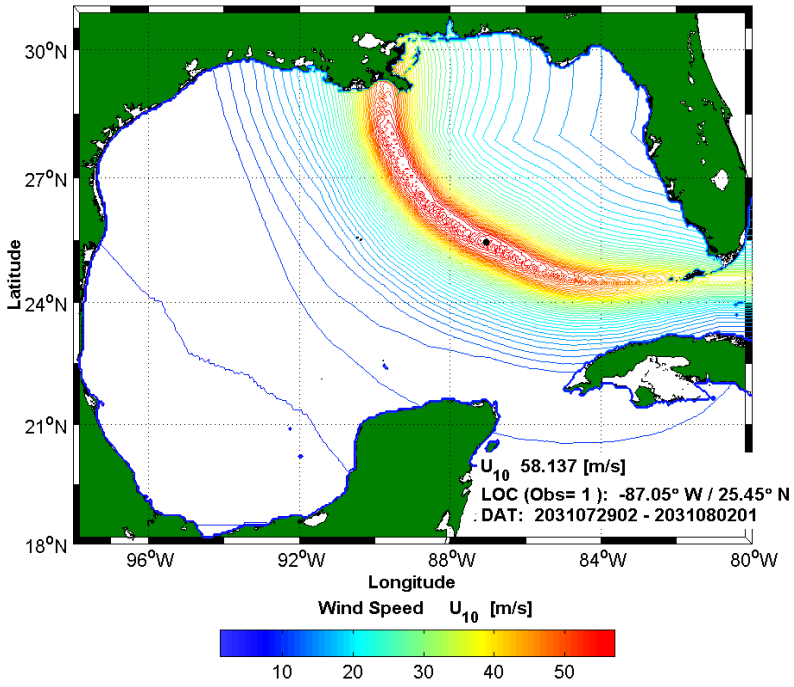

Figure 14.4. Synthetic Hurricane No. 26 Wind Field Along Track

USACE 2011

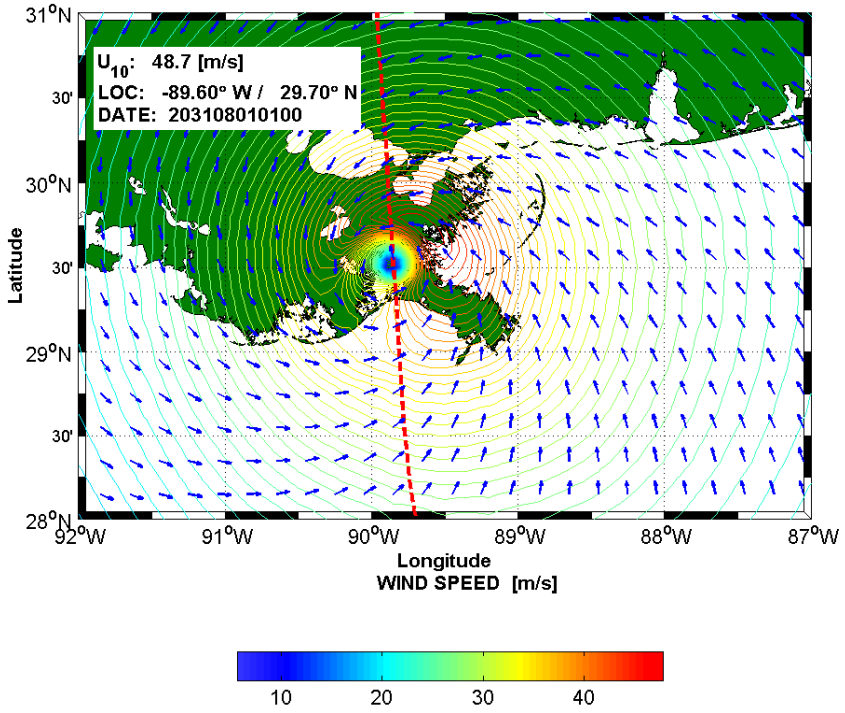

Figure 14.5. Synthetic Hurricane No. 26 Landfall Wind Field

USACE 2011

The vortex model incorporated a linear decay prior to landfall for CP, R_{max} and Holland B. Individual hurricanes decayed by somewhat different amounts according to track and forward speed and thus landfall conditions are more variable than GoM peak conditions. No storm made landfall at Category 5.

Given the set is a Surge Response-OS and not a JPM-OS, Resio et al did not assign joint probabilities to the individual 152 storms.[2] In designing the OS to be representative of a simplistic landfall surge response the authors did not consider special regional surge response characteristics.

Bias and Uncertainty

The reports describe the treatment of the five JPA uncertainties listed in Table 13.1 as follows.

1. ε_P—uncertainty regarding hurricane climatology (joint probability) for selected attributes:
   - Research on GMH CPD, R_{max}, V_f, θ (see Part I, Sections 1 and 3) was utilized to establish the joint probability expression. The ***p***(CPD) is combined with the overall reach hurricane return frequency as a Gumbel distribution with the parameters (a_0 and a_1) varying for 1° longitude increments. Resio et al illustrated the general regional varying values for a_0 and a_1 but did not explicitly provide values for individual increments or the (aleatory) uncertainty bands.

[2] The authors did state that the total of 152 storms GMHs would conservatively represent a record of 853 years, at an average GMH/L-151 return period of 5.6 years. They note this return period is less than taking the GMH/L-60 return period of 16 years and estimating an equivalent GMH/L-151 return period of 16/2.5 or 6.4 years.

- Resio et al did not explicitly provide values for σ_{Rmax} and σ_{Vf}. Resio et al suggested dependency of σ_{Rmax} (epistemic uncertainty) on CPD.

2. ε_W—wind field uncertainties not encompassed in the joint probability:
   - The variability in the CPD-V_{max} relationship (as illustrated by Hurricane Katrina, which made landfall at a borderline Category 4/5 CPD but with strong Category 3 winds), was not explicitly discussed.
   - The team addressed epistemic uncertainty in the Holland B—ε_B—which was estimated to have a linear response in surge, with σ_B equal to about 0.1 to 0.2 * SWL.
   - Other uncertainties contributing to ε_W (e.g., asymmetry, IKE, spiral banding, eye wall replacement,) were addressed to some degree with the PBL representation of hindcast winds (see below).
3. ε_{OS}—epistemic uncertainty associated with the surge response benchmark and the OS:
   - Resio et al selected the OS strictly to represent the surge response—as opposed to a surge hazard or wind hazard response. Simplifications associated with an idealized coastline model, which neglects the influence of complex coastal features (see Section 13.3)—such as the blocking of westward driven surge by the Mississippi River Delta and localized wind setup over large coastal bays, sounds, and lakes—were not addressed with respect to selection of the OS set CPD, R_{max}, and V_f values.. The team did not quantify potential errors/uncertainties associated with limited representation of surge response.
   - The general error of a 1° landfall spacing scheme based on an idealized coastal model was noted as being up to 20%, 9%, and 4% for storms with R_{max}.of 11.5, 23, and 34.5 mi, respectively. However, the potential spatial error associated with the proposed OS—accounting for the distribution of the 30 CPD-R_{max}-V_f-θ combinations and secondary landfalls—was not addressed. For example, with the 152-storm OS some locations along the coast may have a disproportionate share of smaller R_{max} landfalls, and might be subject to greater error. Furthermore, the team's limited investigation of coastal feature influence on spacing did not account for important local conveyance and wind setup effects (see Section 13.4).
   - Resio et al suggested an σ_ϑ based on the influence of track variability on wave setup, with σ_ϑ equivalent to 20% of the wave setup contribution to SWL, or about 0.02 to 0.06 * SWL.
4. ε_ψ—epistemic uncertainty associated with the high resolution surge model:
   - Resio et al defined the portion of σ_ψ associated with ADCIRC-STWAVE as 1.75 to 2.5 ft. This σ_ψ appears to be consistent with the Hurricane Katrina hindcast validation.
   - Resio et al discussed additional relative error associated with the PBL model in contributing to hindcast errors. They suggested that the combined PBL and ADCIRC-STWAVE model σ_ψ was on the order of 2.0 to 3.5 ft.—which equates to a 90% confidence band width of ±3.3 to 5.8 ft.
5. ε_T—epistemic uncertainty associated with tides:
   - The suggested value for σ_T is 0.66 ft (IPET 2009).

The values for $(\sigma_\vartheta^2 + \sigma_B^2)^{0.5}$ and $(\sigma_\psi^2 + \sigma_T^2)^{0.5}$ are therefore about 0.1 to 0.2 * SWL and 2.1 to 3.6 ft, respectively. For a SWL of 10 ft, the overall combined epistemic uncertainty σ_e is $(\sigma_\vartheta^2 + \sigma_B^2 + \sigma_\psi^2 + \sigma_T^2 +)^{0.5}$ and equates to about 2.3 to 4.1 ft—or 90% confidence band widths of ±3.8 to 6.8 ft.

Production and Post-Processing

The production runs included simulation of the 152-storm Surge Response OS with the following:

- Wind and atmospheric pressure forcing conditions throughout the model domain for all 152 storms using the PBL vortex model.
- The ADCIRC-STWAVE model validated for Hurricanes Katrina and Rita, (see Section 11 for a full discussion of the model limitations). The FIS production model included modified acceleration terms, the implicit/explicit numerical method, a constant eddy viscosity value of 50 m^2/s, a time step of 1 s, and node Manning's *n* and wind sheltering coefficients assigned based on land cover data and associated values from technical literature.
- Two modified versions of the 2005 mesh validated for Hurricane Katrina.
  - The current FIS documentation describes a 2007 mesh reflecting post-Katrina improvements to the HSDRRS—e.g., outfall canal gates (vSL15v3_2007_r09). However, the 2007 mesh did not include the most recent HSDRRS improvements, such as further height enhancements and construction of the IHNC and Seabrook Surge Barriers.
  - The project team also developed a 2010 mesh depicting further authorized HSDRRS improvements—including height enhancements and the IHNC Surge Barrier (but **not** the Seabrook Barrier), (USACE 2009 and USACE 2010). Limited documentation for the 2010 mesh runs is provided but the team presumably used the same FIS setup and parameters and implemented similar quality control.

  Minor adjustments to both meshes were also performed for individual storms to mitigate instabilities.
- Omission of tidal boundaries and forcing and instead including tides as a linear uncertainty term (see Section 13).
- A combined LMSL and LMMSL adjustments of 1.1 ft NAVD88-2004.65.
- Boundary inflows for the Mississippi and Atchafalaya Rivers, adjusted for surge wave outflow (with inflows presumably at 195,000 and 58,000 cfs as per the tidal validation); and
- WAM and STWAVE (three of four grids in half plane mode and all without friction, per the Hurricane Katrina hindcast) to compute open ocean and nearshore wave conditions and wave radiation stress gradients. STWAVE was loosely coupled with ADCIRC and radiation stress gradients were updated in the ADCIRC model at 30-minute intervals.

Post-processing quality control steps were discussed in the FIS documentation (USACE 2008). The team used a filtering algorithm to identify and smooth non-fatal instabilities in areas of steep terrain gradients. The team animated 25% of the simulations to facilitate additional checks for unphysical results. The FIS documentation does not itemize individual mesh modifications and the magnitude of non-fatal instabilities.[3]

Resio et al (2007) utilized both the refinement and σ smoothing steps in integrating the CDF at each output location (described in Section 13.6). CDF results of the JPA and Surge Response-OS using the 2007 case ADCIRC mesh were provided by Dr. Jay Ratcliff (USACE 2012). According to Resio et al (2007) the combined epistemic σ_e term (equal to about 2.1 ft plus 0.15 *SWL) was employed to modify the CDF. Resio et al (2007) showed that incorporating ε_e in the CDF integration shifted up the 100- and 500-yr SWLs estimates up. For one location, including ε_e increased the estimated 100-yr SWL of 14.8 ft, by 0.4 ft, and the 500-yr SWL by 1.1 ft. Resio et al (2012) subsequently discussed the effect of also incorporating aleatory ε into the integration—indicating that the total ε would raise the 100-yr SWL by more than 1.5 ft.

The FIS project team did not provide a validation of 2007 JPA versus tide gauge CDFs. Figure 14.6 presents a comparison of NOAA's observed return period SWLs and GEV curve for the Grand Isle tide gauge (see Figure 13.3) versus the 2007 JPA CDF results for several nearby locations. The two sources of return period analysis overlap between 50 and 200 years. The tide gauge is located behind Grand Isle close to Barataria Pass. The JPA results indicate Point 62 is most influenced by the combination of frontal dune sheltering and Barataria Pass. The 100-yr SWL results for Point 62 was 7.8 ft versus 7.1 ft for the gauge CDF. This slight relative over-prediction could be a result of under-prediction of the 100-yr SWL by the GEV curve (the highest return period surge actually matches closely with JPA result).

Figure 14.7 depicts the FIS JPA CDFs around the east-bank HSDRRS for the post-Katrina 2007 case. As noted above, these CDFs have not been corrected for bias (under-prediction) from the Hurricane Katrina hindcast validation for the ADCIRC-STWAVE model. The CDFs are subject to the Resio et al treatment of uncertainty described above. Any errors and uncertainties in the CDFs in Figure 14.7 are likely to be greater at more extreme return periods.

The USACE collected gauge data for Lake Pontchartrain at Frenier and West End beginning in 1931, with observations extending to May 2005 for Frenier and the present for West End. Both sets of observations have significant gaps—September 1965 to January 1969 for Frenier and November 1946 to March 1949 for West End. To date, there has been no published annual series of SWL maximums (in a common vertical datum) for the two gauges. Such a series would require addressing data gaps based on other evidence. Development of annual maximum series for these two gauges could assist in validating the surge CDFs for the south shore of Lake Pontchartrain.

In response to queries from independent technical review (USACE 2007) the project team did employ some available (but very limited) surge data to evaluate the JPA CDFs at four locations—south shore Lake Pontchartrain, IHNC, MRGO near Bayou Bienvenue, and Mississippi Coast just east of the state line. The results showed that the JPA underestimated surge hazard relative to the gauge analysis, which was influenced by the Hurricane Katrina observations. The project team employed the JPA to assess the return period for Hurricane Katrina HWMs and noted that the very long estimated return period of Katrina HWMs—e.g., 660 years for the south shore of Lake Pontchartrain—"are a concern."

[3] The documentation notes that for one synthetic storm, over each time-step (1 s) an average of 6% of the domain area had a relative mass conservation error exceeding ±0.01%. Further breakdown of this error was not provided.

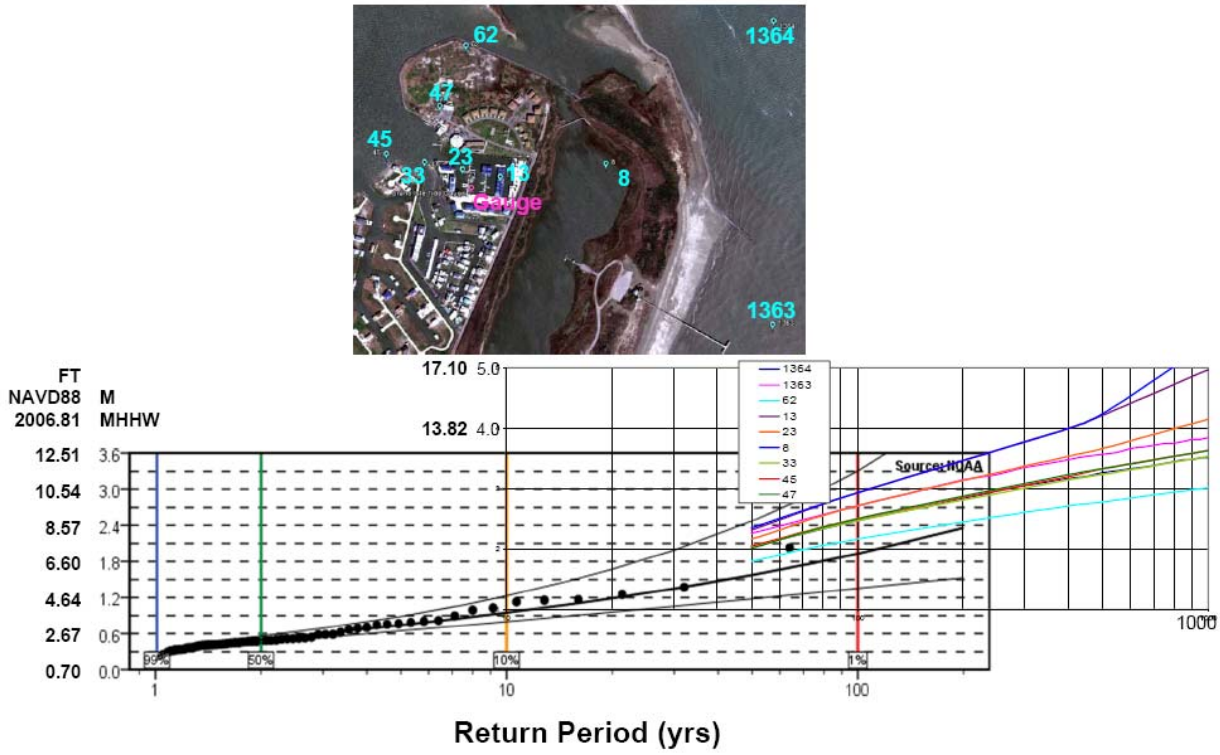

Figure 14.6. JPA versus Tide Gauge Return Frequency Analysis Grand Isle LA
NOAA (http://tidesandcurrents.noaa.gov/est/est_station.shtml?stnid=8761724) and USACE 2012

For comparison purposes Figure 14.8 presents CDF curves developed by the USACE in 1966, following Hurricane Betsy, as part of improving the New Orleans area hurricane protection system (USACE 1966). Surge elevations in Figure 14.8 are given in ft MSL, which must be converted to NAVD88-2006.81. These curves were developed using methods that pre-dated application of JPA. The 1966 estimated 100-yr surge SWL along the south shore of Lake Pontchartrain and along the MRGO near Chalmette in Figure 14.9 are approximately 9.2 and 11.2 ft NAVD88-2006.81, compared to the JPA estimates for the 2007 condition of 8.8 and 17.5 ft NAVD88-2006.81 in Figure 14.7.

In 1988 the USACE developed surge CDFs for the design of levees in east-bank St. Charles Parish (Figure 14.10). For a location east of the Bonnet Carre Spillway Figure 14.9 shows that the 1988 estimated 100-yr surge SWL was 10.8 ft NAVD88-2006.81, compared to 11.4 ft NAVD88-2006.81 in Figure 14.7.

According to FIS documentation, following construction of CDFs at all output locations the team applied only limited spatial smoothing of the return period results. A linear blending algorithm was applied to southeast Louisiana locations near the Mississippi state line due to differences in results between the southeast Louisiana and Mississippi JPAs. (See description of the Mississippi surge JPA methodology below.) The blending region was a few miles wide and modified surge hazard values were determined by interpolating between fully weighted Mississippi and Louisiana study values on the respective sides of the blending region. The differences in 100-yr surge SWL between the two studies were not reported, but may have reached 20 percent, another indication of study uncertainty. Near latitude 30.256 the 100-yr SWL was noted as 13.2 ft west of the Pearl River (USACE 2012) but 16 ft east of the Pearl River (per nearby AE Zone, Hancock Co., Preliminary FIRM Panel 295, FEMA November 2007).

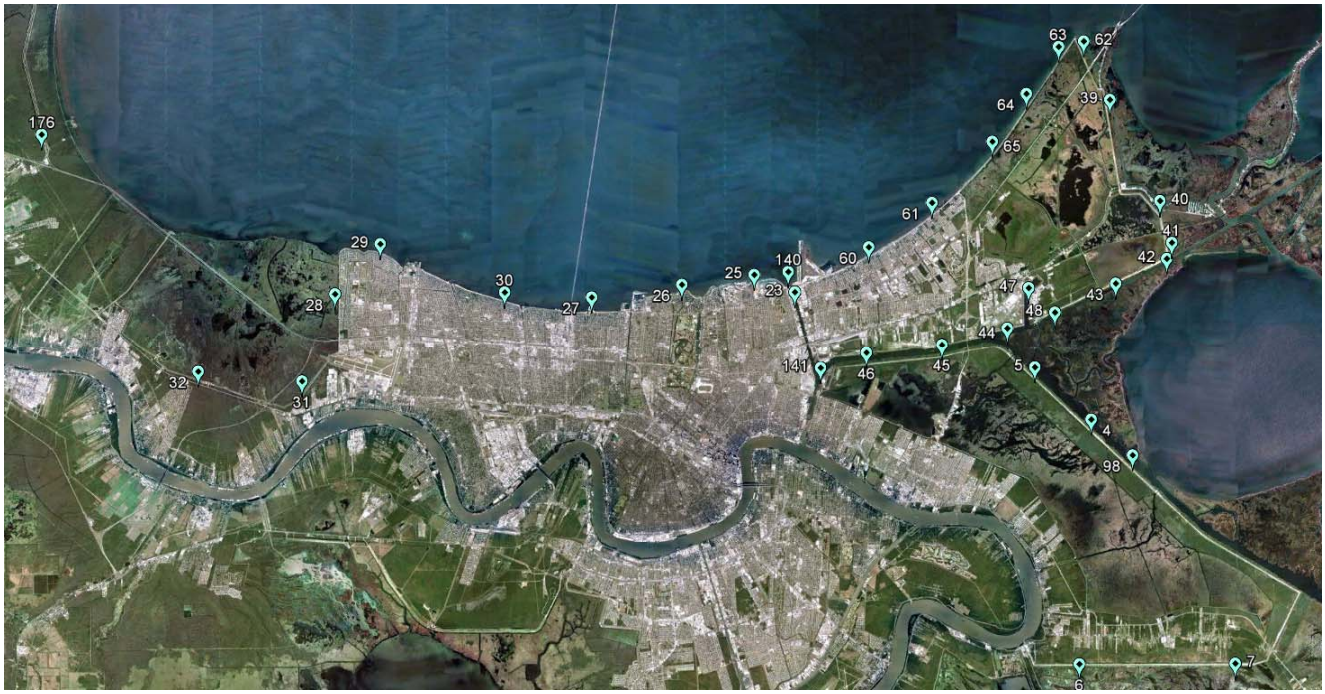

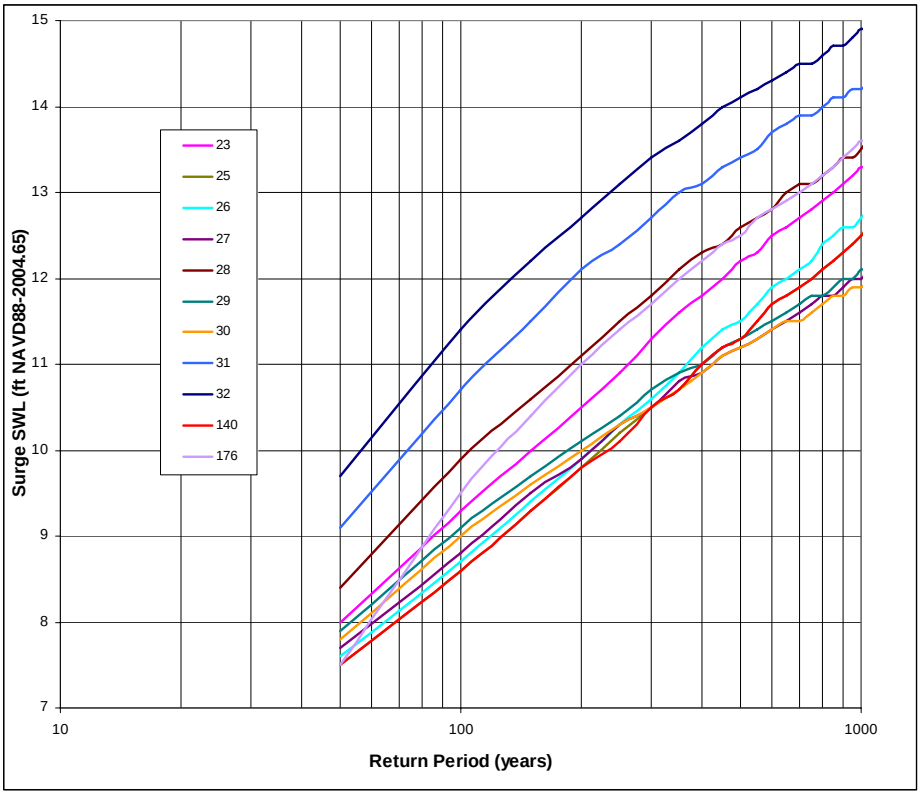

Figure 14.7. Surge SWL CDFs for 2007 FIS, East-Bank New Orleans
USACE 2012

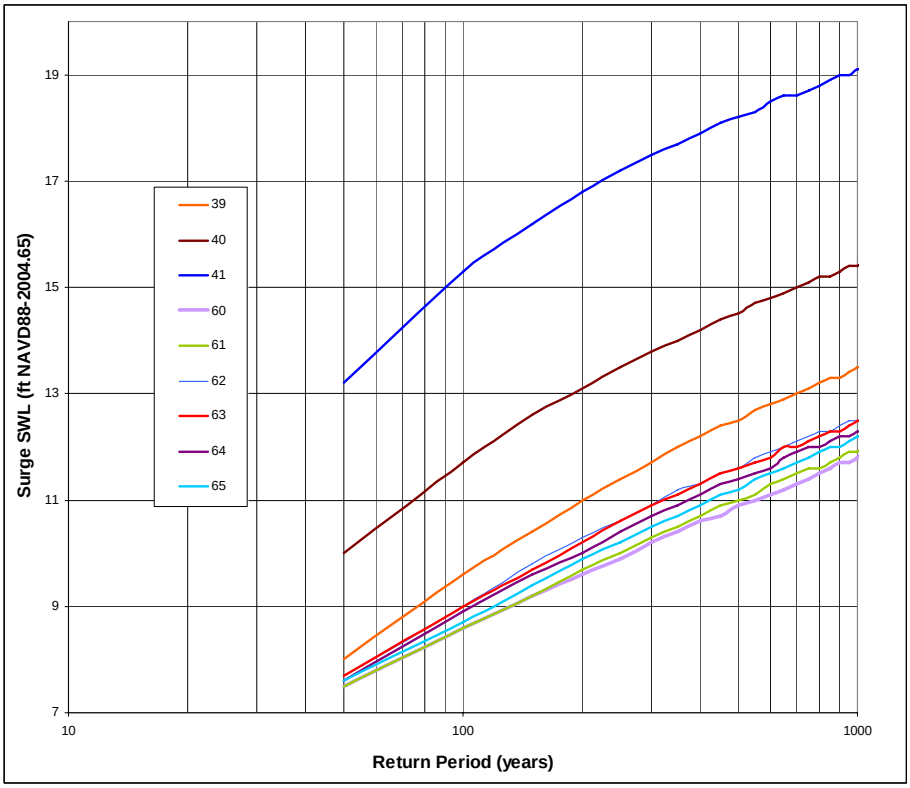

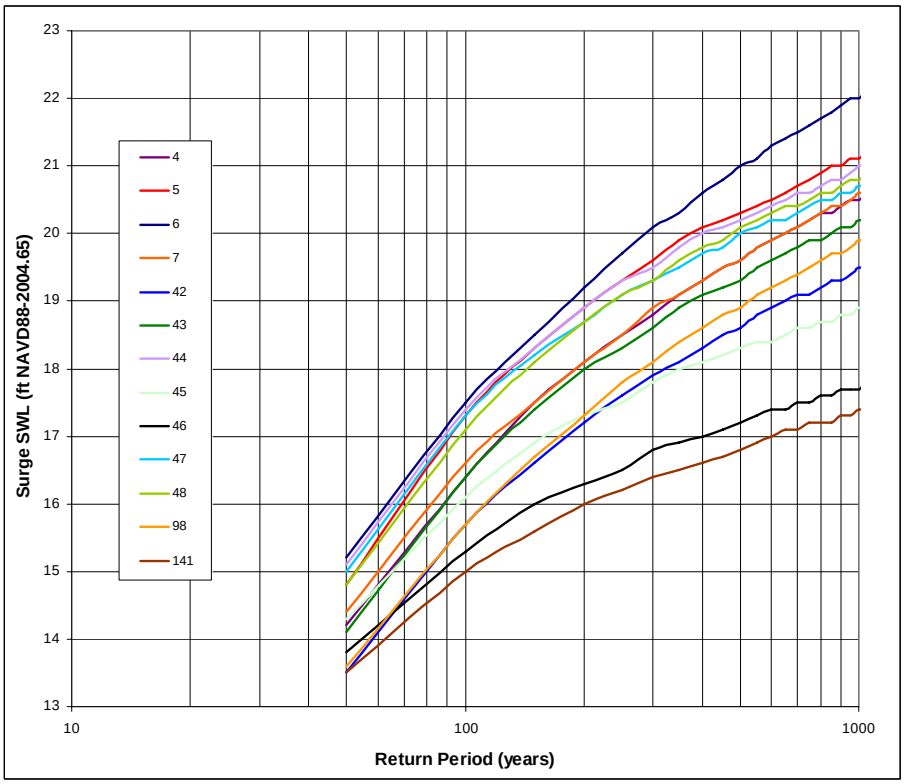

Figure 14.7. Surge SWL CDFs for 2007 FIS, East-Bank New Orleans (continued)

USACE 2012

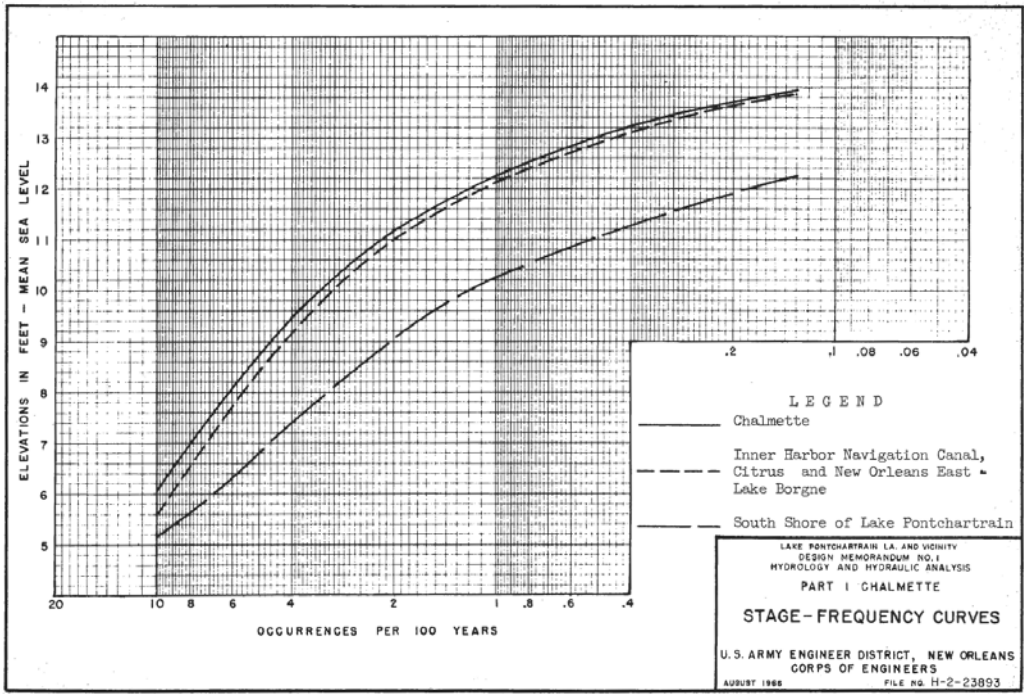

Figure 14.8. 1966 CDFs for East-Bank New Orleans Area

Subtract 1 ft to convert MSL to NAVD88-2006.81

USACE 1966

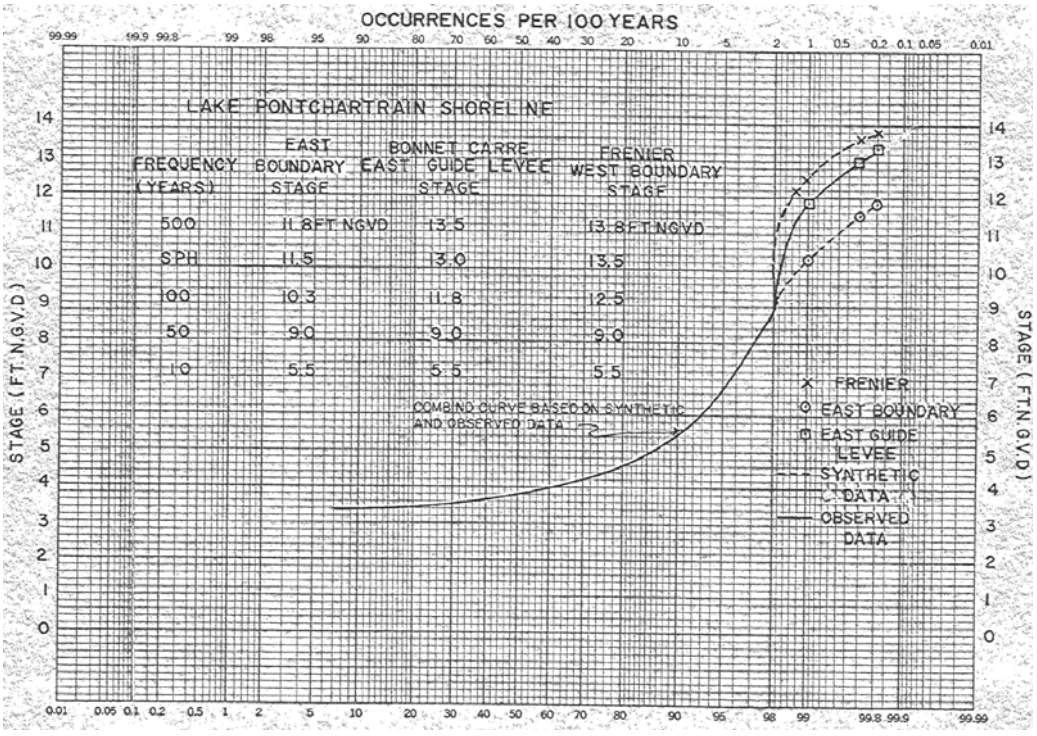

Figure 14.9. 1988 CDFs for East-Bank St. Charles Parish

Subtract 1 ft to convert MSL to NAVD88-2006.81

USACE 1989

As previously discussed (see Section 13.6) confidence limits for CDF curves are not typically prepared as part of the FIS documentation and were not made available for the 2007 CDF results. Resio et al suggested that the Gumbel distribution could be used to represent the surge SWL return frequency at any location, and noted that confidence limits for the resulting Gumbel curve could be computed (Resio et al 2007). However, no Gumbel curves of surge SWL hazard or associated confidence limits were provided.

Wave Hazards

FEMA FIS contractors[4] analyze overland wave hazards associated with the 100-yr SWL hazard using WHAFIS as described in Sections 9.2 and 13.7. In accordance with FIS requirements, special wave hazard zones, termed VE Zones—in which the overland wave height, or the depth of wave runup, associated with the 100-yr SWL exceeds 3 ft—are delineated on the FIRMs (see Figure 14.10). FEMA has completed FIRMs for several coastal southeast Louisiana parishes (Tangipahoa, Livingston, St. James, and St. John the Baptist), and proposed a preliminary FIRM for St. Tammany Parish. FEMA is preparing preliminary FIRMs for those parishes that include some areas enclosed by the HSDRRS (St. Charles, Jefferson, Orleans, St. Bernard, and Plaquemines). For each FIS the 100-yr SWLs will be taken from the foregoing surge JPA.

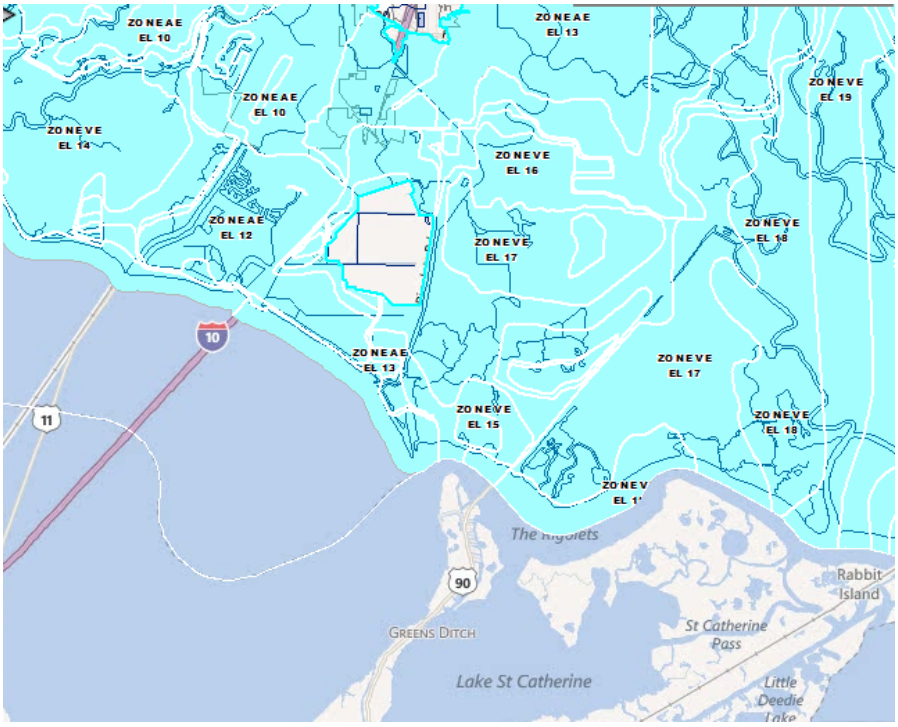

Figure 14.10. Example of Wave Hazard Areas (VE Zones) Shown on FIRM
http://lamp.lsuagcenter.com/?FIPS=22103

[4] The USACE did not perform overland wave analysis for southeast Louisiana coastal FISs. FEMA retained independent engineering firms to perform the analysis and prepare the FIRMs.

A detailed review of the application of WHAFIS in each parish—including inputs regarding 1D transect locations, topography, friction, boundary conditions, etc.—is beyond the scope of this Report. St. Tammany Parish, which include sizeable communities outside of the HSDRRS and exposed to overland wave hazards (e.g., eastern Slidell LA), is currently contesting the accuracy of inputs to the proposed WHAFIS analyses. Local officials contend that VE Zones are smaller than proposed by FEMA.

14.2. IPET Study

The IPET study (IPET 2009, see Volume VIII, Appendix 9) for southeast Louisiana required a separate JPA approach from the FIS. In order to conduct further hazard analysis of HSDRRS overtopping, breaching, and polder inundation (see Section 17) IPET needed an actual JPM-OS, with probabilities assigned to specific storms in the set and their individual associated surge events.

The IPET study took 76 of the 152 Resio et al Surge Response-OS storms affecting the New Orleans metropolitan area—reasonably similar to L-60—and assigned joint probabilities for each storm. Attachment 1 includes the information on the IPET 76-storm set. The overall average return frequency for GMH/L-60 reflected in the IPET set is 0.0745, or an average return period of 13.4 years (reasonably close to 5.6*2.5). No confidence intervals were provided with the joint probabilities but they would likely be greater than those discussed in Section 3 for V_{max} alone.

Figure 14.11 shows the IPET JPM-OS V_{max} return period distribution based on the 76-storm probabilities compared to a) the Gumbel distribution for L-60 based on escalated recent frequencies for GMH activity over the last 60-years, and b) the Resio et al distribution based on the 1941 to 2005 period (both previously given in Figure 3.18). The figure indicates that the 76-storm set overstates V_{max} at return periods below 200 years but understates V_{max} above a 200-year return period, flattening out dramatically between 153 mph (106-year return period) and 155 mph (885-year return period). This range corresponds to the borderline Category 4/5 storm, such as represented by Hurricane Katrina's landfall CP. This flattening out is consistent with the fact that the Resio Surge Response-OS did not contain any Category 5 landfall storms. Figure 14.11 shows that storms below the Category 4/5 are generally over-represented in the IPET JPM-OS, while storms above this intensity are under-represented. Strong Category 3 storms—e.g., Katrina's landfall V_{max} of 126.5-mph—appear to be over-represented, i.e., they have a shorter return period. The IPET Report provided no discussion of whether their JPM-OS was representative of Resio et al's joint probability function, ***p***, applied to L-60.

Surge CDFs were constructed using the results of the 76 storms, presumably without smoothing. The IPET CDF integration code has not been made available.

IPET's improvised 76-storm JPM-OS produced different surge hazard estimates in the vicinity of the HSDRRS than the FIS 152-storm Surge Response-OS. In east-bank St. Charles Parish west of I-310 near the FIS JPA (Point 32 , Figure 14.8) yielded 100- and 500-yr SWL estimates of 11.4 and 14.2 ft, while IPET (see Figure 13.13) produced estimates of 9.7 and 10.7 ft, the latter being 24% lower.

The IPET Study did assess confidence limits for their CDFs. Figure 13.13 illustrates confidence limits for the IPET CDF for St. Charles Parish west of Interstate 310. Note that the figure illustrates confidence limits only for epistemic uncertainties consisting of ε_P, which was not explicitly defined, and ε_ψ, which was defined according to σ_ψ equal to 0.1·SWL. At the 100-yr return period, the estimated surge SWL (50% or median value) is about 9.7 ft, which thus has a σ_ψ of 0.97 ft, or a 90% confidence band (LCL/UCL of 5 to 95%) of ±1.6 ft. The illustrated 90% confidence band is skewed due to the contribution of non-normally distributed ε_P, which spans from about 7.6 to 12.5 ft. (-2.1 to +2.8 ft). The illustrated epistemic uncertainty band thus extends -0.5 and +1.2 ft wider than for ε_ψ alone.

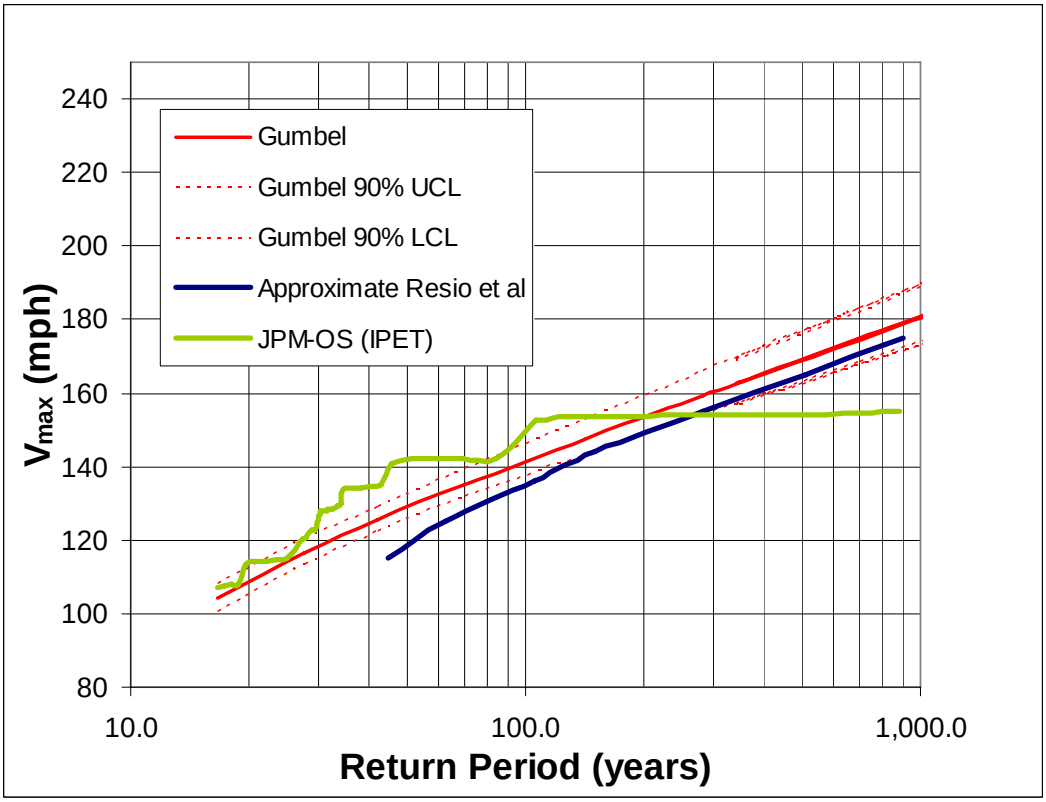

Figure 14.11. Recent Return Period Distribution for L-60 V_{max} versus IPET JPM-OS

IPET defined, but did not illustrate, four sources of normally distributed aleatory uncertainty (σ_B of 0.15·SWL; σ_M parametric of 1.18 ft; σ_M modeling of 0.75 ft; and σ_T of 0.66 ft) which would combine for an additional σ of 2.1 ft at the median estimate of 9.7 ft. Combining the epistemic and aleatory normal distributed uncertainties ONLY yields a total σ_Σ of 2.3 ft, or a 90% confidence band of ±3.8 ft, somewhat less than the lower bound of the total normally distributed σ_Σ associated with the Resio et al approach (noted above). Inclusion of ε_P means the overall magnitude of uncertainty is even higher.

Although the IPET JPA was not representative of the FIS JPA, it—together with the uncertainty information—provided a basis for a preliminary stochastic analysis of residual flood hazards (overtopping, breaching, and polder inundation) and associated risks (see Part IV).

14.3. Southwest Louisiana FIS

The southeast Louisiana project team also a completed surge JPA for southwest Louisiana using the same Surge Response-OS. The southwest study also employed 152 storms distributed among the same 19 combinations of CP-R_{max}-V_f and landfall spacing as in the southeast Louisiana study—but on western tracks. ADCIRC-STWAVE production model, setup and parameters for the southwest study, together with steps for treatment of uncertainty and bias, production, and post-processing steps, were reported to be the same as used in the southeast study. The report does not indicate that any adjustments were made to production SWL results to account for ADCIRC-STWAVE model Hurricane Rita hindcast validation bias (see Section 11).

The southwest Louisiana study report does not present a comparison of stochastic CDF curves versus local tide gauge curves. The NOAA Sabine Pass tide gauge record would seem to provide a reasonable basis for validating the stochastic analysis.

FEMA FIRM mapping contractors for the southwestern Louisiana utilized WHAFIS to identify VE-Zones.[5]

14.4. 2012 Louisiana Master Plan

In 2011 RAND Corporation implemented a highly simplified JPM-OS approach (Louisiana CPRA 2012, Appendix D25) as part of a preliminary investigation into future coastal Louisiana surge hazard. RAND significantly truncated the IPET JPM-OS, which (as noted in Section 14.2) improvised using 76 of the Resio et al Surge Response OS storms for a JPM-OS. RAND first selected 154 storms from the overall 304 Resio et al Surge Response-OS (combined southeast and southwest) to serve as a benchmark. The RAND report stated that they chose the 154 storms to reflect a variety of attributes.

RAND did not introduce any new hurricane climatology information or hurricane JPA. They presumably assigned fractional joint probabilities to each storm based on the Resio et al joint probability expression. RAND then employed the ADCIRC-STWAVE FIS production results for the 154 storms and assigned fraction joint probabilities for each storm to compute benchmark 50-, 100-, and 500-yr return period surges at 449 coastal Louisiana locations. Details on the integration of the CDFs were not presented.

RAND did not provide an evaluation of the 154-storm benchmark's representation of the Louisiana coastal surge hazard. The 154-storm set has inherent limitations as a surge hazard benchmark, given that the original 152 storms for each study (304 combined) were selected by Resio et al to represent surge response and NOT surge hazard. This is especially typified by the absence of any landfalling Category 5 storms.

RAND evaluated a range of subsets from the 154-storm benchmark to select a JPM-OS. RAND ultimately selected a subset of 40 storms, with four storms (combinations of two CPDs and two R_{max}) at 10 coastal landfall points (combined southeast and southwest Louisiana), each at mean V_f and θ. RAND proceeded to employ the 40-storm OS in conjunction with the OCPR2012 model described in Section 11 to evaluate future coastal protection scenarios (see Part V).

Importantly, the 40-storm OS:

- Shares the limitations of the 154-storm benchmark;
- Displays further significant discrepancies in representing the 154-storm benchmark; and
- Is too small to capture important nonlinear surge dynamics and surge hazard response due to the interaction of hurricane attributes and coastal Louisiana features.

The major benefit of the 40-storm JPM-OS was its very small size, which supported its use as an initial tool in assessing alternative future coastal protection scenarios.

[5] As much of the FIS team's focus in 2005-07 was on southeast Louisiana, less attention was apparently paid to mesh details for southwest Louisiana. Following publication of preliminary FIRMs Cameron Parish officials retained a separate team to recommend further improvements to the input for ADCIRC and WHAFIS topography (horizontal alignment and elevation) and hydrodynamic friction (Manning's *n*) for several critical coastal features (e.g., cheniers).

14.5. Mississippi FIS

Concurrent with the southeast Louisiana surge JPA, Toro completed a surge hazard study for coastal Mississippi, (Toro 2008 and URS Corporation 2008). Toro closely coordinated the Mississippi work with Resio et al but choose to develop the Mississippi storm set as a JPM-OS. The Mississippi team evaluated five different JPM-OS in comparison with a benchmark surge hazard using a simplified SLOSH model of the Mississippi coast. The benchmark hazard (referred to in the report as the "Gold Standard") was developed by simulating nearly 3000 storms.

Figure 14.12 compares the benchmark (JPM-Ref) representation of the 100-yr SWL hazard versus the selected JPM-OS (OS6) representation at 147 points along the Mississippi coast. The selected JPM-OS had RMSEs (OS versus benchmark) of 0.47 and 0.59 ft for the 100-yr and 500-yr hazards.

The selected JPM-OS divides the overall probability of a "greater" hurricane (CPD > 48 mb) landfall along the Mississippi coast (estimated at 0.000463 per year per mile or a return period of about 36 years for 1° longitude) into 19 groups, shown in Table 14.2. These 19 groups include five general track θs (see Figure 14.13). Each of the 19 groups contained a number of landfall locations based on tracks offset by R_{max}, for a total set size also of 152 storms.

Six groups have a landfall CPD >100 mb, thus providing for Category 5 landfall storms, unlike the Louisiana Surge Response OS. These 100 mb CPD storms have a total weighted fractional joint probability of 0.091, or an overall return frequency of 0.0000422 per year mile, or an estimated return period of about 395 years for 1° longitude. Figure 14.14 illustrates the JPM-OS joint probabilities for pairs of attributes (which could have been better depicted with contour plots). Toro did not provide information on the uncertainty of these estimated joint probabilities.

The Mississippi project team did not address implications of the simplified SLOSH model limitations in the JPM-OS selection and JPA. While the Mississippi coast is more linear and smoother than the southeast Louisiana coast, it does include several notable irregularities (e.g., St. Louis and Biloxi Bays). Toro did not develop wind return frequency results and validate the Mississippi JPM-OS versus a wind hazard benchmark (e.g., Vickery et al's wind return studies).

The Mississippi production runs employed the calibrated/validated ADCIRC-SWAN (loosely coupled) model (see Section 11). Quality control included automated screening of selected station time-series for large SWL oscillations, as well as screening for abrupt changes in peak SWL between adjacent mesh nodes.

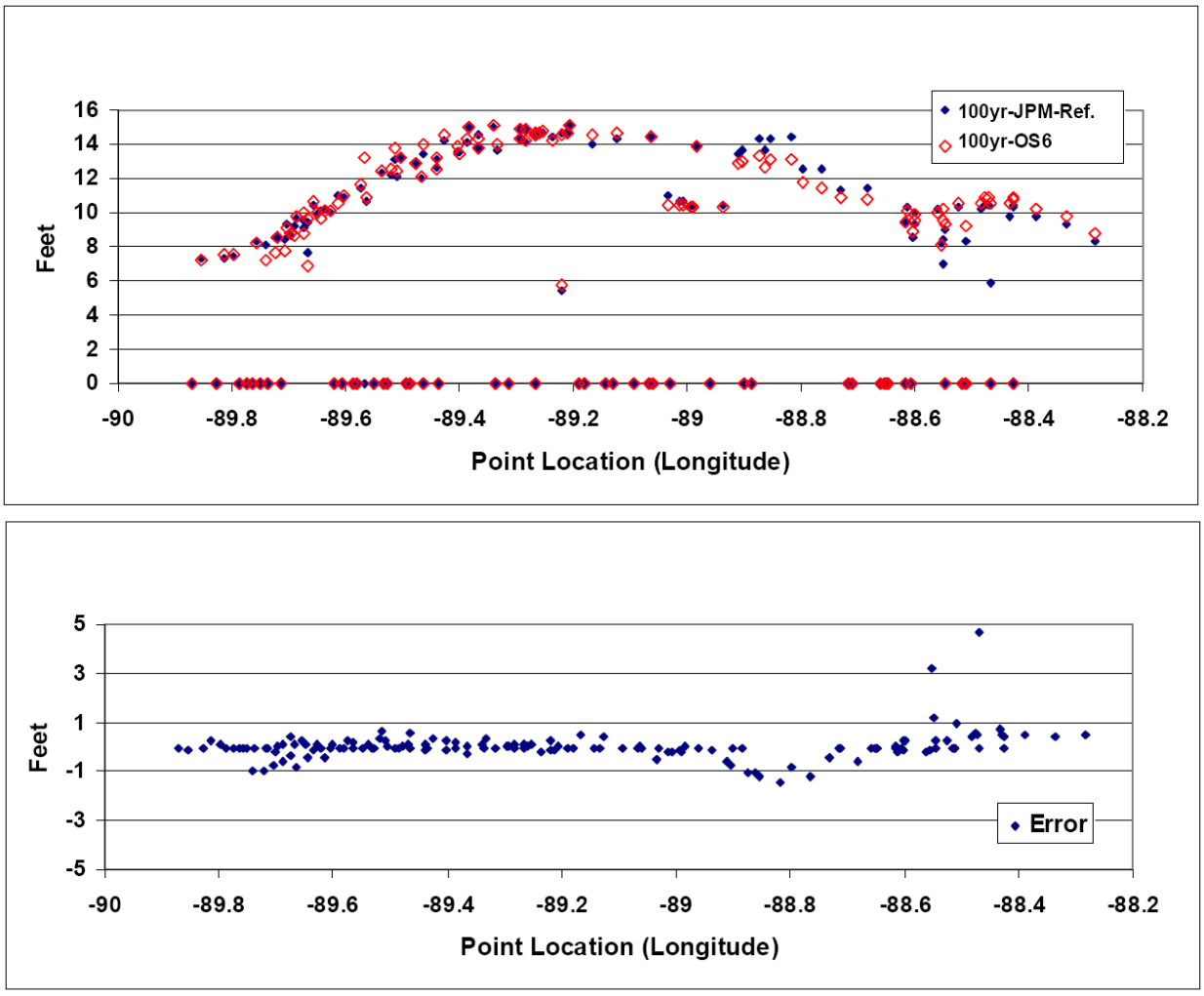

Figure 14.12. Comparison of Benchmark versus JPM-0S 100-yr SWL
URS Corporation 2008

The Mississippi team employed a normally distributed uncertainty term, ε_Σ, consisting of the following components:

1. Uncertainty associated with wind field attributes omitted from the joint probability—ε_W—was defined with a separate σ_B for Holland B of 0.15·SWL ft and σ_{PBL} of 1.17 ft
2. Uncertainty associated with the high resolution ADCIRC-STWAVE surge model—ε_Ψ—was defined with σ_Ψ = 0.77 ft. The combined $\sigma_{PBL\&\Psi}$ = 1.4 ft, much lower than the Resio et al $\sigma_{PBL\&\Psi}$ of 2.0 to 3.5 ft.
3. Uncertainty associated with the tides—ε_T—was defined with σ_T = 0.65ft;
4. Uncertainties regarding hurricane climatology (joint probability) and the JPM-OS—ε_P and $\varepsilon_{JPM\text{-}OS}$—were not defined.

The overall σ_Σ equated to 2.2 ft at a SWL of 10 ft, or a 90% interval of about ±3.4 ft.

Table 14.2. "Greater" Hurricanes for Mississippi JPM-OS

Toro 2008

Landfall CPD mb	GoM R_{max} mile	Landfall V_f mph	Landfall θ	Weighted Fractional Joint Probability
66.69	21.4	13.5	-38.9	0.1330
57.17	45.8	13.5	-12.8 to -13.5	0.1200
49.72	26.4	13.5	-38.9	0.1330
57.17	12.5	13.5	-12.8 to -13.5	0.1200
57.17	23.9	13.5	56.7	0.1080
92.95	16.9	13.3	-12.8 to -13.5	0.0342
78.59	35.4	13.5	-12.8 to -13.5	0.0534
78.59	19.1	9.7	47.3	0.0420
78.59	10.2	13.5	-12.8 to -13.5	0.0534
78.59	19.1	32.5	-12.8 to -13.5	0.0349
70.02	20.7	13.3	-12.8 to -13.5	0.0342
78.59	19.1	9.7	-71.0	0.0420
128.7	13.4	13.3	-12.8 to -13.5	0.0106
103.7	29.1	13.5	-12.8 to -13.5	0.0165
103.7	15.7	9.7	47.3	0.0130
103.7	8.4	13.5	-12.8 to -13.5	0.0165
103.7	15.7	32.5	-12.8 to -13.5	0.0108
94.47	16.7	13.3	-12.8 to -13.5	0.0106
103.7	15.7	9.7	-71.0	0.0130
				Total 0.9991

To post-process the results from the JPM-OS storms run with the ADCIRC-SWAN model the Mississippi team employed a different integration approach from the southeast Louisiana study. The team used the PDF smoothing technique described in Section 13.6, with ε_Σ as a diffusion term (see Figures 13.9 and 13.10). The team did not discuss validation of the JPA CDF versus a CDF that could have been developed from the long-term record at the Biloxi tide gauge. Confidence bands for the JPA CDF were not discussed. The team determined VE Zones associated with the 100-yr SWL hazard using WHAFIS. [6]

[6] Following publication of preliminary FIRMS local Mississippi officials engaged FEMA to improve the input for WHAFIS elevation and wave energy dissipation for several transects.

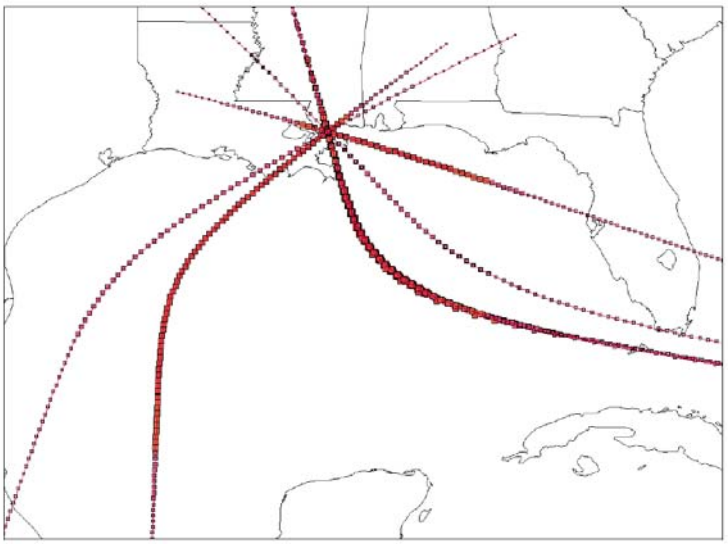

Figure 14.13. "Greater" Hurricane Tracks for Mississippi Coast JPM-OS

Toro 2008

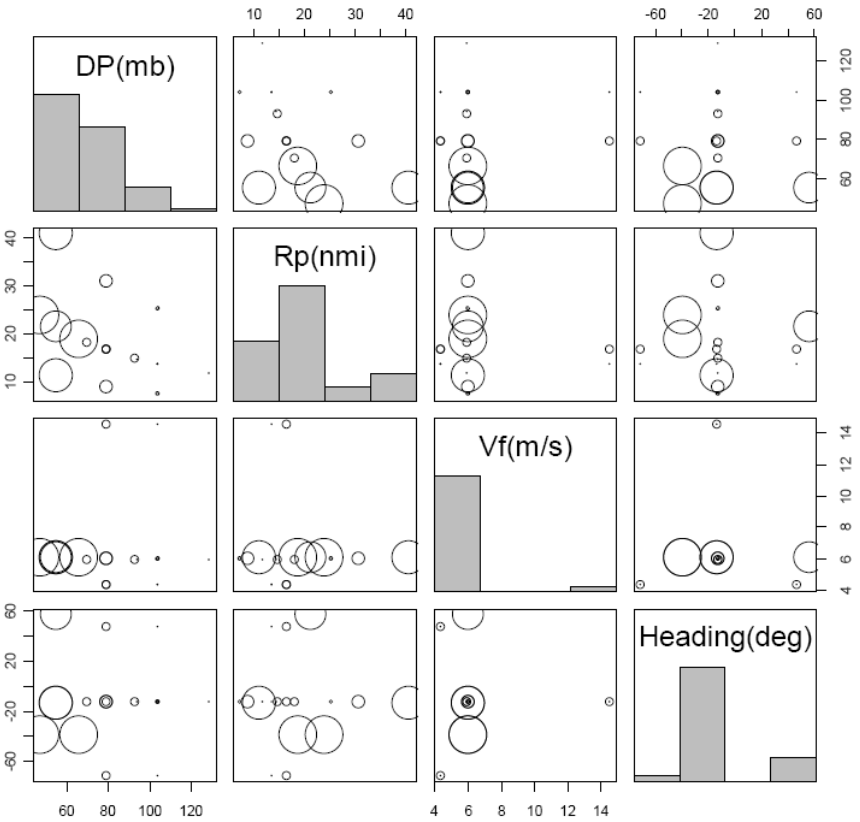

The main diagonal shows the probability distribution of the corresponding quantity (in the form of a histogram). Each off-diagonal scatter diagram shows how each pair of quantities are jointly distributed, with the areas of the circles being proportional to the associated annual rates.

Figure 14.14. JPM-OS Joint Probabilities

Toro 2008

14.6. Other FISs

The Mississippi JPM-OS approach is being employed for two other ongoing GoM coastal FISs, that include key team members from the Mississippi coastal FIS. For the Florida—Big Bend study (less than 100-mi east-west study segment) the surge hazard benchmark was created with 3,263 storms and a regional SLOSH model, resulting in selection of a 159-storm JPM-OS (Northwest Florida Water Management District 2010). A similar approach is being used for Northwest Florida/Alabama by the same team, with the benchmark set and OS reportedly approximating 4,000 and several hundred storms, respectively (Northwest Florida Water Management District 2011).

The North Carolina FIS team is using a 675-storm JPM-OS, with 351 landfalling and 324 bypassing storms. The set reflects combinations of historical tracks with incremental adjustments to storm CDP, R_{max}, Holland B, V_f, , and variations in θ. This set is much larger than the JPM-OS for southeast Louisiana and Mississippi. The North Carolina team compared the return period wind results at five locations for the 675 storm set versus results from Vickery's wind JPA, which employed a much larger Monte Carlo based storm set (see Section 4). Figure 14.15 illustrates the comparison of wind results for one location. The team has indicated that visual comparison of the two wind results supports use of the 675-storm JPM for the hurricane surge return frequency analysis. A measure of the agreement between the two results over the five stations was not included.

The South Carolina and Northeast Florida/Georgia FISs are using JPM-OS. The South Carolina study has a 122-storm JPM-OS, based on comparison with a SLOSH surge hazard benchmark. The number of storms employed in the South Carolina SLOSH benchmark was not available. The Northeast Florida/Georgia study is expected to have on the order 200 to 300 storms. The JPM-OS is being developed in comparison against a lower resolution ADCIRC surge hazard benchmark based on several thousand storms.

The coastal FIS for Texas is being led by the USACE and has utilized the Surge Response-OS used for southeast and southwest Louisiana. Presumably the Texas OS employs the 19 CPD-R_{max}-V_f combinations used for Louisiana. Detailed information on the Texas OS is not currently available. The Texas OS has reportedly included about 360 storms (divided into two 180 storm sets for north and south coastal regions) for a JPA of 100-yr plus return period surge.

Details have not yet been released for these coastal FISs on the treatment of uncertainty, integration procedures, validation against tide gauge CDFs, and result differences at study boundaries.

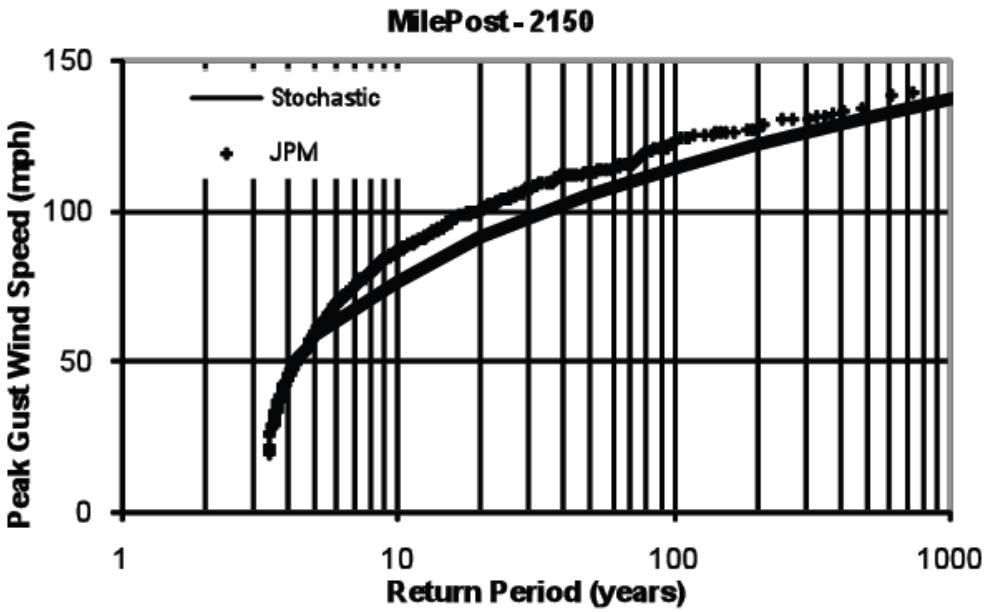

Figure 14.15. Example Comparison of Return Period Wind Gusts from 675-Storm versus Full Monte Carlo JPM

Blanton and Vickery 2008

Part III. Conclusions and Recommendations

Conclusions

Part III has reviewed the state-of-the-practice on hurricane surge return frequency analysis and applications to the CN-GoM. This information supports the following important findings:

1. Surge return frequency analysis can be readily performed with long-term daily tide records using established methods for five CN-GoM gauges (Pensacola, Dauphin Island, Biloxi, Grand Isle, and Sabine Pass). Record lengths, gauge outages, datum issues, local restrictions, the choice of return frequency distribution equations, and extrapolation uncertainties all limit applicability. NOAA's recent analysis of the Grand Isle tide gauge record shows an estimated 100-yr return SWL of 7.1 ft, with 95% confidence intervals of 5.1/11.4 ft. The size of this confidence interval, i.e., -2.0/+4.4 ft (62% for the upper interval), is an important indicator of limitation in surge return estimates.

2. Hurricane JPA (see Part I) can be extended to surge to provide more comprehensive estimates of surge hazard and address some limitations of gauge analysis. Hurricane surge JPA is mathematically expressed in a PDF coupling the analytical joint probability expression, $\boldsymbol{p}$, for hurricane occurrence as a function of hurricane attributes (e.g., CPD, R_{max}, V_f, θ, X) with the high resolution surge response function, $\boldsymbol{\Psi}$, for the same attributes. $\boldsymbol{\Psi}$ must be solved numerically for discrete attribute values using a wind field vortex model (e.g., PBL) coupled with a validated hydrodynamic model (e.g., ADCIRC/STWAVE, described in Part II). Surge PDF results over a wide range of combined attributes are then integrated to provide a surge CDF.

3. There are four established approaches to developing a sufficient number of discrete solutions to the coupled $\boldsymbol{p}$-$\boldsymbol{\Psi}$:

    a. Full-JPM—choose discrete intervals for each attribute to represent $\boldsymbol{p}$ and simulate each storm combination with $\boldsymbol{\Psi}$; joint probabilities based on the combination of attributes are assigned to each storm's surge results; requires a very large number of simulations.

    b. Monte-Carlo-JPM—randomly select storms according to $\boldsymbol{p}$ to construct a reasonably long synthetic record—e.g., 10X the return period of interest—and simulate each storm with $\boldsymbol{\Psi}$; joint probabilities based on the combination of attributes are assigned to each surge result; smaller set than the Full-JPM.

    c. JPM-OS—depending on high resolution $\boldsymbol{\Psi}$ computational requirements, develop a subset from Full/Monte Carlo-JPM to represent $\boldsymbol{p}$ using fractional weightings; further optimize the set to represent a benchmark surge JPA derived with a simplistic $\boldsymbol{\Psi}$ and the Full/Monte Carlo-JPM; the subset is then simulated with the high resolution $\boldsymbol{\Psi}$; weighted joint probabilities of each storm are assigned to each surge result.

    d. Surge Response-OS—as an alternative to JPM-OS, develop a set of storms as needed to depict $\boldsymbol{\Psi}$ only; this set size can be reduced in surge response is assumed to be nearly linear and smooth and interpolation/extrapolation can be used to provide a range of surge response; a large set of discrete $\boldsymbol{p}$-$\boldsymbol{\Psi}$ solutions are provided by combining analytically-derived $\boldsymbol{p}$ with surge values from $\boldsymbol{\Psi}$ defined with the Surge Response-OS; note that the Surge Response-OS and simulation results do not have assigned joint probabilities and cannot be used to support subsequent polder hazard analysis.

4. The use of any of the four surge JPA approaches includes uncertainties which are in addition to uncertainties regarding the hurricane joint probability, $\boldsymbol{p}$ (i.e., the defined hurricane climatology)

and the surge model, $\boldsymbol{\Psi}$. The use of JPM-OS and Surge Response-OS approaches both add significant uncertainties associated with reducing set size. The surge response of certain coastal regions is nonlinear (i.e., the response curve contains notable inflections) and the coupled $\boldsymbol{p}$-$\boldsymbol{\Psi}$ surge hazard may be even more nonlinear. A crucial example is the tilting response of large coastal lakes and bays to local hurricane winds (e.g., Lakes Pontchartrain and Borgne). The OS approaches must contain sufficient storms to represent localized surge response and surge hazard conditions.

5. Altogether there are five major categories of stationary uncertainty in surge JPA:

   i. $\varepsilon_{\boldsymbol{p}}$—aleatory uncertainty in hurricane climatology as defined in $\boldsymbol{p}$, such as uncertainty in return frequency of CPD, and frequency of R_{max}, V_f, and θ;

   ii. $\varepsilon_{\boldsymbol{W}}$—epistemic uncertainty associated with additional hurricane wind field factors excluded from $\boldsymbol{p}$; uncertainty with Holland B (ε_B) is one component; others include intensification and decay;

   iii. ε_{Ψ}—epistemic uncertainty associated with the high resolution surge response model $\boldsymbol{\Psi}$; including winds (PBL), surge (ADCIRC) and waves (STWAVE);

   iv. ε_{OS}—epistemic uncertainties associated with the JPA method (see No. 4 above); uncertainty with the limited number of tracks (ε_{ϑ}) is one component ; and

   v. ε_{T}—tides and pre-storm meteorological conditions affecting the SWL.

   Most sources of uncertainty, with the exception of CPD return frequency, have been treated as normally distributed with an associated $\boldsymbol{\sigma}$, which can be combined into an overall $\boldsymbol{\sigma}_{\Sigma}$. CPD uncertainty is typically skewed and can be assessed using the assigned distribution equation (e.g., Gumbel). Non-stationary uncertainties, such as RSLR, coastal erosion, and subsidence affect future surge return frequency.

6. Numerical integration of the discrete p-Ψ results can include smoothing the PDF and CDF. A σ value can be used; however, a large σ value can distort the CDF. Techniques for refining the discrete results can also aid in smoothing. .

7. Potential bias in a surge JPAs is investigated by comparing the surge JPA CDF versus one derived from a sufficiently long local gauge record (No. 1 above); bias can be further assessed by addressing validation results for key components (such as the high resolution $\boldsymbol{\Psi}$, surge benchmark, and simplified $\boldsymbol{\Psi}$, where used) and lessons from other JPAs.

8. Uncertainty in surge CDFs are evaluated by comparing the computed median curve with confidence intervals accounting for all normally and non-normally distributed sources of uncertainty. FISs do not typically introduce adjustments for uncertainty into final estimates of surge hazard. However, such adjustments are commonly applied in planning and design studies. The final residual uncertainty can be evaluated by comparing the JPA CDF versus local gauge CDF.

9. General inland wave hazards associated with extreme surges are evaluated with simple 1D wave models (e.g., WHAFIS, see Part II). Locations subject to sensitive wind-wave generation conditions, or to complex wave transformations, require more sophisticated 2D and higher-order wave models.

10. The Rayleigh Distribution may over-predict nearshore extreme waves associated with surge SWL peaks lasting only a few hours.

11. Application of hurricane surge JPA to the CN-GoM began in the 1980s. However, hurricane surge JPA was not employed for southeast Louisiana prior to Hurricane Katrina.

12. The FIS surge JPA project team (Resio et al) employed a 152-storm Surge Response-OS for the 151-mi (2.5°) segment for southeast Louisiana. The team developed the storm set with a idealized coastal surge response model. The set included 3 different CPDs, 15 different CPD-R_{max} combinations, and 19 different CP-R_{max}-V_f variations. The set used 9, 7, and 7 landfall locations within the 151-mi range, for three basic variations in θ—central, northeast, and northwest headings. Selected CP-R_{max}-V_f combinations from the 19 variations were used with each of the 23 tracks. The spatial distribution of landfalls within the 151-mi range was adjusted to provide a higher landfall rate in the 60-mi (2.5°) centermost segment—generally in accordance with the Resio et al hurricane intensity-frequency relationship (see Part I).

13. All 152 storms in the Surge Response-OS set were Category 3 or higher in the GoM, including 50 at Category 5. However, none made landfall at Category 5.

14. In designing the Surge Response-OS to be representative of a simplistic regional coastal landfall surge response the authors did not address special nonlinear surge response issues, such as those associated with extreme local winds over Lakes Pontchartrain and Borgne.

15. The southeast Louisiana FIS JPA defined sources of normally distributed uncertainty with total epistemic uncertainty σ_e totaling 2.1 to 3.6 plus 0.1 to 0.2 * SWL. For a 10 ft SWL this equates to a 90% confidence interval of ±3.8 to 6.8 ft. This level uncertainty is generally consistent with that seen in the Grand Isle gauge data (No. 1 above). This σ_e was based on epistemic uncertainties in θ, Holland B, the PBL/ADCIRC/STWAVE model, and tides. Uncertainties associated with other hurricane climatological attributes, and the Surge Response-OS itself were not provided. 2.0 to 3.5 ft. The report does not indicate that any explicit adjustments were made to production SWL results to account for ADCIRC-STWAVE model Hurricane Katrina hindcast validation bias along the south shore of Lake Pontchartrain (>1.5 ft, see Section 11).

16. The current FIS documentation states that production runs for the 152-storm Surge Response-OS were completed with the validated Hurricane Katrina ADCIRC-STWAVE model (including various settings and parameters, see Section 11). The current FIS documentation reflects 2007 mesh updates, but not the IHNC or Seabrook Surge Barrier. The LaCPR Study and HSDRRS design employed the 152-storm Surge Response-OS with a 2010 mesh version which included the IHNC Surge Barrier (but not the Seabrook Barrier) and presumably the same model settings and parameters (see Part IV for a discussion of the 2010 surge JPA results).

17. The southeast Louisiana FIS CDF numerical integration reportedly included both refining and smoothing. The refining utilized piece-wise linear interpolation of the surge response function. Smoothing was applied the discrete values of the integrand and employed the σ_e, which increased the estimated 100- and 500-yr SWLs for one location by 0.4 and 1.1 ft, respectively.

18. The FIS documentation does not contain any validation of the JPA CDFs. This Report provides a comparison of the FIS JPA and NOAA tide gauge CDFs for Grand Isle—which is along the *open coast*—and shows reasonable agreement.

19. In a separate documentation of independent technical review comments and responses, the project team compared JPA results with a limited analysis of regional *interior (sheltered) coast* gauge data (e.g., Lake Pontchartrain, MRGO). The JPA consistently underestimated surge hazard relative to the gauge analysis, primarily due to the extreme surge observations for Hurricane

Katrina. The project team noted that the very long return period estimates for Hurricane Katrina observations—e.g., 660-yrs for the south shore of Lake Pontchartrain—"are a concern."

20. The apparent underestimation of sheltered coast surge hazard versus more reasonable estimation of open coast surge hazard may reflect:

    a. Some underestimation of the recurrence of extreme hurricanes—such as the return period of Hurricane Katrina (see the conclusion of Part I);

    b. The ADCIRC-STWAVE model under-prediction bias in some sheltered areas (see conclusions of Part II); and/or

    c. Limitations of the Surge-Response OS in representing important local nonlinear surge response of sheltered areas.

21. USACE 1966 100-yr surge SWL estimates for south shore Lake Pontchartrain and the MRGO near Chalmette—which pre-dated JPA—were 9.2 ft and 11.2 ft, compared to 8.8 and 17.5 ft for the 2007 JPA. A USACE 1988 100-yr surge SWL estimate for St. Charles Parish west of I-310—based on an extension of the 1966 analysis—was 10.8 ft compared to 11.4 ft for the 2007 JPA.

22. For those parishes with published preliminary FIRMs (at the Part was prepared) the FIS contractor (not the USACE) employed the 1D WHAFIS model to define general inland 100-yr wave hazards (VE Zones) associated with the 2007 JPA 100-yr SWL results. St. Tammany Parish is appealing preliminary FIRMs on the basis of inaccurate 1D transect information and wave transformation parameters.

23. The southeast Louisiana FIS project team also undertook a JPA using the Surge Response-OS approach for southwest Louisiana. The southwest Louisiana FIS employed the same 19 CP-R_{max}-V_f variations and number and variations of tracks, together with the same validated ADCIRC/STWAVE model and 2007 mesh. Following publication of preliminary FIRMs Cameron Parish retained a team to recommend improvements in the local surge and wave JPA results, including modifying model inputs for topography and Manning's *n*.

24. To date there have been two very limited applications of the JPM-OS approach for southeast Louisiana. Both applications supported a JPA used in a "planning level" relative comparison of residual hazards associated with selected protection alternatives (e.g., polder inundation hazards associated with overtopping and breaching). These JPM-OS were not sufficiently developed to provide reasonable estimates of the actual surge or inundation hazard.

    i. IPET improvised use of 76 of the southeast Louisiana Surge Response-OS 152 storms for a JPM-OS. IPET assigned fractional probabilities to individual storms and their surge results, although the set was not developed to include storms with a suitable probability range (i.e., the set was developed as a Surge Response OS and did not include any landfalling Category 5 hurricanes). The IPET 76-storm JPM-OS was not representative of hurricane intensity above the 200-yr return period. IPET's 500-yr surge SWL for St. Charles Parish west of I-310 was 24% lower than the 2007 FIS JPA value. The 76-storm set also has other limitations associated with its small size and not being optimized to represent regional surge hazard.

    The IPET Study defined epistemic and aleatory uncertainty sources totaling to a σ_{Σ} of about 2.6 ft at a 10 ft SWL, or a 90% interval of ±4.3 ft, smaller than identified by the FIS JPA. The IPET study employed only the epistemic portion of the uncertainty—σ of about 1 ft at a 10 ft SWL plus skewed uncertainty associated with ε_{CP}—in the final development of confidence intervals around the JPA.

ii. The 2012 State of Louisiana Master Plan team employed a truncated version of the IPET JPM-OS approach. The Master Plan JPM-OS assigned fractional joint probabilities to 40 of the 152 storms—which included four CP-R_{max} combinations, each applied to 10 basic tracks spaced across the full Louisiana coast (one heading for 10 landfall locations). Given the characteristics of the 152-storm Surge Response-OS, the 40-storm set (like the IPET 76-storm set) was not suitable for representing hurricane intensities above the 200-yr return period. Even more than the IPET set, the 40-storm set has limitations associated with small size and not being representative of the regional and local surge hazards.

25. Since the application of the Surge Response-OS to the Louisiana coastal FIS, ensuing coastal FISs have primarily adopted the JPM-OS approach. Some recent surge JPAs are also expanding the hurricane attributes.

i. One other FIS—for Texas, which is being performed by the same team that undertook the Louisiana FIS—has employed the Surge Response-OS approach. The Texas Surge Response-OS reportedly includes about 360 storms—two 180 storm sets for north and south coastal regions.

ii. The Mississippi FIS used a JPM-OS approach, with a 152-storm set optimized versus hurricane joint probability and further refined to represent a benchmark surge hazard. The team employed the same hurricane attributes used in the Louisiana FIS. The team produced a benchmark surge hazard using a simplified SLOSH model of the Mississippi coast and close to 3,000 storms. The integration approach for the Mississippi project included smoothing using a σ_{Σ} of 2.2 ft at a SWL of 10 ft, equivalent to a 90% interval of about ±3.4 ft. The team determined VE Zones associated with the 100-yr SWL hazard using WHAFIS.

iii. In the GoM, the JPM-OS approach is being employed for the Florida—Big Bend and Northwest Florida/Alabama FISs. In the former study the surge hazard benchmark was created with 3,263 storms and a regional SLOSH model, resulting in selection of a 159-storm JPM-OS. For the latter study, the benchmark set and OS reportedly approximating 4,000 and several hundred storms, respectively.

iv. The North Carolina FIS team is using a 675-storm JPM-OS, reflecting combinations of historical tracks with incremental adjustments to storm CDP, R_{max}, Holland B, V_f, , and variations in θ. The North Carolina team compared the return period wind results at five locations for the 675 storm JPM-OS versus results from Vickery's wind JPA, which employed a much larger Monte Carlo based storm set.

v. The South Carolina and Northeast Florida/Georgia FISs are also using JPM-OS. The former with a 122-storm JPM-OS, based on comparison with a SLOSH surge hazard benchmark. The latter study is expected to have a JPM-OS on the order 200 to 300 storm and is being developed in comparison against a lower resolution ADCIRC surge hazard benchmark employing several thousand storms.

vi. The JPM-OS approach is expected to be employed in upcoming FISs for the Central Atlantic and the West GoM Florida Coasts.

Recommendations

The above conclusions indicate that the JPA approach employed in southeast Louisiana surge hazard analysis is outdated, particularly given advances in other FISs over recent years. They also provide the basis for recommendations to improve hurricane surge hazard analysis for southeast Louisiana. Four specific recommendations to update the surge hazard analysis include:

1. Employ a true JPM-OS approach with a much expanded set size (e.g., hundreds of storms) in the surge JPA. The JPM-OS should be determined using appropriate regional wind and surge benchmarks. The surge benchmark should sufficiently capture critical nonlinear responses and surge hazard conditions—particularly around large sheltered water bodies. Sensitivity tests should be used to examine the scope of regional nonlinear surge response and surge hazard conditions. Alternatively, the revised surge JPA can employ a Monte Carlo JPM or an expanded Surge Response-OS—with sufficient storms addressing nonlinear surge response.
2. Rigorously validate the surge JPA versus tide gauge-based return frequency analyses to evaluate potential bias in JPA results.
3. Employ an integration method which provides the median estimated CDF.. Sensitivity tests should be conducted on possible variations to the integration method to identify the best approach.
4. Define and quantify all sources of normally and non-normally distributed uncertainty contributing to the overall uncertainty in the surge hazard analysis, including uncertainties in the hurricane climatology, wind/surge/wave model, the selected surge JPA method, and set size. Prepare uncertainty intervals for the estimated CDF based on all sources of uncertainty.

The Louisiana CPRA, together with federal partners, should fund critical research to improve surge hazard analysis, including:

1. Expand the number of high quality long-term regional gauge records. Long-term records for several regional USGS and USACE gauges can be enhanced by addressing datum and gap issues.
2. Further evaluate appropriate return frequency distribution equations for the analysis of tide gauge records. In particular, equations should provide reasonable treatment of extreme historical observations.
3. Examine nonlinear surge response and surge hazard conditions for complex coastlines, including sheltered water bodies, particularly for southeast Louisiana.
4. Assess JPM approaches and set size optimization, CDF integration techniques, and the estimation and treatment of hazard uncertainty.
5. Study JPM wind field (10-min average) representation of surge forcing conditions
6. Investigate methods for wave hazard analysis. Such as the appropriate application of 1D overland wave modeling (WHAFIS transect selection and attribution, local wind-wave boundary conditions, wave transformation parameters, etc.) and determining those locations and conditions where more advanced modeling (2D, Boussinesq, etc.) should be applied.

The above recommendations can mitigate systemic and localized bias in estimates of surge hazard. Notably, localized bias is typically of less import to the NFIP than to the community, which must deal with the consequences of over- or under-estimating flood hazards.

However, it is important to recognize the large uncertainty that remains in estimated surge hazard based on either gauge records or JPA—i.e., 50%-plus for the 100-yr return at the 90% confidence level and much higher at the 500-yr return. Much of this uncertainty is associated with limitations inherent in hurricane climatological and surge records. In the near-term, methodological improvements and research are not likely to yield major reductions in uncertainty.

Part III. References

Blanton, B. O., P. J. Vickery, North Carolina Coastal Flood Analysis System: Hurricane Parameter Development, A Draft Report for the State of North Carolina, Floodplain Mapping Project, Technical Report TR-08-06 September 12, 2008.

FEMA, Atlantic Ocean and Gulf of Mexico Coastal Guidelines Update, February 2007.

FEMA, Hancock Co. Preliminary FIRM, Panel 295, November 2007, http://geology.deq.ms.gov/floodmaps/Projects/MapMOD/panels/28045C0295.pdf

Fitzpatrick, P. J., N. Tran, Y. Li, Y. Lau, and C. M. Hill, A Proposed New Storm Surge Scale, Geosystems Research Institute, Mississippi State University, BLDG 1103, Room 108, Stennis Space Center, MS 39529 USA. June 2010. http://www.drfitz.net/uploads/fitz_ocean_surge_scale_ieee_certified.pdf

Ho, F.P and V.A. Myers, Joint Probability Method of Tide Frequency Analysis Applied to Apalachicola Bay and St. George Sound, Florida, NOAA Tech. Rep. NWS 18, 1975.

Interagency Performance Evaluation Task Force (IPET), Performance Evaluation of the New Orleans and Southeast Louisiana Hurricane Protection System, Volumes VIII, Engineering and Operational Risk and Reliability Analysis, U.S. Army Corps of Engineers, June 2009.

Irish, J. L., D. T. Resio and M. A. Cialone, A surge response function approach to coastal hazard assessment. Part 2: Quantification of spatial attributes of response functions, Natural Hazards, Vol. 51, No. 1, 2009

Jonathan, P. and K. Ewans, ,A Spatiodirectional Model for Extreme Waves in the Gulf of Mexico, Journal of Offshore Mechanics and Arctic Engineering, Vo. 133, February 2011.

Jonathan, P. and K. Ewans, Modeling the Seasonality of Extreme Waves in the Gulf of Mexico, Journal of Offshore Mechanics and Arctic Engineering, Vo. 133, May 2011.

Jacobsen, R. W. and N. Dill, Assessing Baseline and Modified Astronomical Tide Propagation in the Pontchartrain Basin Using ADCIRC, for the USACE Louisiana Coastal Protection and Restoration Study, URS Corporation, July 2007.

Louisiana Coastal Protection and Restoration Authority (Louisiana CPRA), Louisiana's Comprehensive Master Plan for a Sustainable Coast, 2012.

McCorquodale, J. A., I. Georgiou , A. G. Retana, D. Barbe, M. J. Guillot, Hydrodynamic modeling of the Tidal Prism in the Pontchartrain Basin, Final Report, for the USACE Louisiana Coastal Protection and Restoration Study, June 2007.

National Research Council of the National Academies, Mapping the Zone: Improving Flood Map Accuracy, Committee on FEMA Flood Maps, Board on Earth Sciences and Resources/Mapping Science Committee, Water Science and Technology Board, The National Academies Press, Washington D. C., 2009.

Needham, H., Identifying Historic Storm Surges and Calculating Storm Surge Return Periods for the Gulf of Mexico Coast, Master's Thesis, Louisiana State University, Department of Geography and Anthropology, May 2010.

NOAA, Tidal and Geodetic Datums: Tidal and Geodetic Relationships, (no date) http://www.laseagrant.org/pdfs/NOAA_TidalGeodeticRelationships.pdf

NOAA, Tides an Currents, Extreme Water Levels, Website. http://tidesandcurrents.noaa.gov/est/

NOAA-NDBC, Website. http://www.ndbc.noaa.gov/

NOAA-NWS, (Ho, F. P., J. C. Su, K. L. Hanevich, R. J. Smith, and F. P. Richards) Hurricane Climatology for the Atlantic and Gulf Coasts of the United States, NOAA Technical Report NWS 38, April 1987.

Northwest Florida Water Management District, Scoping Report for the Coastal Remapping Study of Northwest Florida, Revised December 22, 2010, http://www.nwfwmdfloodmaps.com/pdf/Coastal_Remapping_Study_FinalReport.pdf

Northwest Florida Water Management District, Coastal Modeling and DFIRM Production Technical Approach Report for Coastal Northwest Florida, Revised October 3, 2011, http://www.nwfwmdfloodmaps.com/documents/TechnicalApproachReport10311.pdf

Panchang, V. G. and L Dongcheng, Large Waves in the Gulf of Mexico Caused by Hurricane Ivan, Bulletin of the American Meteorological Society, April 2006.

Resio, D. T., S. J. Boc, L. Borgman, V. J. Cardone, A. Cox, W. R. Dally, R. G. Dean, D. Divoky, E. Hirsh, J. L. Irish, D. Levinson, A. Niederoda, M. D. Powell, J. J. Ratcliff, V. Stutts, J. Suhada, G. R. Toro, and P. J. Vickery, White Paper on Estimating Hurricane Inundation Probabilities, U.S. Army Corps of Engineers, ERDC-CHL, 2007.

Resio, D. T., J. L., and M. A. Cialone, A surge response function approach to coastal hazard assessment. Part 1: Basic concepts, Natural Hazards, Vol. 51, No. 1, 2009.

Resio, D. T., J. L. Irish, J. J. Westerink, N. J. Powell, The Effect of Uncertainty on Estimates of Hurricane Surge Hazards, Natural Hazards, October 2012.

Smith, J. M., Modeling Nearshore Waves for Hurricane Katrina, USACE Engineer Research and Development Center, Coastal and Hydraulics Laboratory, August 2007. http://chl.erdc.usace.army.mil/Media/9/3/7/tnswwrp-07-6.pdf

Suhayda, J. N., Flood Insurance Rate Map Revision Request for Cameron Parish, Vol. I, Cameron Parish Police Jury, 1989.

Toro, G. R., Joint Probability Analysis of Hurricane Flood Hazard for Mississippi, Final Report, Revision 1. Prepared for URS Group, Tallahassee, FL, in support of the FEMA-HMTAP, Flood Study of the State of Mississippi, Risk Engineering, Inc. 4155 Darley Avenue, Suite A Boulder, CO 80305. June 23, 2008.

URS Corporation, Preliminary Flood Frequency Analysis for Hurricane Katrina, for FEMA, 2005

URS Corporation, Mitigation Assessment Team Report, Hurricane Katrina in the Gulf Coast, for FEMA, 2006. http://www.fema.gov/library/viewRecord.do?id=1857

URS Corporation, Mississippi Coastal Analysis Project, Coastal Documentation and Main Engineering Report, Final Report: HMTAP Task Order 18, for Federal Emergency Management Agency, June 17, 2008.

USACE, Lake Pontchartrain, Louisiana and Vicinity, Design Memorandum No. 1, Hydrology and Hydraulic Analysis, Part I Chalmette, August 1966.

USACE, Lake Pontchartrain, Louisiana and Vicinity, Lake Pontchartrain High Level Plan, Design Memorandum No. 18, General Design, St. Charles Parish North of Airline Highway, February 1989.

USACE, Coastal Engineering Manual, EM1110-2-1100, April 2005.

USACE, Southeast Louisiana Joint Surge Study, Independent Technical Review, Final Report, for FEMA, October 15, 2007.

USACE, Flood Insurance Study, Southeast Parishes of Louisiana, Intermediate Submission 2: Offshore Water Levels and Waves, for FEMA, July 2008.

USACE, Louisiana Coastal Protection and Restoration, Final Technical Report, June 2009.

USACE (New Orleans District), Hurricane and Storm Damage Risk Reduction System, Design Elevation Report, Draft Report Version 4.0, August 18, 2010.

USACE, Supporting Information for Southeast Louisiana JPM-OS on 152 Hurricanes Provided by Nancy Powell, 2011.

USACE, Supporting Information for Southeast Louisiana JPM-OS, Results for 2007 Condition, Provided by Dr. Jay Ratcliff together with personal communication on JPM-OS methodology, May 2012

Wamsley, T. V., M. A. Cialone, J. Westerink, and J, M. Smith, Influence of Marsh Restoration and Degradation on Storm Surge and Waves, USACE, ERDC/CHL CHETN-I-77, July 2009.

Xu, L. A Simple Coastline Storm Surge Model Based on Pre-Run SLOSH Outputs, 29th Conference on Hurricanes and Tropical Meteorology, May 2010.

Xu, S. and W. Huang, Integrated Hydrodynamic Modeling and Frequency Analysis for Predicting 1% Storm Surge, Journal of Coastal Research, No. 10052, Pages 253-260. 2008.

Zervas, C. E., Response of Extreme Storm Tide Levels to Long-term Sea Level Change, in Oceans 2005, IEEE, 2005, http://tidesandcurrents.noaa.gov/est/050415-53.pdf

Attachment 1

Attributes for 152 Hurricanes for Southeast Louisiana Hurricane JPA

Sources:

Interagency Performance Evaluation Task Force (IPET), Performance Evaluation of the New Orleans and Southeast Louisiana Hurricane Protection System, Volumes VIII, Engineering and Operational Risk and Reliability Analysis, Appendix 9 Risk Methodology, U.S. Army Corps of Engineers, June 2009.

Resio, D. T., S. J. Boc, L. Borgman, V. J. Cardone, A. Cox, W. R. Dally, R. G. Dean, D. Divoky, E. Hirsh, J. L. Irish, D. Levinson, A. Niederoda, M. D. Powell, J. J. Ratcliff, V. Stutts, J. Suhada, G. R. Toro, and P. J. Vickery, White Paper on Estimating Hurricane Inundation Probabilities, U.S. Army Corps of Engineers, ERDC-CHL, 2007.

USACE, Flood Insurance Study, Southeast Parishes of Louisiana, Intermediate Submission 2: Offshore Water Levels and Waves, July 2008.

Southeast Louisiana JPM-OS Hurricanes

FIS Documentation

No.	GoM CP mb	Peak GoM Winds 30 min (m/s)	(mph)	1-min (mph)	Rmax nm	mile	Vf kn	mph	Track	P or S	θ	Landfall CP mb	Peak Landfall Winds 30 min (m/s)	(mph)	1-min (mph)	SS Category GoM	Landfall
1	960	45	100.7	124.8	11.0	12.7	11	12.7	Central 1	P	0	960	43.1	96.4	119.6	3	3
2	960	43.9	98.2	121.8	21.0	24.2	11	12.7	Central 1	P	0	977	31.5	70.5	87.4	3	2
3	960	42.2	94.4	117.1	35.6	40.9	11	12.7	Central 1	P	0	981	28.9	64.6	80.2	3	2
4	930	52.8	118.1	146.5	8.0	9.2	11	12.7	Central 1	P	0	930	51.2	114.5	142.0	4	4
5	930	52.5	117.4	145.6	17.7	20.4	11	12.7	Central 1	P	0	943	41.2	92.2	114.3	4	3
6	930	51.8	115.9	143.7	25.8	29.7	11	12.7	Central 1	P	0	951	38.8	86.8	107.6	4	3
7	900	57.2	128.0	158.7	6.0	6.9	11	12.7	Central 1	P	0	900	55.3	123.7	153.4	5	4
8	900	58.4	130.6	162.0	14.9	17.1	11	12.7	Central 1	P	0	910	48.4	108.3	134.3	5	4
9	900	57.9	129.5	160.6	21.8	25.1	11	12.7	Central 1	P	0	918	46.6	104.2	129.3	5	3
10	960	45.1	100.9	125.1	11.0	12.7	11	12.7	Central 2	P	0	960	44.2	98.9	122.6	3	3
11	960	43.9	98.2	121.8	21.0	24.2	11	12.7	Central 2	P	0	977	31.7	70.9	87.9	3	2
12	960	42.1	94.2	116.8	35.6	40.9	11	12.7	Central 2	P	0	981	29.0	64.9	80.4	3	2
13	930	52.8	118.1	146.5	8.0	9.2	11	12.7	Central 2	P	0	930	51.3	114.8	142.3	4	4
14	930	52.4	117.2	145.3	17.7	20.4	11	12.7	Central 2	P	0	943	41.3	92.4	114.6	4	3
15	930	51.7	115.6	143.4	25.8	29.7	11	12.7	Central 2	P	0	951	38.9	87.0	107.9	4	3
16	900	57.2	128.0	158.7	6.0	6.9	11	12.7	Central 2	P	0	900	55.4	123.9	153.7	5	4
17	900	58.3	130.4	161.7	14.9	17.1	11	12.7	Central 2	P	0	910	48.5	108.5	134.5	5	4
18	900	57.8	129.3	160.3	21.8	25.1	11	12.7	Central 2	P	0	918	46.7	104.5	129.5	5	3
19	960	45	100.7	124.8	11.0	12.7	11	12.7	Central 3	P	0	960	44.2	98.9	122.6	3	3
20	960	43.7	97.8	121.2	21.0	24.2	11	12.7	Central 3	P	0	977	31.7	70.9	87.9	3	2
21	960	42.2	94.4	117.1	35.6	40.9	11	12.7	Central 3	P	0	981	29.1	65.1	80.7	3	2
22	930	52.8	118.1	146.5	8.0	9.2	11	12.7	Central 3	P	0	930	51.2	114.5	142.0	4	4
23	930	52.3	117.0	145.1	17.7	20.4	11	12.7	Central 3	P	0	943	41.5	92.8	115.1	4	3
24	930	51.7	115.6	143.4	25.8	29.7	11	12.7	Central 3	P	0	951	38.9	87.0	107.9	4	3
25	900	57.2	128.0	158.7	6.0	6.9	11	12.7	Central 3	P	0	900	55.9	125.0	155.1	5	4
26	900	58.1	130.0	161.2	14.9	17.1	11	12.7	Central 3	P	0	910	48.7	108.9	135.1	5	4
27	900	57.7	129.1	160.0	21.8	25.1	11	12.7	Central 3	P	0	918	46.8	104.7	129.8	5	3
28	960	44.9	100.4	124.5	11.0	12.7	11	12.7	Central 4	P	0	960	43.5	97.3	120.7	3	3
29	960	43.8	98.0	121.5	21.0	24.2	11	12.7	Central 4	P	0	977	31.2	69.8	86.5	3	2
30	960	42.1	94.2	116.8	35.6	40.9	11	12.7	Central 4	P	0	981	28.8	64.4	79.9	3	2
31	930	52.6	117.7	145.9	8.0	9.2	11	12.7	Central 4	P	0	930	51.2	114.5	142.0	4	4
32	930	52.6	117.7	145.9	17.7	20.4	11	12.7	Central 4	P	0	943	41.1	91.9	114.0	4	3
33	930	51.7	115.6	143.4	25.8	29.7	11	12.7	Central 4	P	0	951	38.6	86.3	107.1	4	3
34	900	57.3	128.2	158.9	6.0	6.9	11	12.7	Central 4	P	0	900	55.1	123.3	152.8	5	4
35	900	58.1	130.0	161.2	14.9	17.1	11	12.7	Central 4	P	0	910	48.3	108.0	134.0	5	4
36	900	57.8	129.3	160.3	21.8	25.1	11	12.7	Central 4	P	0	918	46.5	104.0	129.0	5	3
37	960	44.9	100.4	124.5	11.0	12.7	11	12.7	Central 5	P	0	960	43.4	97.1	120.4	3	3
38	960	43.7	97.8	121.2	21.0	24.2	11	12.7	Central 5	P	0	977	31.0	69.3	86.0	3	2
39	960	42.2	94.4	117.1	35.6	40.9	11	12.7	Central 5	P	0	981	28.7	64.2	79.6	3	2
40	930	52.7	117.9	146.2	8.0	9.2	11	12.7	Central 5	P	0	930	50.7	113.4	140.6	4	4
41	930	52.3	117.0	145.1	17.7	20.4	11	12.7	Central 5	P	0	943	40.9	91.5	113.4	4	3
42	930	51.8	115.9	143.7	25.8	29.7	11	12.7	Central 5	P	0	951	38.3	85.7	106.2	4	3
43	900	57.2	128.0	158.7	6.0	6.9	11	12.7	Central 5	P	0	900	55.5	124.1	153.9	5	4
44	900	58	129.7	160.9	14.9	17.1	11	12.7	Central 5	P	0	910	48.2	107.8	133.7	5	4
45	900	57.6	128.8	159.8	21.8	25.1	11	12.7	Central 5	P	0	918	46.1	103.1	127.9	5	3
46	960	44.3	99.1	122.9	18.2	20.9	11	12.7	SE 1	P	-45	974	33.0	73.8	91.5	3	2
47	960	43.5	97.3	120.7	24.6	28.3	11	12.7	SE 1	P	-45	980	30.5	68.2	84.6	3	2
48	900	58.3	130.4	161.7	12.5	14.4	11	12.7	SE 1	P	-45	909	55.6	124.4	154.2	5	4
49	900	58.1	130.0	161.2	18.4	21.2	11	12.7	SE 1	P	-45	920	46.3	103.6	128.4	5	3
50	960	44.2	98.9	122.6	18.2	20.9	11	12.7	SE 2	P	-45	974	33.2	74.3	92.1	3	2
51	960	43.3	96.9	120.1	24.6	28.3	11	12.7	SE 2	P	-45	980	30.5	68.2	84.6	3	2
52	900	58.2	130.2	161.4	12.5	14.4	11	12.7	SE 2	P	-45	909	55.4	123.9	153.7	5	4
53	900	58	129.7	160.9	18.4	21.2	11	12.7	SE 2	P	-45	920	46.2	103.3	128.1	5	3
54	960	43.8	98.0	121.5	18.2	20.9	11	12.7	SE 3	P	-45	974	33.0	73.8	91.5	3	2
55	960	43.1	96.4	119.6	24.6	28.3	11	12.7	SE 3	P	-45	980	30.5	68.2	84.6	3	2
56	900	58	129.7	160.9	12.5	14.4	11	12.7	SE 3	P	-45	909	55.5	124.1	153.9	5	4
57	900	57.5	128.6	159.5	18.4	21.2	11	12.7	SE 3	P	-45	920	46.2	103.3	128.1	5	3
58	960	43.6	97.5	120.9	18.2	20.9	11	12.7	SE 4	P	-45	974	32.9	73.6	91.3	3	2

IPET Documentation

No.	Storm Frequency per yr	GoM CP mb	Rmax nm	Vf kn	Holland's B	Track angle at landfall	Track Identifer
1	7.90E-04	960	11	11	1.27	0	1
2	9.19E-04	960	21	11	1.27	0	1
3	4.92E-04	960	35.6	11	1.27	0	1
4	2.50E-03	930	8	11	1.27	0	1
5	2.73E-03	930	17.7	11	1.27	0	1
6	2.30E-03	930	25.8	11	1.27	0	1
7	1.13E-03	900	6	11	1.27	0	1
8	1.39E-03	900	14.9	11	1.27	0	1
9	3.46E-04	900	21.8	11	1.27	0	1
10	7.90E-04	960	11	11	1.27	0	2
11	9.19E-04	960	21	11	1.27	0	2
12	4.92E-04	960	35.6	11	1.27	0	2
13	2.50E-03	930	8	11	1.27	0	2
14	2.73E-03	930	17.7	11	1.27	0	2
15	2.30E-03	930	25.8	11	1.27	0	2
16	1.13E-03	900	6	11	1.27	0	2
17	1.39E-03	900	14.9	11	1.27	0	2
18	3.46E-04	900	21.8	11	1.27	0	2
19	7.90E-04	960	11	11	1.27	0	3
20	9.19E-04	960	21	11	1.27	0	3
21	4.92E-04	960	35.6	11	1.27	0	3
22	2.50E-03	930	8	11	1.27	0	3
23	2.73E-03	930	17.7	11	1.27	0	3
24	2.30E-03	930	25.8	11	1.27	0	3
25	1.13E-03	900	6	11	1.27	0	3
26	1.39E-03	900	14.9	11	1.27	0	3
27	3.46E-04	900	21.8	11	1.27	0	3
28	7.90E-04	960	11	11	1.27	0	4
29	9.19E-04	960	21	11	1.27	0	4
30	4.92E-04	960	35.6	11	1.27	0	4
31	2.50E-03	930	8	11	1.27	0	4
32	2.73E-03	930	17.7	11	1.27	0	4
33	2.30E-03	930	25.8	11	1.27	0	4
34	1.13E-03	900	6	11	1.27	0	4
35	1.39E-03	900	14.9	11	1.27	0	4
36	3.46E-04	900	21.8	11	1.27	0	4
37	7.90E-04	960	11	11	1.27	0	5
38	9.19E-04	960	21	11	1.27	0	5
39	4.92E-04	960	35.6	11	1.27	0	5
40	2.50E-03	930	8	11	1.27	0	5
41	2.73E-03	930	17.7	11	1.27	0	5
42	2.30E-03	930	25.8	11	1.27	0	5
43	1.13E-03	900	6	11	1.27	0	5
44	1.39E-03	900	14.9	11	1.27	0	5
45	3.46E-04	900	21.8	11	1.27	0	5
46	3.50E-04	960	18.2	11	1.27	-45	1
47	3.90E-04	960	24.6	11	1.27	-45	1
48	7.16E-04	900	12.5	11	1.27	-45	1
49	5.48E-04	900	18.4	11	1.27	-45	1
50	3.50E-04	960	18.2	11	1.27	-45	2
51	3.90E-04	960	24.6	11	1.27	-45	2
52	7.16E-04	900	12.5	11	1.27	-45	2
53	5.48E-04	900	18.4	11	1.27	-45	2
54	3.50E-04	960	18.2	11	1.27	-45	3
55	3.90E-04	960	24.6	11	1.27	-45	3
56	7.16E-04	900	12.5	11	1.27	-45	3
57	5.48E-04	900	18.4	11	1.27	-45	3
58	3.50E-04	960	18.2	11	1.27	-45	4.1

Southeast Louisiana JPM-OS Hurricanes

FIS Documentation

No.	GoM CP mb	Peak GoM Winds 30 min (m/s)	30 min (mph)	1-min (mph)	Rmax nm	Rmax mile	Vf kn	Vf mph	Track	P or S	θ	Landfall CP mb	Peak Landfall Winds 30 min (m/s)	30 min (mph)	1-min (mph)	SS Category GoM	SS Category Landfall
59	960	42.9	96.0	119.0	24.6	28.3	11	12.7	SE 4	P	-45	980	30.4	68.0	84.3	3	2
60	900	57.8	129.3	160.3	12.5	14.4	11	12.7	SE 4	P	-45	909	55.3	123.7	153.4	5	4
61	900	57.6	128.8	159.8	18.4	21.2	11	12.7	SE 4	P	-45	920	46.3	103.6	128.4	5	3
66	960	44.4	99.3	123.2	18.2	20.9	11	12.7	SW 1	P	45	974	32.7	73.1	90.7	3	2
67	960	42.9	96.0	119.0	24.6	28.3	11	12.7	SW 1	P	45	980	30.1	67.3	83.5	3	2
68	900	58.8	131.5	163.1	12.5	14.4	11	12.7	SW 1	P	45	909	55.7	124.6	154.5	5	4
69	900	58.3	130.4	161.7	18.4	21.2	11	12.7	SW 1	P	45	920	46.1	103.1	127.9	5	3
70	960	44.2	98.9	122.6	18.2	20.9	11	12.7	SW 2	P	45	974	32.7	73.1	90.7	3	2
71	960	43.6	97.5	120.9	24.6	28.3	11	12.7	SW 2	P	45	980	30.1	67.3	83.5	3	2
72	900	58.6	131.1	162.5	12.5	14.4	11	12.7	SW 2	P	45	909	55.4	123.9	153.7	5	4
73	900	58.2	130.2	161.4	18.4	21.2	11	12.7	SW 2	P	45	920	45.8	102.5	127.0	5	3
74	960	44.1	98.6	122.3	18.2	20.9	11	12.7	SW 3	P	45	974	32.5	72.7	90.1	3	2
75	960	43.6	97.5	120.9	24.6	28.3	11	12.7	SW 3	P	45	980	29.9	66.9	82.9	3	2
76	900	58.6	131.1	162.5	12.5	14.4	11	12.7	SW 3	P	45	909	55.1	123.3	152.8	5	4
77	900	58.2	130.2	161.4	18.4	21.2	11	12.7	SW 3	P	45	920	45.6	102.0	126.5	5	3
Total																	
78	960	44.1	98.6	122.3	18.2	20.9	11	12.7	SW 4	P	45	974	32.6	72.9	90.4	3	2
79	960	43.6	97.5	120.9	24.6	28.3	11	12.7	SW 4	P	45	980	30.0	67.1	83.2	3	2
80	900	58.6	131.1	162.5	12.5	14.4	11	12.7	SW 4	P	45	909	54.9	122.8	152.3	5	4
81	900	58.2	130.2	161.4	18.4	21.2	11	12.7	SW 4	P	45	920	45.7	102.2	126.8	5	3
82	960	40.4	90.4	112.1	17.7	20.4	6	6.9	Central 1	P	0	973	30.5	68.2	84.6	3	2
83	900	55.6	124.4	154.2	17.7	20.4	6	6.9	Central 1	P	0	913	45.5	101.8	126.2	4	3
84	960	40.5	90.6	112.3	17.7	20.4	6	6.9	Central 2	P	0	973	30.5	68.2	84.6	3	2
85	900	55.7	124.6	154.5	17.7	20.4	6	6.9	Central 2	P	0	913	45.5	101.8	126.2	4	3
86	960	40.3	90.1	111.8	17.7	20.4	6	6.9	Central 3	P	0	973	30.3	67.8	84.0	3	2
87	900	55.5	124.1	153.9	17.7	20.4	6	6.9	Central 3	P	0	913	45.2	101.1	125.4	4	3
88	960	40.5	90.6	112.3	17.7	20.4	6	6.9	Central 4	P	0	973	30.2	67.6	83.8	3	2
89	900	55.8	124.8	154.8	17.7	20.4	6	6.9	Central 4	P	0	913	45.3	101.3	125.7	4	3
90	960	40.4	90.4	112.1	17.7	20.4	6	6.9	Central 5	P	0	973	30.0	67.1	83.2	3	2
91	900	55.5	124.1	153.9	17.7	20.4	6	6.9	Central 5	P	0	913	45.1	100.9	125.1	4	3
92	930	48.8	109.2	135.4	17.7	20.4	6	6.9	SE 1	P	-45	946	37.6	84.1	104.3	4	3
93	930	48.9	109.4	135.6	17.7	20.4	6	6.9	SE 2	P	-45	946	37.6	84.1	104.3	4	3
94	930	48.8	109.2	135.4	17.7	20.4	6	6.9	SE 3	P	-45	946	37.5	83.9	104.0	4	3
95	930	48.7	108.9	135.1	17.7	20.4	6	6.9	SE 4	P	-45	946	37.6	84.1	104.3	4	3
97	930	49.3	110.3	136.7	17.7	20.4	6	6.9	SW 1	P	45	946	37.3	83.4	103.5	4	3
98	930	49.2	110.1	136.5	17.7	20.4	6	6.9	SW 2	P	45	946	37.3	83.4	103.5	4	3
99	930	49.3	110.3	136.7	17.7	20.4	6	6.9	SW 3	P	45	946	37.3	83.4	103.5	4	3
100	930	49.3	110.3	136.7	17.7	20.4	6	6.9	SW 4	P	45	946	37.2	83.2	103.2	4	3
101	930	55.9	125.0	155.1	17.7	20.4	17	19.6	Central 1	P	0	944	45.0	100.7	124.8	4	3
102	930	55.8	124.8	154.8	17.7	20.4	17	19.6	Central 2	P	0	944	44.8	100.2	124.3	4	3
103	930	56	125.3	155.3	17.7	20.4	17	19.6	Central 3	P	0	944	44.9	100.4	124.5	4	3
104	930	56	125.3	155.3	17.7	20.4	17	19.6	Central 4	P	0	944	44.5	99.5	123.4	4	3
105	930	56	125.3	155.3	17.7	20.4	17	19.6	Central 5	P	0	944	44.2	98.9	122.6	4	3
106	930	55.9	125.0	155.1	17.7	20.4	17	19.6	SE 1	P	-45	946	44.1	98.6	122.3	4	3
107	930	55.7	124.6	154.5	17.7	20.4	17	19.6	SE 2	P	-45	946	44.3	99.1	122.9	4	3
108	930	55.8	124.8	154.8	17.7	20.4	17	19.6	SE 3	P	-45	946	44.2	98.9	122.6	4	3
109	930	55.4	123.9	153.7	17.7	20.4	17	19.6	SE 4	P	-45	946	44.0	98.4	122.0	4	3

IPET Documentation

No.	Storm Frequency per yr	GoM CP mb	Rmax nm	Vf kn	Holland's B	Track angle at landfall	Track Identifer
59	3.90E-04	960	24.6	11	1.27	-45	4.1
60	7.16E-04	900	12.5	11	1.27	-45	4.1
61	5.48E-04	900	18.4	11	1.27	-45	4.1
63	2.50E-04	960	24.6	11	1.27	45	1
64	3.02E-04	900	12.5	11	1.27	45	1
65	2.01E-04	900	18.4	11	1.27	45	1
66	1.54E-04	960	18.2	11	1.27	45	2
67	2.50E-04	960	24.6	11	1.27	45	2
68	3.02E-04	900	12.5	11	1.27	45	2
69	2.01E-04	900	18.4	11	1.27	45	2
70	1.54E-04	960	18.2	11	1.27	45	3
71	2.50E-04	960	24.6	11	1.27	45	3
72	3.02E-04	900	12.5	11	1.27	45	3
73	2.01E-04	900	18.4	11	1.27	45	3
74	1.54E-04	960	18.2	11	1.27	45	4
75	2.50E-04	960	24.6	11	1.27	45	4
76	3.02E-04	900	12.5	11	1.27	45	4
77	2.01E-04	900	18.4	11	1.27	45	4
76	**7.45E-02**						
62	Not Provided	960	18.2	11	1.27	45	1

IPET 63, 64, 65 appear to be FIS 79, 80, 81

No.	Storm Frequency per yr	GoM CP mb	Rmax nm	Vf kn	Holland's B	Track angle at landfall	Track Identifer
78	Not Provided	960	17.7	6	1.27	0	1
79	Not Provided	900	17.7	6	1.27	0	1
80	Not Provided	960	17.7	6	1.27	0	2
81	Not Provided	900	17.7	6	1.27	0	2
82	Not Provided	960	17.7	6	1.27	0	3
83	Not Provided	900	17.7	6	1.27	0	3
84	Not Provided	960	17.7	6	1.27	0	4
85	Not Provided	900	17.7	6	1.27	0	4
86	Not Provided	960	17.7	6	1.27	0	5
87	Not Provided	900	17.7	6	1.27	0	5
88	Not Provided	930	17.7	6	1.27	-45	1
89	Not Provided	930	17.7	6	1.27	-45	2
90	Not Provided	930	17.7	6	1.27	-45	3
91	Not Provided	930	17.7	6	1.27	-45	4.1
92	Not Provided	930	17.7	6	1.27	45	1
93	Not Provided	930	17.7	6	1.27	45	2
94	Not Provided	930	17.7	6	1.27	45	3
95	Not Provided	930	17.7	6	1.27	45	4
96	Not Provided	930	17.7	17	1.27	0	1
97	Not Provided	930	17.7	17	1.27	0	2
98	Not Provided	930	17.7	17	1.27	0	3
99	Not Provided	930	17.7	17	1.27	0	4
100	Not Provided	930	17.7	17	1.27	0	5
101	Not Provided	930	17.7	17	1.27	-45	1
102	Not Provided	930	17.7	17	1.27	-45	2
103	Not Provided	930	17.7	17	1.27	-45	3
104	Not Provided	930	17.7	17	1.27	-45	4.1

Southeast Louisiana JPM-OS Hurricanes

FIS Documentation

No.	GoM CP mb	Peak GoM Winds 30 min (m/s)	30 min (mph)	1-min (mph)	Rmax nm	Rmax mile	Vf kn	Vf mph	Track	P or S	θ	Landfall CP mb	Peak Landfall Winds 30 min (m/s)	30 min (mph)	1-min (mph)	SS Category GoM	SS Category Landfall
111	930	56.2	125.7	155.9	17.7	20.4	17	19.6	SW 1	P	45	946	43.7	97.8	121.2	4	3
112	930	56	125.3	155.3	17.7	20.4	17	19.6	SW 2	P	45	946	43.4	97.1	120.4	4	3
113	930	56.1	125.5	155.6	17.7	20.4	17	19.6	SW 3	P	45	946	43.3	96.9	120.1	4	3
114	930	56	125.3	155.3	17.7	20.4	17	19.6	SW 4	P	45	946	43.6	97.5	120.9	4	3
115	960	44.2	98.9	122.6	17.7	20.4	11	12.7	Central 1b	S	0	973	33.0	73.8	91.5	3	2
116	900	58.2	130.2	161.4	17.7	20.4	11	12.7	Central 1b	S	0	913	47.6	106.5	132.0	5	4
117	960	44.2	98.9	122.6	17.7	20.4	11	12.7	Central 2b	S	0	973	33.1	74.0	91.8	3	2
118	900	58	129.7	160.9	17.7	20.4	11	12.7	Central 2b	S	0	913	47.8	106.9	132.6	5	4
119	960	44.2	98.9	122.6	17.7	20.4	11	12.7	Central 3b	S	0	973	33.3	74.5	92.4	3	2
120	900	58	129.7	160.9	17.7	20.4	11	12.7	Central 3b	S	0	913	48.0	107.4	133.1	5	4
121	960	44.1	98.6	122.3	17.7	20.4	11	12.7	Central 4b	S	0	973	33.1	74.0	91.8	3	2
122	900	58	129.7	160.9	17.7	20.4	11	12.7	Central 4b	S	0	913	47.7	106.7	132.3	5	4
123	960	44.1	98.6	122.3	17.7	20.4	11	12.7	SE 1b	S	-45	974	33.3	74.5	92.4	3	2
124	960	43.8	98.0	121.5	17.7	20.4	11	12.7	SE 2b	S	-45	974	33.1	74.0	91.8	3	2
125	960	43.7	97.8	121.2	17.7	20.4	11	12.7	SE 3b	S	-45	974	32.7	73.1	90.7	3	2
126	900	58	129.7	160.9	17.7	20.4	11	12.7	SE 1b	S	-45	919	46.4	103.8	128.7	5	3
127	900	57.9	129.5	160.6	17.7	20.4	11	12.7	SE 2b	S	-45	919	46.5	104.0	129.0	5	3
128	900	57.8	129.3	160.3	17.7	20.4	11	12.7	SE 3b	S	-45	919	45.8	102.5	127.0	5	3
131	960	44.2	98.9	122.6	17.7	20.4	11	12.7	SW 1b	S	45	974	32.9	73.6	91.3	3	2
132	900	58.3	130.4	161.7	17.7	20.4	11	12.7	SW 1b	S	45	919	46.0	102.9	127.6	5	3
133	960	44.2	98.9	122.6	17.7	20.4	11	12.7	SW 2b	S	45	974	32.8	73.4	91.0	3	2
134	900	58.3	130.4	161.7	17.7	20.4	11	12.7	SW 2b	S	45	919	45.8	102.5	127.0	5	3
135	960	44.2	98.9	122.6	17.7	20.4	11	12.7	SW 3b	S	45	974	32.9	73.6	91.3	3	2
136	900	58.3	130.4	161.7	17.7	20.4	11	12.7	SW 3b	S	45	919	45.8	102.5	127.0	5	3
137	960	40.5	90.6	112.3	17.7	20.4	6	6.9	Central 1b	S	0	973	30.1	67.3	83.5	3	2
138	900	55.6	124.4	154.2	17.7	20.4	6	6.9	Central 1b	S	0	913	45.1	100.9	125.1	4	3
139	960	40.4	90.4	112.1	17.7	20.4	6	6.9	Central 2b	S	0	973	30.0	67.1	83.2	3	2
140	900	55.7	124.6	154.5	17.7	20.4	6	6.9	Central 2b	S	0	913	45.1	100.9	125.1	4	3
141	960	40.3	90.1	111.8	17.7	20.4	6	6.9	Central 3b	S	0	973	30.2	67.6	83.8	3	2
142	900	55.6	124.4	154.2	17.7	20.4	6	6.9	Central 3b	S	0	913	45.3	101.3	125.7	4	3
143	960	40.6	90.8	112.6	17.7	20.4	6	6.9	Central 4b	S	0	973	29.9	66.9	82.9	3	2
144	900	55.8	124.8	154.8	17.7	20.4	6	6.9	Central 4b	S	0	913	45.0	100.7	124.8	4	3
145	930	48.8	109.2	135.4	17.7	20.4	6	6.9	SE 1b	S	-45	946	37.5	83.9	104.0	4	3
146	930	48.9	109.4	135.6	17.7	20.4	6	6.9	SE 2b	S	-45	946	37.6	84.1	104.3	4	3
147	930	48.8	109.2	135.4	17.7	20.4	6	6.9	SE 3b	S	-45	946	37.2	83.2	103.2	4	3
149	930	49.3	110.3	136.7	17.7	20.4	6	6.9	SW 1b	S	45	946	37.3	83.4	103.5	4	3
150	930	49.4	110.5	137.0	17.7	20.4	6	6.9	SW 2b	S	45	946	37.0	82.8	102.6	4	3
151	930	49.4	110.5	137.0	17.7	20.4	6	6.9	SW 3b	S	45	946	37.5	83.9	104.0	4	3
152	930	55.8	124.8	154.8	17.7	20.4	17	19.6	Central 1b	S	0	944	44.7	100.0	124.0	4	3
153	930	55.8	124.8	154.8	17.7	20.4	17	19.6	Central 2b	S	0	944	44.5	99.5	123.4	4	3
154	930	55.9	125.0	155.1	17.7	20.4	17	19.6	Central 3b	S	0	944	44.8	100.2	124.3	4	3
155	930	56	125.3	155.3	17.7	20.4	17	19.6	Central 4b	S	0	944	44.6	99.8	123.7	4	3
156	930	55.9	125.0	155.1	17.7	20.4	17	19.6	SE 1b	S	-45	946	44.3	99.1	122.9	4	3
157	930	55.6	124.4	154.2	17.7	20.4	17	19.6	SE 2b	S	-45	946	44.1	98.6	122.3	4	3
158	930	55.3	123.7	153.4	17.7	20.4	17	19.6	SE 3b	S	-45	950	42.9	96.0	119.0	4	3
160	930	56	125.3	155.3	17.7	20.4	17	19.6	SW 1b	S	45	946	43.6	97.5	120.9	4	3
161	930	56.2	125.7	155.9	17.7	20.4	17	19.6	SW 2b	S	45	946	43.6	97.5	120.9	4	3
162	930	55.9	125.0	155.1	17.7	20.4	17	19.6	SW 3b	S	45	946	43.9	98.2	121.8	4	3
Total	**152**																

	in GoM	at Landfall
Number of Category 1	**0**	**0**
Number of Category 2	**0**	**45**
Number of Category 3	**50**	**80**
Number of Category 4	**61**	**27**
Number of Category 5	**41**	**0**

IPET Documentation

No.	Storm Frequency per yr	GoM CP mb	Rmax nm	Vf kn	Holland's B	Track angle at landfall	Track Identifer
105	Not Provided	930	17.7	17	1.27	45	1
106	Not Provided	930	17.7	17	1.27	45	2
107	Not Provided	930	17.7	17	1.27	45	3
108	Not Provided	930	17.7	17	1.27	45	4
109	Not Provided	960	17.7	11	1.27	0	1.5
110	Not Provided	900	17.7	11	1.27	0	1.5
111	Not Provided	960	17.7	11	1.27	0	2.5
112	Not Provided	900	17.7	11	1.27	0	2.5
113	Not Provided	960	17.7	11	1.27	0	3.5
114	Not Provided	900	17.7	11	1.27	0	3.5
115	Not Provided	960	17.7	11	1.27	0	4.5
116	Not Provided	900	17.7	11	1.27	0	4.5
117	Not Provided	960	17.7	11	1.27	-45	1.5
118	Not Provided	960	17.7	11	1.27	-45	1.5
119	Not Provided	960	17.7	11	1.27	-45	2.5
120	Not Provided	900	17.7	11	1.27	-45	2.5
121	Not Provided	900	17.7	11	1.27	-45	3.5
122	Not Provided	900	17.7	11	1.27	-45	3.5
123	Not Provided	960	17.7	11	1.27	45	1.5
124	Not Provided	900	17.7	11	1.27	45	1.5
125	Not Provided	960	17.7	11	1.27	45	2.5
126	Not Provided	900	17.7	11	1.27	45	2.5
127	Not Provided	960	17.7	11	1.27	45	3.5
128	Not Provided	900	17.7	11	1.27	45	3.5
129	Not Provided	960	17.7	6	1.27	0	1.5
130	Not Provided	900	17.7	6	1.27	0	1.5
131	Not Provided	960	17.7	6	1.27	0	2.5
132	Not Provided	900	17.7	6	1.27	0	2.5
133	Not Provided	960	17.7	6	1.27	0	3.5
134	Not Provided	900	17.7	6	1.27	0	3.5
135	Not Provided	960	17.7	6	1.27	0	4.5
136	Not Provided	900	17.7	6	1.27	0	4.5
137	Not Provided	930	17.7	6	1.27	-45	1.5
138	Not Provided	930	17.7	6	1.27	-45	2.5
139	Not Provided	930	17.7	6	1.27	-45	3.5
140	Not Provided	930	17.7	6	1.27	45	1.5
141	Not Provided	930	17.7	6	1.27	45	2.5
142	Not Provided	930	17.7	6	1.27	45	3.5
143	Not Provided	930	17.7	17	1.27	0	1.5
144	Not Provided	930	17.7	17	1.27	0	2.5
145	Not Provided	930	17.7	17	1.27	0	3.5
146	Not Provided	930	17.7	17	1.27	0	4.5
147	Not Provided	930	17.7	17	1.27	-45	1.5
148	Not Provided	930	17.7	17	1.27	-45	2.5
149	Not Provided	930	17.7	17	1.27	-45	3.5
150	Not Provided	930	17.7	17	1.27	45	1.5
151	Not Provided	930	17.7	17	1.27	45	2.5
152	Not Provided	930	17.7	17	1.27	45	3.5